GDAŃSK UNIVERSITY OF TECHNOLOGY

The author of the doctoral dissertation: Tomy Muringayil Joseph.
Scientific discipline: Chemical Sciences

DOCTORAL DISSERTATION

Title of doctoral dissertation: Copolymerisation studies of cardanol-based monomers towards the development of novel thermoplastic elastomers via ATRP

Title of doctoral dissertation (in Polish): Badania kopolimeryzacji monomerów na bazie kardanolu w kierunku opracowania nowych elastomerów termoplastycznych poprzez ATRP

Supervisor *signature*	Auxiliary supervisor *signature*
Prof. Józef Tadeusz Haponiuk	Dr K.I. Suresh

Gdańsk, year 2023

GDAŃSK UNIVERSITY OF TECHNOLOGY

STATEMENT

The author of the doctoral dissertation: Tomy Muringayil Joseph

I, the undersigned, declare that I am aware that in accordance with the provisions of Art. 27 (1) and (2) of the Act of 4th February 1994 on Copyright and Related Rights (Journal of Laws of 2021, item 1062), the university may use my doctoral dissertation entitled:

Copolymerization studies of cardanol-based monomers towards the development of novel thermoplastic elastomers via ATRP.

for scientific or didactic purposes.[1]

Gdańsk, *Signature of the PhD student*

Aware of criminal liability for violations of the Act of 4th February 1994 on Copyright and Related Rights and disciplinary actions set out in the Law on Higher Education and Science (Journal of Laws 2021, item 478), as well as civil liability, I declare, that the submitted doctoral dissertation is my own work.

[1] Art 27. 1. Educational institutions and entities referred to in art. 7 sec. 1 points 1, 2 and 4–8 of the Act of 20 July 2018 – Law on Higher Education and Science, may use the disseminated works in the original and in translation for the purposes of illustrating the content provided for didactic purposes or in order to conduct research activities, and to reproduce for this purpose disseminated minor works or fragments of larger works.

2. If the works are made available to the public in such a way that everyone can have access to them at the place and time selected by them, as referred to in para. 1, is allowed only for a limited group of people learning, teaching or conducting research, identified by the entities listed in paragraph 1.

GDAŃSK UNIVERSITY OF TECHNOLOGY

I declare, that the submitted doctoral dissertation is my own work performed under and in cooperation with the supervision of **Prof. Józef Tadeusz Haponiuk** and the auxiliary supervision of **Dr K.I. Suresh**.

This submitted doctoral dissertation has never before been the basis of an official procedure associated with the awarding of a PhD degree. All the information contained in the above thesis which is derived from written and electronic sources is documented in a list of relevant literature in accordance with Art. 34 of the Copyright and Related Rights Act.

I confirm that this doctoral dissertation is identical to the attached electronic version.

Gdańsk, *Signature of the PhD student*

I, the undersigned, agree to include an electronic version of the above doctoral dissertation in the open, institutional, digital repository of Gdańsk University of Technology.

Gdańsk, *Signature of the PhD student*

GDAŃSK UNIVERSITY OF TECHNOLOGY

DESCRIPTION OF DOCTORAL DISSERTATION

The Author of the doctoral dissertation: Tomy Muringayil Joseph

Title of doctoral dissertation: Copolymerisation studies of cardanol-based monomers towards the development of novel thermoplastic elastomers via ATRP.

Title of doctoral dissertation in Polish: Badania kopolimeryzacji monomerów na bazie kardanolu w kierunku opracowania nowych elastomerów termoplastycznych poprzez ATRP.

Language of doctoral dissertation: English

Supervisor: Prof. dr hab. inż. Józef Tadeusz Haponiuk

Auxiliary supervisor*: Dr. K.I. Suresh

Date of doctoral defense: <day, month, year>

Keywords of the doctoral dissertation in Polish: <słowa kluczowe> ATRP, styren, akrylan kardanylu, metakrylan pentadecylofenylu, kopolimeryzacja, elastomery termoplastyczne.

Keywords of the doctoral dissertation in English: ATRP, Styrene, Cardanyl acrylate, Pentadecylphenyl methacrylate, Copolymerization, Thermoplastic Elastomers

Summary of doctoral dissertation in Polish:

W ramach badań opracowano polimery i kopolimery na bazie kardanolu, wykorzystując naturalnie występujący zasób organiczny z przemysłu spożywczego, płyn z łupin orzechów nerkowca (CNSL). Badanie pokazuje potencjał CNSL w zakresie zaspokojenia wielu potrzeb materiałowych w różnych zastosowaniach poprzez unikalną modyfikację kardanolu (addycja grup akrylowych/metakrylowych) w celu umożliwienia kopolimeryzacji ze styrenem za pomocą polimeryzacji rodnikowej z transferem atomu (ATRP). Zdolne do polimeryzacji pochodne kardanolu, (PDPMA/CA) wykazywały korzystne właściwości podczas syntezy przy różnymi stosunkach komonomerów, co ilustruje efektywne wykorzystanie pochodnych biomasy. Uzyskanie wąskiej dyspersji masy molowej i poznanie cech związanych z architekturą makromolekularną to dwie korzyści płynące z zastosowania techniki ATRP. Ta modyfikacja może znacznie poprawić syntezę kopolimerów na bazie surowców odnawialnych w kierunku polepszenia ich właściwości. Ponadto, wykorzystując "zasady zielonej chemii", odpowiedni proces polimeryzacji może umożliwić łatwą i czystą syntezę polimerów z

zasobów odnawialnych. W tych badaniach optymalizacja procesu polimeryzacji miała kluczowe znaczenie dla precyzyjnego kontrolowania masy cząsteczkowej i struktury polimeru. Część dyskusji koncentruje się na badaniu różnych dodatkowych cech i / lub zastosowań polimerów na bazie kardanolu, które wynikają z ich architektury makromolekularnej.

W pierwszej części pracy zastosowano technikę polimeryzacji rodnikowej z transferem atomu (ATRP) do zbadania zachowania kopolimeryzacyjnego styrenu i metakrylanu pentadecylofenylu (PDPMA) przy różnych proporcjach molowych monomerów. Wykorzystując informacje ze spektroskopii 1H NMR, określono składy kopolimerów i współczynniki reaktywności za pomocą metod Finemanna-Rossa i Kelena-Tudosa. Wyniki wskazują na preferencję do przyłączania styrenu z tendencją do kopolimeryzacji naprzemiennej, a powstały kopolimer był bogaty w styren przy dowolnym składzie mieszaniny monomerów, pomimo wzrostu stężenia PDPMA. Długość sekwencji styrenu zmniejsza się wraz ze wzrostem zawartości PDPMA w wyjściowej mieszaninie monomerów, a długość sekwencji określona na podstawie danych dotyczących współczynnika reaktywności sugeruje, że długość sekwencji PDPMA jest mniej więcej stała. Charakterystyka molekularna kopolimerów za pomocą GPC pokazuje, że masa cząsteczkowa i polidyspersyjność zależą od składu wyjściowej mieszaniny monomerów. W zależności od jej składu, masa cząsteczkowa kopolimeru wynosiła od 3000 do 22 000 g/mol, a polidyspersyjność wynosiła od 1,3 do 2,19. Zachowanie kopolimerów podczas przemiany zeszklenia zmieniało się w zależności od składu wsadu, a ich stabilność termiczna wzrastała wraz ze wzrostem zawartości styrenu. Morfologia rozdzielonych faz została zaproponowana przez analizę morfologiczną wykonaną przy pomocy TEM.

W drugiej części pracy metodą ATRP została wykorzystana do zbadania zachowania kopolimeryzacyjnego akrylanu kardanylu (CA) i styrenu przy różnych proporcjach monomerów. Wykorzystując dane ^{1}H NMR dotyczące składu, wykorzystano metody Finemanna-Rossa i Kelena-Tudosa do oszacowania składu kopolimeru i współczynników reaktywności. Wyniki pokazują, że pomimo zwiększenia procentowej zawartości CA we wsadzie, styren kopolimeryzował preferencyjnie z tendencją do przyłączania naprzemiennego i że powstały kopolimer był bogaty w styren dla wszystkich składów wyjściowej mieszaniny reakcyjnej. Zgodnie z obliczeniami długości sekwencji opartymi na danych dotyczących współczynnika reaktywności, długość sekwencji CA jest w przybliżeniu stała, podczas gdy długość sekwencji styrenu spada wraz ze wzrostem stężenia CA we wsadzie. Badania GPC wykazują, że skład wyjściowej mieszaniny reakcyjnej wpływa na masę cząsteczkową i polidyspersyjność kopolimerów.

W zależności od stosunku monomerów w mieszaninie wyjściowej polidyspersyjność kopolimeru wynosiła od 1,18 do 3,45, a jego masa cząsteczkowa wynosiła od 2551 do 6934 g/mol. W zależności od składu wsadu zmienia się zachowanie kopolimerów w przemianie zeszklenia, a gdy zawartość styrenu wzrasta, wzrasta również stabilność termiczna kopolimerów. Wyniki badania pęcznienia pokazują, że otrzymane kopolimery mają głównie charakter hydrofobowy. Te wyniki zostały zweryfikowane za pomocą badań metodami podczerwieni i magnetycznego rezonansu jądrowego przeprowadzonych przed i po zmydlaniu. Biorąc pod uwagę zmienny stopień nienasycenia kardanolu, przedstawione tutaj kompleksowe badania charakterystyki strukturalnej mają kluczowe znaczenie dla opracowania przyjaznych dla środowiska metod zrównoważonego procesu chemicznego wykorzystującego ten odnawialny zasób. Badanie morfologii metodą TEM ujawniło fazową strukturę rdzenia-powłoki w przypadku wytworzonej kompozycji sty-co-CA70.

Zbadano czynniki, takie jak elastyczność łańcucha głównego, mobilność łańcucha bocznego i zachowanie podczas krystalizacji, aby zrozumieć wpływ tych czynników na monomery akrylanowe i metakrylanowe i ich polimery. Badania reologiczne i adhezyjne wskazują na możliwość regulowania właściwości adhezyjnych kopolimerów styren-PDPMA/CA i ich użyteczność w klejach topliwych. Możliwość regulowania właściwości adhezyjnych umożliwia precyzyjne dostosowanie charakterystyk wiązania dla różnych podłoży i różnych zastosowań. Ta wszechstronność zwiększa wydajność, trwałość, elastyczność i odporność na środowisko klejów, zwiększając ich użyteczność w różnych branżach. W badaniu omówiono również wpływ ligandów monomerów, w szczególności w przypadkach PMDETA i dNbpy, na konwersję, masę cząsteczkową i polidyspersyjność oraz wpływ struktury monomeru na przemiany termiczne w monomerach i polimerach. Wszystkie ulepszenia są bezpośrednio związane z wprowadzeniem elastycznych łańcuchów alkilowych C15 do kardanolu. W ten sposób CA może zastąpić monomery na bazie ropy naftowej w produkcji utwardzanych powłok o unikalnych właściwościach i wysokiej zawartości struktur pochodzących z biomasy. Badane właściwości pozwalają lepiej zrozumieć czynniki, które należy wziąć pod uwagę przy projektowaniu układów polimerowych.

Summary of the doctoral dissertation in English: The research developed cardanol-based polymers and copolymers, utilising a naturally occurring organic resource from the cashew industry, Cashew Nut Shell Liquid (CNSL). The study demonstrates the potential of CNSL to meet many materials needs in different applications through the unique modification of cardanol (addition of acrylic/methacrylic groups) to allow copolymerise with styrene by Atom Transfer Radical Polymerization (ATRP). The polymerisable monomers derived from cardanol (PDPMA/CA), exhibited favourable properties upon synthesis, with varying comonomer ratios illustrating the efficient utilisation of biomass derivatives. Gaining narrow molar mass dispersion and learning more about the characteristics associated with macromolecular architecture are two benefits of using the ATRP technique. This modification may significantly improve the synthesis of biomass-based copolymers with superior properties. In the meantime, using "green" chemical principles, the polymerisation process may make it possible to easily and cleanly synthesise polymeric molecules from renewable resources. In this research, optimising the polymerisation process was crucial for precisely controlling the molecular weight and design of the polymer. The discussion part of the thesis is focused on the investigation of different additional characteristics and uses of the polymers that result from macromolecular architecture by comparing them with cardanol-based polymers.

In the first section of the experiment, the Atom Transfer Radical Polymerization technique was used to examine the copolymerisation behaviour of styrene and pentadecylphenyl methacrylate (PDPMA) at various monomer feed ratios. Using composition information from ^{1}H NMR spectroscopy, the copolymer composition and reactivity ratios were determined using the Finemann-Ross and Kelen-Tudos methods. The results indicate a preference for the addition of styrene with an alternation tendency, and the resulting copolymer was rich in styrene at any feed composition, despite an increase in the feed's PDPMA concentration. Styrene sequence length decreases with increasing PDPMA content in the feed, and sequence length determined based on reactivity ratio data suggests that PDPMA sequence length is more or less constant. The molecular characterisation of the copolymers by GPC shows that molecular weight and polydispersity depend on the composition of the feed. Depending on the composition of the feed, the molecular weight of the copolymer ranged from 3000 to 22,000 g/mole, and the polydispersity was between 1.3 and 2.19. The behaviour of the copolymers during the glass transition varied depending on the feed composition, and their thermal stability increased as the styrene level rise. A phase-separated morphology was proposed by the morphological analysis done by TEM.

The second part of the work designed by the atom transfer radical polymerisation method was used to examine the copolymerisation behaviour of styrene and cardanyl acrylate (CA) at varied monomer feed ratios. Using ^{1}H NMR composition data, the Finemann-Ross and Kelen-Tudos methods were used to estimate the copolymer composition and reactivity ratios. The findings show that, despite increasing the CA percentage in feed, styrene copolymerised preferentially with an alternation tendency and that the resultant copolymer was rich in styrene at all feed compositions. According to sequence length calculations based on reactivity ratio data, the sequence length of CA is roughly constant while the sequence length of styrene falls as the CA concentration in feed rises. GPC research demonstrates that the feed content affects the molecular weight and polydispersity of the copolymers. According to the feed mix, the polydispersity of the copolymer ranged from 1.18 to 3.45 and its molecular weight was between 2551 and 6934 g/mole. Depending on the feed composition, the copolymers' glass transition behaviour changes, and when the styrene content raise, the copolymers' thermal stability rises as well. Swelling experiments show that the copolymers investigated in this study are mostly hydrophobic in nature. This finding was verified using infrared and nuclear magnetic resonance studies performed before and after saponification. Given the variable degree of unsaturation in cardanol, the comprehensive structural characterisation investigations reported here are critical for developing environmentally friendly methods for a sustainable chemical business using this renewable resource. TEM examination of the morphology revealed a phase-separated core-shell structure in the case of sty-co-CA_{70} composition produced.

Factors like main chain flexibility, side chain confinement and crystallisation behaviour were explored to understand the impact of these factors on acrylate and methacrylate monomers and polymers. Rheological and adhesion tests indicate the tunability of the adhesion properties of styrene-PDPMA/CA copolymers and their utility in hotmelt adhesives. The tunability in adhesion properties enables precise customisation of bonding characteristics for diverse substrates and applications. This versatility enhances adhesives' performance, durability, flexibility, and environmental resistance, enhancing their utility across various industries. The study also discussed the impact of ATRP ligands, specifically PMDETA and dNbpy, on conversion, molecular weight, and polydispersity, and the influence of monomer structure on thermal transitions in monomers and polymers. All the improvements are directly linked to the introduction of flexible C_{15} long alkyl chains of cardanol. Thus, CA can replace petroleum-based monomers in producing curable coatings with unique properties and high biobased content. The properties investigated enhance understanding of factors to consider when building polymeric systems.

I want to thank all those without whom this work would not have been possible.

Thank you very much:

Prof. Józef T. Haponiuk

for the substantive direction of this doctoral dissertation,
comprehensive help, time devoted to me, and faith in me.

Dr. K. I. Suresh

for the unique atmosphere in the laboratory,
always express help, motivation, and cooperation.

Prof. Sabu Thomas

for valuable tips, motivation, and joint search
for solutions to difficult questions and situations.

I am also very grateful to my family and friends
for invaluable support, great understanding, patience
and help in many life situations.

Table of Contents

CHAPTER-II

MATERIALS, MONOMER SYNTHESIS AND CHARACTERIZATION TECHNIQUES

CHAPTER IV

ATR COPOLYMERIZATION OF STYRENE AND CARDANYL ACRYLATE (CA)

CHAPTER-V

DISCUSSION ON STUDY OUTCOME - EVALUATION ON ATRP SYNTHESIS OF CARDANOL-BASED MONOMERS AND POLYMERS SYNTHESIZED VIA ATRP

List of Figures

Page No.

List of tables

Page No.

List of schemes

Page No.

List of abbreviations

CRP	-	Controlled radical polymerization
ATRP	-	Atom Transfer Radical Polymerization
FRP	-	Free radical polymerization
LRP	-	Living radical polymerization
NMP	-	Nitroxide Mediated Polymerization
RAFT	-	Reversible Addition/Fragmentation Chain Transfer Polymerization
GTP	-	Group transfer polymerization
DT	-	Degenerative transfer
PRE	-	Persistent radical effect
TERP	-	Organotellurium-mediated live radical polymerization
SBRP	-	Organostibine-mediated polymerization
ATRA	-	Atom transfer radical addition
SMMA	-	Styrene–methyl methacrylate copolymer
SBC	-	Styrene-butadiene copolymers
SB		Styrene-butadiene rubber
MABS	-	Methyl methacrylate-acrylonitrile-butadiene-styrene copolymers
ASA	-	Acrylonitrile-styrene-acrylate copolymer
SMA	-	Styrene-maleic anhydride
CNSL	-	Cashew nutshell liquid
PDP	-	Pentadecylphenol
PDPMA	-	Pentadecylphenylmethacrylate
CA	-	Cardnyl Acrylate
St	-	Styrene
EB	-	Ethyl benzene
M_wD	-	Molecular weight distribution
PDI	-	Polydispersity index
CuBr	-	Copper(I) bromide

PMDETA	-	*N*,*N*,*N*',*N*',*N*''-pentamethyldiethylenetriamine
EBriB	-	Ethyl-2-bromoisobutyrate
TEA	-	Triethylamine
D.C.M.	-	Dichloromethane
Na_2CO_3	-	Sodium carbonate
THF	-	Tetrahydrofuran
^{1}H NMR	-	Proton nuclear magnetic resonance
^{13}C NMR	-	Carbon-13 nuclear magnetic resonance
FT-IR	-	Fourier transform infrared spectroscopy
TEM	-	Transmission electron microscopy
FR-KT	-	Finemann-Ross and Kelen-Tudos
GPC	-	Gel permeation chromatography
DSC	-	Differential scanning calorimetry
TGA	-	Thermogravimetric analysis
T_g	-	Glass transition temperature
PET	-	Polyethelyleneterepthalate
PA	-	Pentadecylphenylacrylate
PMA	-	Pentadecylphenylmethacrylate
dNbpy	-	4,4'-Di-5-nonyl-2,2'-bipyridine

AIM & OBJECTIVE

The study aimed to document the characteristics and properties of the synthesized copolymer derived from cardanol, a cashew industry byproduct and a naturally occurring organic resource. The main points of the dissertation as objectives are furnished below:

- Synthesis of Pentadecylphenyl methacrylate (PDPMA) and Cardanyl acrylate (CA) monomer from cardanol, a by-product of the cashew processing industry, and a renewable resource.
- Synthesis of Styrene-co-PDPMA/CA with controllable molecular weight and narrow polydispersity index by ATRP of the monomers and styrene with various feed ratios (PDI).
- Structural characterization of synthesized copolymers by IR, Mass ^{1}HNMR and ^{13}C spectroscopy.
- Molecular weight determination of copolymers by Size Exclusion Chromatography.
- Polydispersity, Reactivity ratios of monomers, and sequence length of copolymers calculated using Finemann-Ross (FR), and Kelen-Tudos (KT) parameters.
- Thermogravimetric Analysis (TGA) and Differential Scanning Calorimetry (DSC) to characterize the thermal properties of Styrene-co-PDPMA/CA copolymers.
- TEM analysis and evaluation the morphology of the synthesized copolymer.
- Rheological studies of Styrene-co-PDPMA/CA copolymers at low-high-temperature ranges.
- Adhesion properties of the synthesized copolymers.

The main objective of this study is to investigate and evaluate the development of well-defined homo & block copolymers through Atom Transfer Radical Polymerization techniques (ATRP). Initially, the research focuses on polymer synthesis using ATRP at a suitable ppm level of a metal catalyst, the concentration of the initiator, and reaction temperature for the controlled polymerization to achieve the maximum yield. After optimizing the proper Monomer: Ligand: Catalyst ratio at an optimum temperature, the research focuses on synthesizing copolymers using ATRP with different monomer feed ratios. Hence, the study focuses on preparing polymers (homo/block) that use ppm level of metal catalyst deprived of affecting the productivity of polymerization. The role of the ATRP initiator is crucial, and the halogen requirement to fulfill its purpose makes it easy to adopt the polymerization method. Most of the study conducted for this thesis focuses on synthesizing styrene with acrylate/methacrylate-based homo- and copolymers by ATRP to achieve controlled molecular weight distribution and narrow MWD with minimal copper catalyst consumption.

The polymerization was studied and optimized under the lowest possible copper concentration for the controlled copolymers, essential in obtaining narrow-block copolymers. Structural characterization of synthesized copolymers can be carried out by IR, Mass, ^{1}HNMR and ^{13}C spectroscopy. Molecular weight determination of copolymers was performed by Size Exclusion Chromatographic technique (SEC) to evaluate the molecular weight distribution. Polydispersity, reactivity ratios and sequence length of copolymers were calculated using Finemann-Ross (FR) and Kelen-Tudos (KT) methods. Another aspect of the study was investigating synthesised copolymers' thermal stability and adhesion properties. The findings from this research will undoubtedly help improve our understanding of the factors that must be considered when synthesizing homo and block copolymers utilizing ATRP for various applications. The living radical polymerization method chosen for the current study was examined regarding its historical evolution and applicability since the present thesis is about the "Synthesis of monomersand their polymerization by ATRP process." The background of the current investigation in general and the work on ATRP was addressed. Another crucial subject will be the application oflive radical polymerization in developing amphiphilic polymeric systems.

Scheme A & B depicts the proposed design for bulk ATRP of styrene-co-PDPMA/CA at 95 °C.

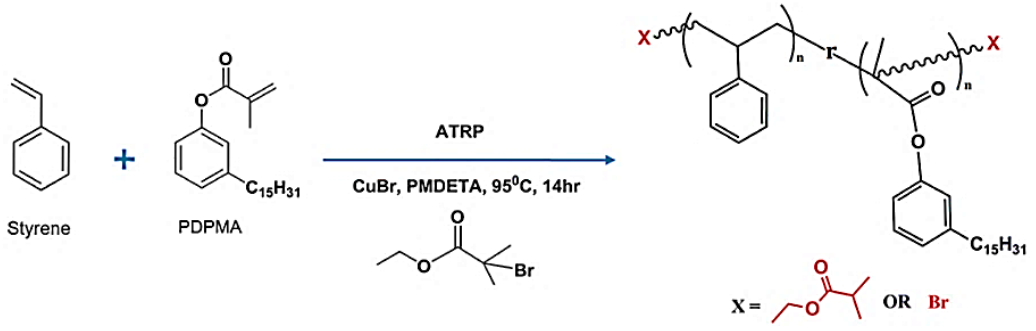

Scheme A. Schematic representation of styrene-co-PDPMA via ATRP.

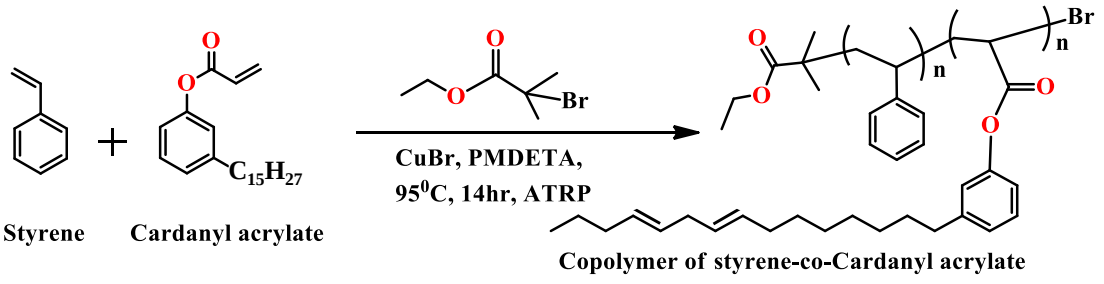

Scheme B. Schematic representation of styrene-co-CA via ATRP.

Since the proposed work aims to the copolymerization studies of polymerizable monomers from cardanol by ATRP, the entire thesis is designed as follows:

Chapter I	**INTRODUCTION.**
Chapter II	**MATERIALS, MONOMER SYNTHESIS, AND CHARACTERIZATION TECHNIQUES.**
Chapter III	**ATR COPOLYMERIZATION OF STYRENE AND PENTADECYLPHENYL METHACRYLATE.**
Chapter IV	**ATR COPOLYMERIZATION OF STYRENE AND CARDANYL ACRYLATE.**
Chapter V	**DISCUSSION ON STUDY OUTCOME - EVALUATION ON ATRP SYNTHESIS OF CARDANOL-BASED MONOMERS AND POLYMERS SYNTHESIZED VIA ATRP**

SCOPE OF RESEARCH ON ATRP

Polymer chemists have long prioritized synthesizing bio-based polymers with well-defined compositions, topologies, and functionalities, which enable Controlled Radical Polymerization (CRP) techniques, already commercialized for synthesizing polymers. The fundamental part in CRP area, Atom Transfer Radical Polymerization (ATRP) research is divided into three main areas: (1) developing a structure-reactivity correlation for each ATRP process component; (2) creating new, more effective, selective, affordable, and green catalytic systems for ATRP; and 3) establishing an association between the macroscopic properties of materials produced via ATRP and their structure. Radical polymerization (RP) is the most common polymer manufacturing process, with almost half of the polymer production which is due to the factors associated with it. These are: (i) easy to implement the process in industrial plants, (ii) water tolerant, (iii) compatibility of various monomers, and (iv) fast polymerization reactions. However, the FRP's major drawback is that it cannot produce polymers with exact molecular weight control and narrow molecular weight distribution, making it challenging to synthesize polymers with tailor-made chemical composition. CRP techniques address these issues by addressing uncontrolled side reactions, active bimolecular termination, and chain transfer reactions.

ATRP makes it possible to apply radical polymerization easily and potentially in combination with the transition metal redox process, making the FRP method distinctive. Polymers with narrow polydispersity and controlled molecular weight may be readily prepared using ATRP. The reaction can be conducted at ambient temperature, utilizing diverse monomers, initiators, catalysts, and other components. Functional groups can also be added at the chain ends by functionalized ATRP initiators or halogen replacement by nucleophilic substitution. Copper has been widely adopted as a transition metal catalyst for ATRP, which has led to its widespread application in the industrial synthesis of polymers from a wide range of acrylates, styrenes, methacrylates, acrylonitrile, and other vinyl monomers. End-functionalized polymers and copolymers offer numerous applications, including block, graft, and star copolymer synthesis, surface modification, and compatibilization in polymer blends, adhesives, and coatings. The pharmaceutical, oil, agricultural, paper, and detergent sectors are just some of the many that benefit from block copolymers' use as thermoplastics, associative polymers with hydrophilic and hydrophobic segments, and surfactants.

CHAPTER-I. INTRODUCTION

Renewable resources are gaining increasing importance as alternatives to fossil fuels, serving as raw materials energy sources. Biomonomers, derived from renewable sources, offer sustainable alternatives to petroleum-based polymers, reducing environmental impact and fostering a circular economy through biodegradable materials, waste reduction, and responsible resource management. The utilization of cashew nut shell liquid (CNSL) exemplifies this pursuit. CNSL, a byproduct from cashew processing, yields cardanol—a naturally occurring phenolic compound. Distillation of CNSL produces cardanol, which contains a lengthy hydrocarbon side chain. This unique structure enables cross-linking and imparts desirable traits to coatings, like progressive drying and water resistance. Cardanol serves diverse applications—epoxy curing agents, paints, adhesives, and more—thanks to its excellent electrical insulation and thermal stability, making it a sustainable alternative to petroleum-based phenols. Furthermore, cardanol's molecular structure allows tailored polymer creation, enhancing properties through chemical modification. This renewable phenolic lipid is sourced from cashew nut shells, offering promise in various industries. It can be incorporated into polymer chains using Atom Transfer Radical Polymerization (ATRP), leading to advanced materials with enhanced properties such as adhesion, durability, and corrosion resistance, valuable in coatings, adhesives, and high-performance applications. Since the presenting investigation deals with the **"*Synthesis of monomers and their polymerization by ATRP process*"**, deliberating the historical evolution, significance and rationale of the living radical polymerization process will be worthwhile. Background of the recent investigation in general and work on living radical polymerization processes, i.e., ATRP, will be discussed. Further, applications of ATRP, particularly in synthesizing thermoplastic elastomers, will be reviewed. Finally, the aim and objective of the present investigation will be outlined.

1. LIVING RADICAL POLYMERIZATION: AN OVERVIEW

1.1. Significance of polymers

Polymer chemistry and technology is a fascinating subject in chemistry, chemical engineering, and material science, affecting various disciplines such as electronics, medicine, and materials like plastics, rubbers, fibers, films, elastomers, and structural materials. The significance of polymers has grown, making it challenging to envision human life without their contributions. Novel polymeric entities are being synthesized precisely due to their lightweight structure, optical transparency, processability, and high electrical and mechanical characteristics. Various structural parameters influence the properties of these polymers, while formulations and compositional interactions lead to divergent outcomes.[1] Polymers, crucial in modern society, have evolved from traditional building materials to everyday artefacts, transforming various industries.[2] Synthetic orchestration involves monomer combination to create polymer chains with divergent properties, using natural and synthetic substrates, dating back to the mid-19th century.[3]

The polymer industry has experienced exponential growth, surpassing the metals sector's scope. Both natural and synthetic polymers significantly improve human existence and societal standards. Their contributions include sustenance preservation, transportation, telecommunication, medical interventions, nutritional enhancement, and historical documentation. The symbiosis between synthetic and natural polymers is essential in today's complex environment. Scientific inquiry is crucial in addressing fundamental issues like sustenance provision, potable water availability, air quality protection, energy resource utilization, and human health and well-being.[4] The complexity of polymers arises from learning foundational science, which includes facts, theories, and practical uses. This knowledge applies to individuals in various fields, including medicine, engineering, physics, chemistry, and biomedical sciences, as well as those seeking intellectual acumen. Polymers have transformative potential in fabricating various commodities, including coatings, elastomers, adhesives, amalgamations, plastics, fibres, and niche products like caulks, ceramics, and composites. The fundamental underpinnings of polymers' behaviour reveal their quintessential principles across the entire polymer spectrum, with some exceptions grounded in elemental precepts. Researchers from diverse disciplines actively engage in polymer research, involving over half of chemists, chemical engineers, and mechanical engineers.[5]

Polymers and polymer chemistry significantly influence emerging domains in pharmaceuticals, biomedicine, molecular biology, biochemistry, and biophysics. Exploring high-molecular-weight compounds is a rapidly expanding field that transcends chemistry sub-disciplines and interdisciplinary pursuits. Polymer science is a specialized, comprehensive investigation sphere encompassing chemistry and diverse scientific branches. As experts from various fields explore new territories, scientific domains burgeon dynamically, shaping and catalyzing polymer research endeavours, cementing its trajectory in scientific progress.[6] Polymer synthesis involves applying complex concepts, chemical tenets, and advanced methodologies to complex macromolecular structures and materials. This intricate endeavour demands the forefront of chemical techniques and transcends traditional boundaries in chemistry, physics, biology, and medical sciences. Polymer science requires newcomers to combine insights from these disciplines, showcasing its multifaceted nature.[7]

1. 2. World scenario of monomers and polymers.

The contemporary era is dominated by polymers, which play a crucial role in various domains of human existence. With global production reaching 150 million metric tons, polymers profoundly impact industries, agriculture, and medical applications. However, this growth relies heavily on monomers derived from non-renewable oil reserves, accounting for 80% of the feedstock. The complex dynamics of polymerization, resource utilization, and sustainability highlight the complex dynamics shaping our polymer-dependent world.[8] Global oil production is around 3 million metric tons, with 4% dedicated to monomer synthesis and 96% to energy generation. Monomer synthesis from oil poses significant carbon dioxide emissions, contributing to the "greenhouse effect" and environmental degradation. Researchers are now focusing on creating monomers from renewable and sustainable resources, leading to a paradigm shift in polymer feedstock utilization.[9]

1. 3. Polymerization

Classifying polymers remains a persistent difficulty, with no universally accepted categorization. Polymer research has evolved into two discrete classification frameworks: condensation and addition polymers, characterized by structural divergence and the dichotomy between step and chain polymerizations. However, the terminology can cause confusion and misunderstandings. "condensation addition" emphasizes compositional attributes or structural intricacies, while the "step-chain" classification focuses on the mechanisms orchestrating polymerization events.[10]

1. 4. Radical polymerization

Radical polymerization is a mature technique with millions of tons of vinyl-based homo and copolymers produced yearly. Free radical polymerization is frequently used in commercial and academic settings to synthesize various polymeric materials. Reasons for its widespread use include its resistance to water and protic environments, its compatibility with a wide variety of functional group monomers, and its simplicity of synthesis. Dispersed aqueous systems (emulsion, mini-emulsion, and suspension polymerization) are used to perform radical polymerizations, with a focus on the role that operating in a heterogeneous environment has in determining the polymerization rate, etc.[11] These methods have considerably reduced the complexity of the laboratory setting and found broad commercial success. Unlike ionic and coordination polymerizations, radical polymerizations need the lack of oxygen for the polymerization or copolymerization of a wide variety of vinyl monomers, including functional monomers. The reactions may be carried out over a wide temperature range, generally between 0 and 100 °C, and various solvents and other contaminants are tolerated.

The primary drawback of traditional radical polymerizations is the inability to regulate the resulting polymer's molecular architecture. Due to their sluggish initiation, quick propagation, and susceptibility to various termination processes, polymers with large molecular weights and a broad polydispersity are often generated with relatively limited architectural control. The physical and mechanical properties of the polymers reflect these qualities. Consequently, radical polymerization was disregarded as a viable option for high-throughput synthesis of complex polymers with a wide range of topologies. Radical polymerization is a versatile and simple polymer science technique synthesizing various polymers with tailored properties, including commodity plastics and advanced materials. It is ideal for large-scale production in packaging, automotive, electronics, and construction industries. However, it requires a deep understanding of molecular weight distribution and microstructure to harness its potential fully. Advancements in controlled radical polymerization techniques enhance its utility by enabling precise tuning of polymer architectures and properties.[12]

1.5. Living Polymerizations: prerequisites

Anionic polymerization of styrene with sodium napthanilide in 1956 was the first example of "living" polymerization, which has since been shown to be one of the most effective ways for controlled polymer synthesis.[12] Well-defined polymers with regulated chain end functions and block and graft copolymers were made possible by developing ionic polymerization techniques. Polymers with well-defined topologies and molecular weights may be generated using living polymerization, which excludes unwanted side reactions. When the initiation rate is higher than or equal to the propagation rate, the resultant polymers have narrow polydispersity parameters, often falling within the range of 1.1. Even though styrenes and 1,3-dienes were the only nonpolar hydrocarbon monomers that could be used in live anionic polymerization, this process has recently been extended to include polar monomers such as (meth)acrylates and other functional derivatives.[13] Several functional groups and monomer families are incompatible with the developing polymer chain's terminal. However, these polymerization procedures required stringent reaction conditions, including ultra-pure chemicals, the absence of water and oxygen, and often extremely low temperatures. Not only are there restrictions on the quantity of monomers that may be used, but functionalities included in the monomers might have unintended consequences. A similar explosion has happened in previously hard-to-control polymerizations, such as cationic, coordination, ring-opening, and ring-opening metathesis polymerization.[14]

1.6. Living Radical Polymerizations

Living radical polymerizations are a significant advancement in polymer chemistry, enabling the controlled growth of polymer chains with well-defined end groups and narrow molecular weight distributions. This transformative approach relies on the reversible deactivation of propagating radicals, allowing for the manipulation of reaction kinetics and the preservation of active species. Techniques like ATRP, RFT, and NMP contribute to expanding tailor-made materials with intricate structures and functionalities for various applications.[15]

A significant focus of polymer chemistry has been the creation of polymers with precisely controlled properties. In the 1980s, "iniferters" - chemical compounds that simultaneously acts as an initiator, transfer agent, and terminator were presented by Otsu et al.[15], and in the 1990s, various live radical polymerizations were suggested. Compared to traditional anionic living polymerizations, the number of systems and suggested approaches for regulating radicals has increased significantly in recent years.[15] The methods described here minimize the extent or probability of radical bimolecular termination and give equal opportunity for propagation to all polymer terminals by quickly establishing a dynamic equilibrium between a small amount of growing free radicals and a large majority of dormant species. The molar ratio of monomers to the quiescent species, in this case, the initiator, determines the final chain length, which is almost constant.[16] In ATRP and degenerative transfer (DT), dormant chains can be alkyl halides; in reversible addition-fragmentation chain transfer processes (RAFT), they can be thioesters; in nitroxide-mediated radical polymerization (NMRP), they can be alkoxyamines; and in group transfer polymerization (GTP), they can be organometallic species.[17]

1.6.1. Fundamentals for LRP

The basics of LRP, in general, can be summarized as follows:

- Fast initiation, when compared to propagation, since all chains should begin to grow essentially simultaneously and retain functionality.
- Fast exchange between active and dormant species, so that the majority of the growing chains are in the dormant state and only a fraction is present as propagating free radicals.
- The propagation rate should not depend on the D.P.
- The polymerization reaction should be free of termination and transfer reactions.
- To facilitate chain growth and minimize termination events, it is important to maintain a relatively low concentration of the propagating radicals ($[P_n^{\cdot}] < 10^{-7}$ M).
- There should be only single type of propagating species, and if different propagating species are present, their conversion between them should be extremely rapid.
- There should be a direct linear relationship between the monomer conversion and the number average molecular weight (M_n) of the polymer.

1.6.2. Mechanism

The production of well-defined polymers relies on the principles of LRP, which aims to minimize termination effects and ensure rapid initiation. This approach ensures that all active polymer chains have an almost equal opportunity to grow, resulting in polymers with low dispersity ($Đ_M$). Central to all LRP systems is establishing a dynamic equilibrium between propagating radicals and various dormant species. Radicals can either be temporarily trapped in a deactivation/activation process, as shown in **Scheme 1 (a)**, or participate in a reversible transfer process involving degenerative exchange, as depicted in **Scheme 1 (b)**.[18] The first method depends on what is known as the Persistent Radical Effect (PRE). The PRE is a unique kinetic phenomenon that imparts a self-regulating characteristic to specific LRP systems.

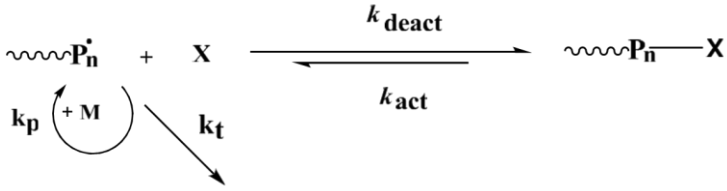

Scheme 1 (a). Equilibrium between propagating radicals and dormant species in LRP by activation/deactivation process.

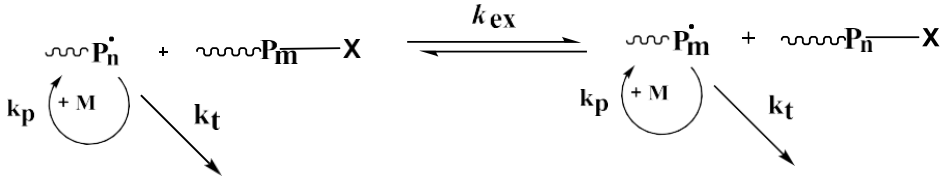

Scheme 1 (b). Equilibrium between propagating radicals and dormant species in LRP by the degenerative exchange process.

The propagating radicals, denoted as $P_n^{\cdot}$, are swiftly captured during the deactivation step (with a rate constant of deactivation, k_{deact}), where they interact with species X. This species is typically a stable radical, like a nitroxide, or an organometallic entity such as a cobalt porphyrin occurs with a deactivation rate constant represented as k_{deact}.[19] The dormant species can be activated (k_{act}) through various means, such as spontaneous thermal activation, light exposure, or a suitable catalyst. This activation process is aimed at regenerating the active growth centers. While radicals have the capacity to propagate (k_p), they also face the possibility of termination (k_t). However, it's worth noting that persistent radicals (denoted as X) cannot undergo termination with each other; instead, they can (reversibly) form cross-couplings with the growing species (k_{deact}). As a result, each instance of radical-radical termination leads to the irreversible accumulation of X. Over time, the concentration of X progressively increases following a unique 1/3 power law. Consequently, both the concentration of radicals and the probability of termination decrease as time elapses. In this scenario, the growing radicals predominantly interact with X, which is present at concentrations over 1000 times higher, rather than reacting with each other. In systemsobeying the PRE, a steady state of growing radicals is established through the activation– deactivation process rather than initiation–termination as in conventional RP.[20] In the systems based on degenerative transfer (DT) **Scheme 1 (b**)), the activation occurs via a bimolecular radicaltransfer between a dormant and an active species. The exchange process (k_{ex}) usually proceeds via a short-lived intermediate that can sometimes be considered a transition state. In addition- fragmentation systems, the intermediate's lifetime can delay polymerization or participate in sidereactions like trapping growing radicals or initiating new chains.

1.6.3. Advances of LRP than FRP

LRP and FRP proceed via the same radical mechanism, exhibit similar chemo-, regio- and stereo-selectivities, and can polymerize a similar range of monomers. However, several important advances of LRP exist, as summarized below:

- The lifetime of growing chains is extended from <1 s in FRP to >1 h in LRP through the participation of dormant species and intermittent reversible activation.
- Initiation is slow, and the free radical initiator is often left unconsumed at the end of an FRP. In most LRP systems, initiation is very fast and near instantaneous growth of all chains can be achieved, ultimately enabling control over chain architecture.
- Nearly all chains are dead in FRP, whereas in LRP the proportion of dead chains is <10%.
- The rate of polymerization in LRP is often slower than in FRP. However, the rates may be comparable in certain cases.
- A steady state radical concentration is established in FRP with similar rates of initiation and termination, whereas in LRP systems based on the PRE, a steady radical concentration is reached by balancing the rates of activation and deactivation.
- Termination usually occurs between long chains and constantly generated new chains in FRP, while in LRP systems based on the PRE, all chains are short at the early stages of the reaction and become progressively longer; thus, the termination rate significantly decreases with time. In DT processes, new chains are constantly generated by a small amount of conventional initiator, and therefore, termination is more likely throughout the reaction.

1.6.4. Functionality in LRP

The synthesis of low-M_W polymers with high levels of functionality holds considerable promise for LRP. Since propagating radicals are generally functional group tolerant, most LRP methods may include functional monomers and initiators into a (co)polymer.[12] It is also possible to confer functionality on discrete regions of a macromolecule. This may involve adding side functional groups to a polymer backbone either directly or via a protected intermediate. Chain ends may be converted to other functional groups or used as functional initiators to integrate new end groups. In reversible addition-fragmentation transfer (RAFT) polymerization, for instance, dithioesters have been converted to thiols, alkoxyamines have been converted to alkyl chlorides, and alkyl halides (R-X) have been converted to allyl, hydroxy, amino, azido, and ammonium or phosphonium groups in ATRP with excellent yields.[21] In telechelics and stars, inactive species are transformed into multifunctional polymers by linear chain growth in two directions. Certain regions of macromolecules may also be engineered to perform new functions. This includes the functional core of stars, the centres of two-directionally grown chains, and periodically repeated segments prepared by ATRP or click coupling. With the ability to modify macromolecular design as a jumping-off point for synthesis, numerous new polymeric materials are being developed, heralding the dawn of the smart polymer' era.

1.6.5. The different types of LRPs

Two classes of LRP methodology can be distinguished about the mechanism involved in the activation-deactivation equilibrium. The key difference is between PRE-based and DT-based systems. Systems based on the PRE were given the general term SFRP. NMP and cobalt-mediated polymerization are two examples of SFRPs.[12] Reversibly trapping carbon-centered radicals and being unable to cross-propagate with the monomer are two of the unique properties of the radicals provided by certain nitroxides and cobalt porphyrin complexes. The ATRP is a catalytic process based on the PRE.[22] An atom or group (often a halogen atom) caps the ends of the chains in their inactive state; this is removed by a transfer mediated by a transition metal catalyst in a redox reaction. Copper catalysts have been the focus of most research, although iron, cobalt, nickel, and ruthenium catalysts have also been utilized. These DT-based systems include iodine transfer, RAFT, organotellurium-mediated live radical polymerization (TERP), and organostibine-mediated polymerization (SBRP).[23] In DT-based systems, activation happens by ambimolecular radical transfer of an inactive species to an energetic one. The monomer units are incorporated into the CTA to produce the polymer. Between the two phases of activation and deactivation, the molar mass of the CTA grows. The word "degenerative" refers to the fact that the initial CTA and inactive chains have the same chemical structure besides the number of monomer units.

2. ATOM TRANSFER RADICAL POLYMERIZATION (ATRP)

Radical polymerization techniques allow for the production of tons of polymers annually, with multiple polymerization processes, moderate reaction temperatures, and insensitivity to external impurities. However, they cannot control the architecture of the synthesized polymers, which is essential for their optimal properties. Controlled radical polymerization (CRP) techniques are key in designing and developing self-healing polymers, providing excellent control over molecular weight, molecular weight distribution, and architecture. Radical polymerization has revolutionized the field of polymers, allowing the synthesis of low polydispersity functional polymers with well-defined molecular architecture. A living polymerization does not involve any unwanted side reactions, and all polymer chains are simultaneously initiated such that the chain ends of the synthesized polymer are active indefinitely. However, polymerizations with 100% living characteristics are not possible in reality. An ideal living polymerization technique should consist of the following features:

- An increase in molecular weight concerning monomer addition and time leads to first-order kinetics with respect to the monomer.
- The degree of polymerization is directly proportional to the initial monomer to initiator concentration ratio.
- The polydispersity index is close to unity.
- The polymerization is living, and the reaction continues after adding more monomers after all the previous monomers have been consumed.

Living polymerization has opened up new possibilities for designing and developing novel polymeric materials with definite architectures and compositions. ATRP is a controlled living polymerization technique that has emerged as one of the most successful synthetic techniques. ATRP is a versatile and powerful CRP technique widely studied and used as the key synthetic route for developing functional polymers. Customising molecular properties produces innovative materials like blocks, graft, star copolymers, surface-modified polymers, adhesives, and coatings. Because self-healing needs specialized features inside polymers, ATRP is a helpful tool in their development. ATRP is the primary reaction responsible for the constant growth of polymeric chains during polymerization. It is mechanistically related to atom transfer radical addition (ATRA). Still, unlike ATRA, it involves the reactivation of the formerly formed alkyl halide adduct with the unsaturated monomer and the forming additional monomer units in the propagation step. ATRP is a modification of Kharasch's addition reaction used to synthesize highly functional small organic molecules and polymeric materials with precise molecular weight, molecular weight distribution, composition, and molecular architecture. Mitsuo Sawamoto and Krzysztof Matyjaszewski first introduced ATRP in 1995, and it has become a highly applicable technique for the synthesis of a large number of polymers due to its tolerance towards functionalities and impurities and reasonable control over molecular weight and structure[22] which gained rapid interest due to its applicability. As ATRP advances, it supports sustainable bio-based materials adhering to green chemistry principles, improving sustainability in various industrial sectors.

2.1. Fundamentals of ATRP

ATRP is a controlled polymer chemistry process that enables precise polymer synthesis with defined compositions, topologies, and functionalities. The ATRP gets its moniker from the atom transfer step, a critical elementary process in the regular growth of polymeric chains. ATRP originates from the ATRA reactions, catalyzed by transition metal complexes that seek to produce 1:1 adducts of R-X and alkenes. Most initiating systems consist of an organic halide and a transition metal complex (activator) at a lower oxidation state. Transition metal complexes in their higher oxidation state coordinate with halide ligands (deactivators), activating the carbon-halogen bond of the halogen compound to generate the carbon radical species (via one-electron oxidation of the metal complex associated with abstraction of the halogen by the metal species; see Schemes **2a** and **2b**). After interacting with the monomer, the newly produced carbon radical species forms an adduct radical, which is eventually capped by the halogen on the metal complex at a higher oxidation state or by combining with a different monomer molecule.[20,24] By reducing the highly rapid propagation of a specific emerging radical chain end, the halogen-capping reaction of the radical species limits the development of extraordinarily long polymer chains, particularly in the early phases of polymerization. The metal catalyst may also re-create the expanding radical species by re-activating the carbon-halogen bond formed during adduct formation or at the chain termination of an oligomer or polymer. The covalent species with the carbon-halogen terminal is called a "dormant" species here. However, it is analogous to the "living" species in other reversible but heterolytic anionic and cationic polymerizations. By reversibly activating the carbon-halogen terminal with a metal catalyst, the length of the resulting polymer chains may be controlled with high precision.

Furthermore, with the accumulation of the deactivator as a consequence of the Persistent Radical Effect (PRE), there is a shift in the equilibrium between radical and dormant species. This equilibrium is governed by the ratio of the activation rate to the deactivation rate (k_{act}/k_{deact}) and is skewed towards the dormant species. Consequently, the immediate concentration of radicals is restricted by this phenomenon, leading to a deceleration in the apparent reaction rate. As a result, bimolecular radical termination reactions (involving the formation of P_n-P_n at rate k_t) arehindered, allowing for precise control over the molecular weight (M_W).[12,16,25]

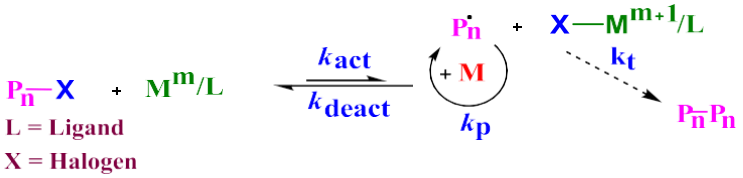

Scheme 2a. ATRP Equilibrium between R-X and metal complex in the lower oxidationstate and alkyl radical and metal complex in the higher oxidation state.

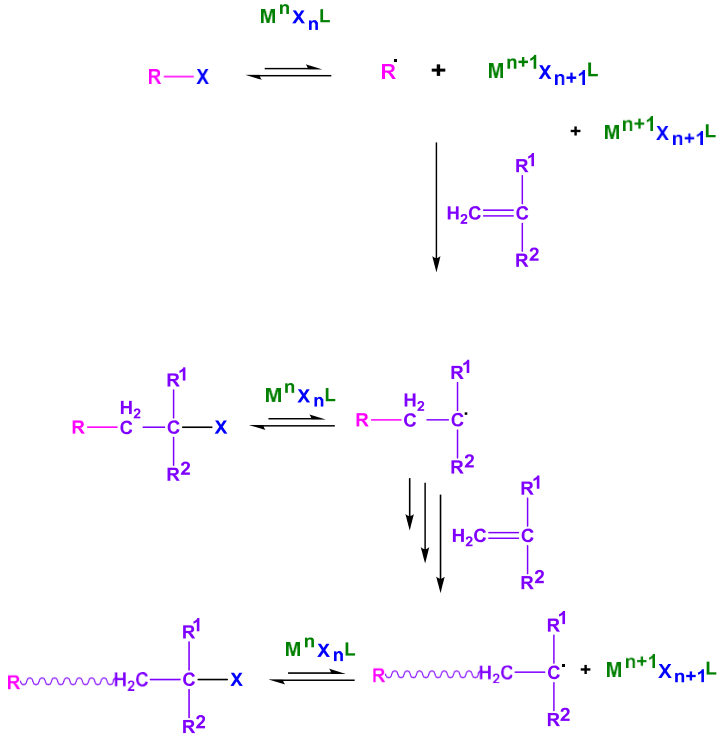

Scheme 2b. ATRP mechanism.

An activator refers to a copper (I) species complexed with two ligands, while a deactivator corresponds to a copper (II) species. In Scheme 3, we can observe the parameters k_a, k_d, k_p, and k_t applied to a bulk styrene polymerization conducted at 110°C. As the polymer chain elongates and the system's viscosity increases, there is a significant reduction in the rate factors associated with termination[26]. In fact, the gradual decrease in kt over time is a characteristic feature of many LRP systems. To gain a comprehensive understanding of the function of various components in ATRP, including monomers, initiators, catalysts, ligands, and solvents, is of utmost importance.

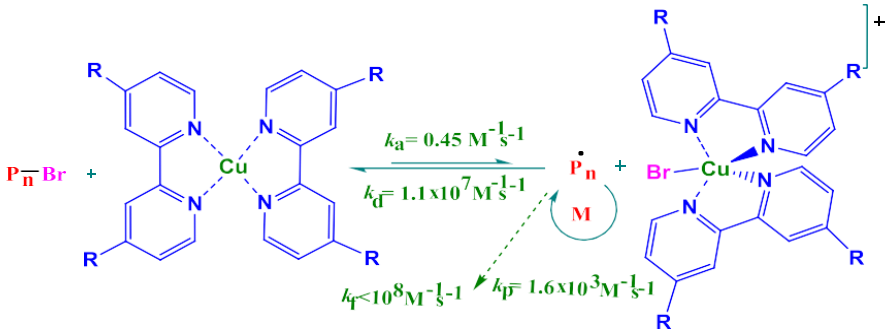

Scheme 3: Values of the rate constant for activation (k_a), deactivation (k_d), propagation (k_p), and termination (k_t) for a bulk styrene polymerization at 110 °C. [84]

2.2. Design of the initiating systems in ATRP - a multicomponent System

Initiating systems for transition-metal catalyzed ATRP consist of a metal complex and an initiator. The catalyst, a metal complex, permits radical species to be produced from the initiator or the terminal of a dormant polymer. It is essential to select the metal complexes and initiators based on the monomer structures to control radical polymerisation. By incorporating additional substances, such as additives or switching solvents, the rate and control of polymerization can also be accelerated. Catalyst, initiator with a movable (pseudo) halogen, and monomer (made of a transition metal species with any appropriate ligand) are the three parts of the ATRP system. An additive is employed on occasion. Elements like solvent and temperature must be considered for a successful ATRP.

2.2.1 Transition metal complexes

Various transition metal complexes have been applied in ATRP experiments with the aim of enhancing radical generation. To achieve this, the metal centre must undergo a single electron transfer process, which involves extracting a halogen or pseudohalogen and expanding its coordination sphere.[27] ATRP serves as a method for producing molecules devoid of halogen or pseudohalogen elements. This is achieved through the reversible generation of propagating radicals from dormant chain ends that were initially terminated by halogens or pseudohalogens in the presence of transition metal complexes. The resulting polymer structure is intricately governed by the thermodynamics and kinetics of this atom transfer process. The formation of these radicals invariably leads to their termination, and the relative rate constants for propagation, deactivation, and activation play a substantial role in determining the fraction of terminated chains. Transition metals employed in ATRP predominantly belong to groups 7 (Re), 8 (Fe, Ru), 9 (Rh), 10 (Ni, Pd), and 11 (Cu) [28]. It's noteworthy that early transition metals may exhibit a strong affinity for H and O atoms, potentially leading to B-hydrogen abstraction and coordinationwith ester groups. To effectively participate in the one-electron oxidation process, the halogen atom transfer must be unidirectional and exclusive to the particular transition metal complex.

The prerequisites for an efficient catalyst are:

- Two readily available oxidation states separated by one electron;
- Reasonable affinity towards a halogen atom;
- Relatively strong complexation with ligands;
- An expandable coordination sphere to accommodate a (pseudo) halogen.

The choice of catalyst and ligand combination plays a pivotal role in establishing an atom transfer equilibrium and regulating the exchange rate between dormant and active species. An effective catalyst needs to satisfy specific criteria, including possessing a metal core with a notable affinity for halogens and a coordinating sphere capable of expanding during oxidation. Concurrently, the ligand should form a robust complex with the catalyst, facilitate the solubilization of the transition metal salt, and modulate the redox potential of the metal

center. In the context of this study, copper (I) bromide was utilized to investigate ATRP reactions involving acrylic and methacrylic monomers.[29]

There are several guidelines for an efficient ATRP catalyst, which are:

- Fast and quantitative initiation ensures that all the polymer chains start to grow simultaneously.
- The balance between the alkyl halide and the transition metal significantly favors the dormant species. This equilibrium position leads to the majority of polymer chains being in a dormant state, resulting in a low radical concentration. Consequently, the impact of radical termination reactions on the overall polymerization process is greatly reduced.
- Fast deactivation of the active radicals by halogen transfer ensures that all polymer chains grow at approximately the same rate, leading to a narrow $Đ_M$.
- Relatively fast activation of the dormant polymer chains provides a reasonable polymerization rate.

2.2.2. Ligand

ATRP ligands are essential in controlled radical polymerization, regulating kinetics, chain length distribution, and end-group functionality. They interact with transition metal catalysts, allowing for tailored conditions and increased versatility for various monomers and applications. The exploration and development of novel ligands contribute to polymer science advancements and innovative materials with tailored properties. The ligand plays a crucial role in ATRP by controlling the complex's solubility in the reaction mixture and maintaining the complex's stability over a wide range of monomers, solvents, and temperatures. In atom transfer rapid proton exchange (ATRP), the ligand's primary role is to ensure that the transition-metal salt is soluble in the organic medium and adjust the metal centre's redox potential for maximum reactivity and kinetics.[30] It can fine-tune selectivity and force the complex to carry out the necessary one-electron transfer operation for ATRP. As the catalyst is immobilized, the ligands can also make the catalyst easier to remove and recycle.

ATRP relies on copper and iron-mediated ligands, with copper and iron being the most effective, while phosphorous, sulfur, and oxygen-based ligands have less success. When the metal centre is subjected to steric hindrance, catalytic activity is diminished, and activity decreases with the number of coordinating sites, $N_4 > N_3 > N_2 >> N_1$, and with the number of linking C atoms, $C_2 > C_3 >> C_4$. The potential for side reactions, such as those between amines and phosphines and alkyl halides, is crucial when choosing the ligand. Most transition metals, including ruthenium, rhodium, rhenium, nickel, iron, and palladium, have been combined with phosphorous ligands in ATRP. Phosphines are phosphorous-based ligands with high catalytic activity and effective polymerization control, while cyclopentadienyl, indenyl, and 4-isopropyl toluene types are also employed. Oxygen ligands based on phenolsand carboxylic acids have also been considered.[22,24]

2.2.3. Initiators

The initiator R-X is often employed in ATRP, and a rapid and quantitative start is recommended. The monomer conversion rate and the monomer concentration ratio at the start of the process determine the Mn of ATRP-prepared polymers:

$$M_n = \frac{[\text{Monomer}]_0}{[\text{Initiator}]_0} \times \text{Monomer Conversion} \times MW_{Monomer +} \; MW_{\text{Initiator}}$$

Were,

M_n = Number average molecular weight,
$[\text{Monomer}]_0$ = Initial concentration of monomer,
$[\text{Initiator}]_0$ = Initial concentration of initiator,
MW = Molecular weight

In ATRP, the R group and halide atom X must be strategically selected depending on the monomer and catalyst/ligand. Initiators may be chosen from various organic halogen-containing molecules, including sulfonyl chlorides, polyhalogenated compounds, R-X with activated substituents on the -carbon, and many more. While R-X (X = Cl, Br) simple initiators are often used in ATRP, polyhalogenated substances are also valid options. Macro-initiators may also be employed, such as polymers that have been ATRP-prepared, polymers that contain halogens, or polymers that have had their terminal halogens functionalized. If the initiation rate is more than or equal to the observed propagation rate, and the initiation is quantitative, then the Mw and M in ATRP may be effectively controlled.

Many factors can influence the initiation rate, including:

- The bond strength of the carbon-halide bond: Alkyl chlorides typically have a higher bond strength than alkyl bromides, which lowers the activation coefficient (k_a) of alkyl chlorides.
- The stability of the generated radicals will often rise with the number of alkyl side groups on the radical core, making them simpler to produce. In that regard, tertiary halides willbe superior to secondary halides, which will be superior to primary halides as initiators.The
- potential creation of anions: when the initiators produce radicals with very low electron counts, outer-sphere electron transfer may occur during activation, creating radical anions susceptible to side reactions.

How many halogen atoms are in the R-X used as initiators doesn't matter. The structure of the initiator and the number of halogen atoms determine whether synthesized polymers have a linear (using R-X with a single halogen atom) or star- or brush-like (many halogen atoms in the initiator) design. Many potential initiator functional groups exist within the R-X.

The following are the primary benefits of synthesizing polymers by ATRP while employing functional initiators:

- Direct functionalization
- No post-polymerization modification is required
- Yields α-telechelic polymers
- Multiple applicable functionalities (more than those attainable via nucleophilic substitution of ω-end halogen atom).

2.2.4. Monomers

ATRP has effectively polymerised different monomers, including acrylamide/methacrylamide monomers. It has proven difficult because polyacrylamides create robust complexes with transition metal ions; the link between the polymer and halide atom is strong, and the halide atom at the polymer chain end is eliminated by nucleophilic attack. However, there have been reports of some success using these monomers. Several acrylamide derivatives, including N-hydroxyethyl acrylamide, N N-dimethyl acrylamide, N-tert-butylacrylamide, and N-(2-hydroxypropyl) methacrylamide, have successfully undergone ATRP.[31] Monomers significantly impact the ATRP reaction, influencing the concentration of propagating radicals and the rate of radical deactivation. Several factors can explain this effect, including:

- Similar to how the solvent affects polymerization, the monomer's solubility parameters and how copper-complex formation is impacted will also have an impact.
- The monomer's kp influences the rate of polymerization. When a monomer with a fast polymerization rate is employed, several monomer additions per activation/deactivation step may occur, leading to a broadening of the DM, particularly at low conversion and low initiator efficiency.
- In polymerization, each monomer employed will produce an alkyl halide with a particular redox potential. As a result, the radical concentration in the system will change due to changes in the (de)activation constant and atom transfer equilibrium constant (K_{eq}).
- Along with halogen atom exchange, some halide-containing polymer end-groups can interact specifically with the copper species involved.

Each monomer in ATRP has its equilibrium constant ($k_{eq} = k_{act}/k_{deact}$) for active and inactive species, even when using identical catalysts and conditions. Multiplying k_p by keq yields the polymerization rate. Therefore, the polymerisation rate will be exceedingly sluggish if k_{eq} is too low. This may be one reason why vinyl acetate, halogenated alkenes, and olefins, less reactive monomers, have not been polymerized thus far. This necessitates picking out the ATRP-optimal catalyst, ligand, solvent, temperature, and additives for each monomer.[22,25]

2.2.4.1. Styrene

Metal complexes of copper, ruthenium, rhodium, iron, and rhenium" catalyze the controlled polymerization of styrene and substituted styrene. It is possible to achieve tightly regulated molecular weights and narrow PDIs in a copper-based system composed of 1-PEBr/CuBr/dHbpy.[32] These compounds, combined with an initiator containing bromide oriodide, can be used to polymerize styrene under well-controlled conditions. Even a chloride initiator can afford narrow polydispersities when linked with the Ru-Cp* ($RuCl(C_5H_5)(PPh_3)_2$) complex in the presence of Al(O-*i*Pr)3 at 80 °C in toluene. To achieve regulated molecular weightwith monomer conversion, a series of substituted styrene were polymerized with the 1- PEBr/CuBr/bpy system in diphenyl ether at 110 °C. By increasing the reactivity of the monomerand breaking the C-X bond in the inactive species, electron-withdrawing substituents acceleratedthe polymerization process. The rhenium complex effectively controls molecular weights and polydispersity indices in synthesized polymers, with M_w/M_n ratios ranging from 1.2 to 1.3, regardless of electron-donating or electron-withdrawing groups in the reaction system.[33,34]. Based on the reaction conditions, the Cu-based catalyst system polymerizes 4-(Chloromethyl) styrene, which features a reactive C-Cl link in the monomer, to create hyperbranched or linear polymer.[35]

2.2.4.2. Methacrylates

ATRP of methacrylates with precisely controlled molecular weights and narrow polydispersities (M_w/M_n = 1.1-1.2) can be prepared, depending on the metal catalysts and initiator system. Methacrylates are highly reactive monomers since the radical stabilization by methyl/ester substituents requires relatively mild metal complexes. However, copper/bpy-based systems need careful consideration of unique factors such as polar solvent usage and halogen exchange reactions.[36] Using sulfonyl chlorides and 2-halonitriles as initiators in ATRP of MMA promotes controlled polymerization due to their high apparent rate constants, improving efficiency. This allows the creation of broad molecular weight ranges (M_n = 1000 to 180 000) with limited polydispersity. Isopropyl methacrylate, n-butyl methacrylate, 2-(dimethylamino) ethyl methacrylate, 2-(hydroxyethyl) methacrylate, silyl-protected HEMA, oligo (ethylene oxide)-substituted methacrylates, etc., all polymerize successfully.[37]

2.2.4.3. Acrylates

Copper-based systems and alternative catalysts like Ru, Fe, Ni, and Re effectively control molecular weights and reduce polydispersities in poly(acrylate)s, enabling polymer chemists to optimize synthesis with desired ATRP properties. CuBr/dHbpy/BPN system afforded controlled molecular weight of poly (MA) with very narrow polydispersities in bulk at 110 °C. The polymerization temperature may be adjusted to generate polymers by changing the catalyst in a suitable amount of time. For instance, at ambient temperature and utilizing a catalyst of 0.05 mol% CuBr/MesTREN, poly (MA) with M, = 12600 and PDI = 1.10 was produced in 1 hour. Well-defined polymers and functional polymers have been synthesized by ATRP of ethyl acrylate, methyl acrylate, isobornyl acrylate, n-butyl acrylate, tert-butyl acrylate, glycidyl acrylate and 2-hydroxyethyl acrylate.[38,39]

2.2.5. Solvents

The rate of the polymerization process and atom transfer equilibrium are both affected by the solvent used, making the choice of solvent very important. It is quite familiar that polar solvents improve the solubility of the catalyst complex.[40] Sometimes, a solvent must be used, especially if the synthesized polymers are insoluble in their monomers. Various solvents, such as water, alcohol, dimethylformamide, ethylene carbonate, benzene, toluene, xylene, diphenyl ether, ethyl acetate, and many more, have been used to work with different monomers. Numerous factors influence the choice of solvent; among them, the fundamental criterion for choosing a solvent is minimal chain transfer. It is also essential to consider the solvent-catalyst-other-parts-of-the-ATRP-system interactions. Proper solvent selection and control are crucial for successful copper-based ATRP, preventing solvent-induced catalyst poisoning (such as carboxylic acid or phosphine poisoning in Cu-based ATRP) and mitigating side reactions (polar solvent in particular) for controlled reaction characteristics.[24]

2.3. Mechanisms

ATRP generates carbon-centered radical species reversibly, enabling controlled polymerization and well-defined structures and properties. A radical scavenger, stereochemical structures, copolymerizations, electron spin resonance, mass spectrometry analyses, and other techniques were used to probe the radical process.[41] Inactive polymer chain terminals, covalent C-H or C-Y bonds, and unsaturated C-C double bonds resulted from the process being quenched by radical scavengers such as TEMPO (Y), 1,1-diphenyl-2-picrylhydrazyl (DPPH), and galvinoxyl. Under the same circumstances, the tacticity of PMMA achieved with different metal-catalyzed ATRP was almost identical to that obtained by conventional radical initiators like AIBN. Advanced mass spectrometry techniques, including MALDI-TOF MS, ESI-MS, and TOF-SSI MS, have been used to study the terminal groups and polymers in metal-catalyzed ATRP.[42] These findings collectively indicate the presence of relatively stable carbon-halogen terminals.

2.3.1. Kinetic studies on ATRP

The design of well-defined macromolecules relies on understanding the size and influence of kinetic factors in CRP. The molecular weight distribution, rate of polymerization, and the distribution of comonomers in a particular polymer segment are all determined by kinetics. Understanding and measuring the kinetic parameters depend on the measurement of these parameters. The metal complex in the higher oxidation state (e.g., $X\text{-}Mt^{m+1}/L_n$) and the creation of propagating radicals (R*) as a result of a reversible (pseudo)halogen transfer between a transition metal complex (Mt^m/L_n) and a quiescent species (R-X) provide the mechanistic foundation for ATRP. A transition metal complex (Mt^m/L_n) at a lower oxidation state serves as the activator in deactivation reactions involving radicals and oxidized metal complexes ($X\text{-}Mt^{n+1}$/Ligand). The activation and deactivation rates for these processes are k_{act} and k_{deact}, respectively. Like in regular radical polymerization, where monomers are added to regularly produced radicals to construct the polymer chain at a pace determined by the propagation rate constant k_p. Also, ATRP has termination reactions (k_t), most often involving radical coupling and disproportionation.

The equation for a given monomer, M, illustrates how the location of the ATRP equilibrium controls the polymerization rate.[22,41,43]

$$\mathbf{R_p = k_p[M][P^*] = k_p[M]k_{ATRP}\frac{[PX][M_t^Z\ L_n]}{[XM_t^{Z+1}L_n]}}$$

The rate constants (k_{act} and k_{deact}) and their ratio K_{ATRP} by a specific catalyst are crucial indicators of the catalyst's activity in polymerization. The ligand L significantly influences these rate constants and overall catalytic performance. In the absence of chain termination and transfer reactions, the polydispersity index of a polymer synthesized via ATRP can be calculated using an equation that describes the relationship between the deactivator (*D*), concentrations of initiator (*RX*) and the propagation (k_p) and deactivation (k_{deact}) rates, and the monomer conversion (*q*), which provides a comprehensive understanding of polymerization kinetics and molecular characteristics control.

$$\mathbf{\frac{M_w}{M_n} = \left[\frac{([RX]0 - [RX]t)k_p}{k_{deact}\ [D]}\right]\left[\frac{2}{q} - 1\right]}$$

A catalyst can achieve polymers with a lower polydispersity index (lower k_p/k_{deact}) by facilitating faster deactivation of growing chains. However, increasing deactivator concentrations leads to slower polymerization rates with decreased polydispersity index. Incorporating Cu^{II} halides (5-10%) into copper-based ATRP feedstock improves initiation step efficiency, resulting in better control and lower polymerization rates. This is because the deactivation rate is increased, improving the efficiency of the initiation step.[44] This optimization enables the synthesis of well-defined polymers with desirable molecular characteristics.

2.4. Precision Polymer Synthesis

Metal-catalyzed ATRP efficiently synthesises controlled polymer architectures like block copolymers, end-functionalized polymers, gradient/statistical copolymers, comb, graft, star, and hyperbranched polymers. This technique allows controlled synthesis from various monomers under mild reaction conditions.

2.4.1. Functionalized Polymers (a- and w-End Functionalized Polymers)

A functionalized organic halide (R-X) initiator is used in ATRP to create polymers having an α -end group. The polymerization process results by attaching functional groups to the α -functional group, the majority of which are hydroxyl-functionalized, carboxyl-functionalized, etc.[24,45] For the polymerization of hydrophilic monomers like OEGMA in aqueous solution, salt-type initiators such $NaCOO(C_6H_4)\ CH_2X$ (X = Br, Cl) are used. Polymers with lengthy hydrophilic segments at one end may be produced using an oligo (ethylene oxide) unit initiator. For the production of polymer brushes, etc., to create thiol-functionalized PMMA, thiols also give excellent binding towards a metal surface, such as gold.

Initiators such as allyl chloride and allylbromide work well with CuX catalysts for polymerizing styrene, whereas allyl compounds with distant halogens are helpful for initiating the polymerization of methacrylates. In reverse ATRP,a functional azo initiator is utilized in the presence of higher oxidation state transition metal catalysts like $FeCl_3/PPh_3$ to enable the synthesis of α-end-functionalized polymers.[46,47] A functionalized quencher terminates ω-end functionality after the ATRP process. The Ru- catalyzed polymerization of MMA can be effectively quenched by using silyl-enol etherscontaining a phenyl group or α-(siloxy)styrenes, leading to the synthesis of α-end functionalizedPMMA with a ketone group. Similarly, the Cu-catalyzed polymerization of MA produces allyl- functionalized polymers when allyl tri-n-butyl stannane is added as a quenching agent. Metal- catalyzed polymerizations can interact with allyl compounds, resulting in the inactivation of the C-X terminal. By quenching the Cu-catalyzed polymerization of MMA and MA with allyl alcohol, a B-bromo alcohol terminal can be created. Sodium azide or trimethylsilyl azide in the presence of tetra butyl ammonium fluoride transformed PSt, PMA, and P*n*BA into an azide group. The reaction between polystyrene with an azide end group and C_{60} was studied after the azide group was transformed into an amino group using PPh_3/H_2O or $LiAlH_4$.

2.5. Controlling parameters in ATRP

2.5.1. Temperature

The rate of an ATRP relies a lot on the reaction temperature. The operating temperature depends primarily on the targeted molecular weight, the catalyst/ligand system, and the monomer used. At elevated temperatures, the reaction rate in ATRP is enhanced due to the increased solubility of the catalyst system. This temperature dependence is attributed to the elevation of both the atom transfer equilibrium constant and the rate constant for radical propagation as the reaction temperature increases. A greater k_p/k_t ratio is achieved at elevated temperatures, allowing for finer regulation of the polymerization process due to the increased activation energy for propagation (k_p) relative to the radical termination (k_t).[48]

2.5.2. Percentage of conversion

The high monomer conversions in ATRP slow down the rate of propagation considerably. Therefore, to retain the living characteristic of the synthesized polymer, the reaction should be stopped before complete conversion. Although no effect on polydispersity may occur, end-group loss may occur under prolonged reaction times for complete monomer conversion. Hence, a 90-95% monomer conversion is optimum for obtaining living polymers with a high degree of chain-end functionality or synthesising block copolymers with specific architectures.[49,50]

2.5.3. Concentration of the initiator

The initiator concentration influences molecular weight and polymerization, affecting the number of active chains formed. The chosen initiator's efficiency is also crucial. Rapid initiation with minimal chain transfer and termination reactions results in a consistent number of growing

polymer chains directly proportional to the initial initiator concentration. The Molecular weight and degree of polymerization decrease with an increase in the initial concentration of initiator $[I]_o$in a general ATRP process.[51] The initiator concentration and initial monomer concentration $[M]_o$is related to the degree of polymerization.

2.5.4. Additives

The reversible activation-deactivation reactions in ATRP maintain a low but constant concentration of active radial species and reduce the termination reactions by radical combination and disproportionation. Yet, industrial applications may need to be improved due to the slower polymerization rate of ATRP as compared to traditional radical polymerization techniques. So, additives play a crucial role in increasing the ATRP rate while keeping the inherent living characteristics intact. Sometimes, additives also help in starting an ATRP reaction. Adding highly polar solvents such as water in small amounts can accelerate the ATRP rate, while adding strong nucleophiles like phosphines terminates the polymerization process.[52]

2.6. Advantages of ATRP

ATRP offers advantages over conventional radical-based polymerization techniques, enabling complex polymer synthesis with diverse topologies, controlled molecular weight, and temperature control. This living system can be controlled, making it a valuable tool for various applications.[53] Thus, ATRP is a robust method for developing polymers with diverse architectures and controlled chemical composition. It allows uniform growth of polymer chains in various media, including solution, microemulsion, miniemulsion, dispersion, suspension, emulsion, and bulk.[54]

2.7. Synthesis of functional polymers by ATRP

The most essential characteristic of ATRP is its ability to synthesize functional polymers. The presence of functionalities enhances the efficacy of polymers and is necessary for the progress of various features of structure-property relationships. Three distinct synthetic approaches were devised, each incorporating site-specific functional groups to enable the controlled synthesis of well-defined polymers through ATRP as follows: [25,55]

- By utilizing functional ATRP initiators
- By direct polymerization of functional monomers and
- By end-group transformation chemistry.

Besides, the post-polymerization modification of polymer chains based on the first two approaches can also be carried out. The first two methods yield polymers with chain end-functionality, while the last method yields polymers with multiple functionalities throughout the backbone.

2.8. Synthesis of polymers with controlled macromolecular architecture by ATRP

Polymers with varying macromolecular architectures have been successfully developed using ATRP. Topologically well-controlled polymers include those with cyclic structures, grafted from multifunctional backbones, grafted into functional backbones, copolymers formed using di/multifunctional initiators, and linear chains of controlled dimensions and polydispersity. Segmented copolymers, such as block and graft systems, periodic and gradient copolymers, and others, were designed using ATRP to regulate chain composition precisely. In addition to being functionally tolerant, ATRP can be end-functionalized with good results after polymerization.[20]

2.9. Block Copolymers

ATRP can create di, tri, or multi-block copolymers when the polymer chain end consists of an activated halide. Block copolymers can be prepared by synthesizing macroinitiators through ATRP or alternative methods. The growth of blocks can be accomplished either by employing a single macroinitiator or by introducing a second monomer in a nearly complete reaction.

2.9.1. Block Copolymers Synthesized by ATRP

ATRP is a versatile method for synthesizing block copolymers from monomers like styrenes and (meth)acrylates. It employs sequential monomer addition and initiator from isolated macroinitiator, focusing on alkyl or related methacrylates. The ATRP method, catalyzed by Ru, Cu, and Ni, ensures the successful preparation of these copolymers. Narrow polydispersity block copolymers, such as AB5889 and ABA, are prepared by performing a successive polymerization of MMA and nBMA under ruthenium catalysis. Using macroinitiator techniques and mostly copper catalysts, methyl acrylate diblock copolymers of tert-butyl acrylate and isobornyl acrylate have been synthesized.[56] Ni, Cu, and Fe catalysts were used to create a diblock copolymer (AB or BA) comprising MMA (A) and MA (B).

Since poly(methacrylate)s have more active C-X terminals than poly(acrylates), block copolymerization from PMMA may be carried out using a sequential or macroinitiator approach with significant results. Slightly more polydisperse (M_w/M_n, = 1.4-1.5) MMA/styrene block copolymers were synthesised using Cu and Fe catalysts.[57] The macroinitiator was produced using a copper-based method, yielding diblock copolymers of the acrylate/styrene AB and BA types. The block copolymers may have acrylamide and vinylpyridine segments added to them.[58] Copper-catalyzed sequential copolymerization of 2-[(trimethylsilyl)oxy] ethyl acrylate and n-butyl acrylate yielded amphiphilic forms by hydrolyzing the silyl group.[59] Amphiphilic block copolymers containing hydroxy groups originated from iron- and copper-catalyzed styrene/p-acetoxystyrene block copolymers. AB or ABA types, with a pendant amino group, are formed when (meth)acrylates are copolymerized with 2-(dimethylamino)ethyl methacrylate using a copper catalyst.[60]

2.9.2. Block Copolymers via Combination of Other Polymerizations

Block copolymers can be made by combining ATRP with other polymerization techniques such as anionic, cationic, conventional radical, ionic ring-opening, and ring-opening metathesis polymerization. Carbon-halogen terminals can be introduced through chemical modification of the polymer terminal or by initiating the polymerization process using halogenated initiators.[61] Without any modifications, ATRP may be initiated by carbon-X bonds produced by cationic polymerization in biological systems. Polystyrene with a C-Cl terminal can be obtained through living cationic polymerization using R-Cl/Lewis's acid. This C-Cl terminal can then serve as a starting point to synthesize block copolymers with ATRP acrylates and methacrylates. Esterification using 2-bromopropionyl and 2-bromoisobutryl halides is another strategy, which involves converting the chlorine terminal into hydroxyl functionalities. Carbanionic terminals obtained from living anionic polymerization can be transformed into C-X bonds using ATRP.[62] These methods can often be implemented using polystyrene polymers. Through a series of reactions with styrene oxide and 2-bromoisobuty bromide, the polystyrene terminal was converted into polyisoprene and bromide.[20] Copper catalysts facilitate asymmetric thermo-reversible polymerization (ATRP) for (meth)acrylates and styrene, forming controlled molecular weight block copolymers with well-defined compositions and narrow polydispersity indexes (M_w/M_n = 1.1-1.2). This efficient process ensures well-defined block copolymers with narrow polydispersity indexes. The block copolymer's intermediate segment, which contains the fluorescent dye, may be transformed to add functional groups at the junction of the polyisoprene and polystyrene segments.[63]

Various block copolymers can be produced by converting cationic ring-opening polymerization of THF into copper-catalyzed radical polymerization of acrylates, methacrylates, and styrene. Nickel-catalyzed ATRP can also be combined with living ring-opening polymerization of e-caprolactone using aluminium alkoxide or alkyl aluminium to synthesize linear or dendrimer-like star block copolymers.[64] these block copolymers were initially synthesized using ATRP with CBr_3CH_2OH, utilizing the C-Br bond as a radical initiating site and the hydroxyl group for subsequent ROP. By hydrosilylation of 3-butenyl-2-bromoisobutyrate, the silane terminal of PDMS or block copolymers of styrene and DMS can be converted into the C-Br terminal, facilitating the inclusion of poly(dimethylsiloxane) segments into the block copolymers.[65]

Block copolymers with the second block formed by ATRP have shown effective incorporation of monomers without radical stabilizing substituents such as vinylidene chloride, vinyl acetate, ethylene, etc.[66] Initiating the ATRP of nBA at 30 °C in the presence of CuBr/Me_6TREN complex, the azo compounds with activated halogen atoms play a key role without destroying the diazene. To create a block copolymer (M_n = 41 800; PDI = 3.56), the resultant P*n*BA (M_n = 7500; PDI = 1.15) containing the central azo unit was dissolved in VOAc.[67] Polymerization of VOAc was also initiated at 90 °C using 2,2'-azobis [2-methyl-N-(2-(4-chloromethylbenzoyloxy) ethyl) propionamide]. To get PVOAc-b-PS (M, = 91 600; PDI = 1.8), a Cl-terminal group on PVOAc (M, = 47 900; PDI =2.21) was employed as a macroinitiator in the ATRP of styrene.[24]

2.10. Random Copolymers

The ease with which various monomer pairings can be copolymerized to true random/statistical copolymers makes radical polymerization stand out as a significant benefit.[60] ATRP has copolymerized methacrylates, acrylates, and styrenes randomly or statistically using controlled molecular weights and narrow polydispersities.[25] The monomer reactivity ratios and sequences closely resemble traditional free radical polymerization. Besides, emulsion polymerization produced random copolymers of nBMA and MMA. Two monomers were nearly simultaneously consumed during the polymerization process to achieve a random or statistical distribution of repeat units along the polymer chains. The inclusion of functional groups to the polymer chains of styrene-based random copolymers can be made possible by copolymerizing with functional styrene derivatives. Styrene and p-acetoxy styrene copolymerization resulted in random copolymerization, hydrolyzed to produce styrene/p-vinyl phenol copolymers.[68] The randomly distributed benzyl ether groups and benzyl acetate were converted into benzyl bromide, in the presence of copper catalysts, and then used to start the controlled radical polymerization of styrene to produce graft copolymers. Ruthenium and copper catalysts can be used to create methyl methacrylate copolymers with acrylamide and maleimide. Both copolymers' PMMA chains contain amide groups dispersed at random.[69]

2.11. Segmented block copolymers

Figure 1 shows segmented block copolymers are multi-block copolymers in which rigid, crystallizable blocks are alternated with more pliable, soft blocks. The soft, amorphous phase created by the continuous segments makes the material elastic at low temperatures.[70] The stiff segments are physical crosslinks providing solvent resistance and material dimensional stability. The rigid segments are typically rapid crystallizing segments, like esters or amide groups, and the ability of urea and urethane groups to hydrogen self-associate is well documented.[71]

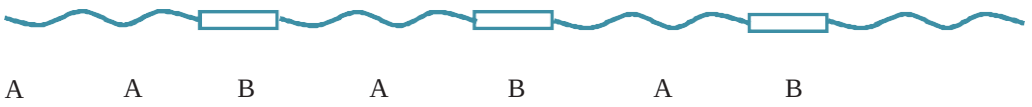

Figure 1. Segmented block copolymer representation: (A) flexible segment, (B) rigid segment.

The shape and morphology of segmented block copolymers are determined by phase separation between flexible and rigid segments, resulting from liquid-liquid demixing or crystallization processes. TPEs with crystallization-induced phase separation have a soft phase and dispersed crystalline lamellae in their morphology[72] (**Figure 2**). Cella's theory (phase B) suggests lamellae of segmented block copolymers undergo perpendicular crystallization of stiff segments. A few crystalline stiff segments will combine with amorphous segments (A). Soft phase glass transition temperature increases due to incomplete phase separation in TPE-Es.[73]

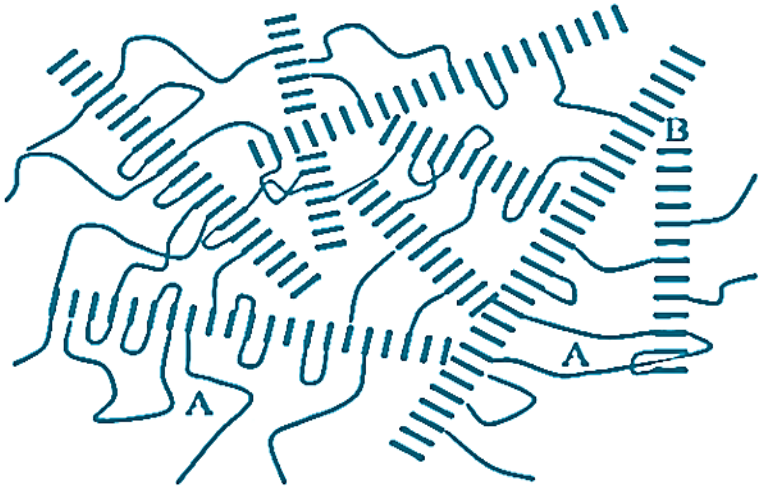

Figure 2. The schematic diagram depicts Cella's[73] two-phase morphology of segmented copolymers with rigid segments, with (A) amorphous phase and (B) crystalline lamellae.

During liquid-liquid demixing in polyurethanes, the phase separation results from thermodynamic incompatibility between the segments. In this process, the flexible and rigid urea/urethane segments undergo phase separation, followed by partial crystallization of the rigid segments. The resulting morphology comprises crystalline rigid segments within the polyether phase, non-crystallized stiff segments distributed in the soft phase, and a complex liquid-liquid demixed hard phase containing both partially and non-crystallized segments.

2.11.1. Uniform Rigid Segment

The distribution of rigid segment lengths notably impacts the characteristics of segmented block copolymers. Commercially available segmented block copolymers often exhibit random distributions of rigid segment lengths. However, incorporating uniform rigid segments can enhance segmented block copolymers' properties. For example, polyurethanes with uniform rigid segments exhibit higher degrees of crystallinity and narrower glass transition ranges than those with random rigid segments. This is attributed to the increased phase separation between the flexible and rigid segments in the presence of uniform rigid segments.[74] Besides, polyether (ester amide) s (PEEA) characteristics with regular rigid amide segments were carefully examined.[75] The practically full crystallization of the hard, homogeneous amide segments. PEEAs with uniform rigid segments are transparent and have a relatively high and sharp melting temperature, a low Tg, high crystallinity, and a rubbery plateau independent of temperature. Block copolymers with rigid segments of the same size typically show a two-phase morphology with essentially no rigid segments dissolving in the soft phase.

2.11.2. Soft segment

The extended flexible soft segment significantly impacts mechanical properties, solvent resistance, weather resistance, and low-temperature characteristics. The composition and molecular weight of soft segments also impact the shape of polyurethanes. Soft segments with average molecular weights of 2000–2500 are usually used to produce thermoplastic elastomers.[76]

2.12. Polystyrene (PS)

Polystyrene (PS) is a readily available and well-known high-molecular-weight linear polymer with diverse applications. Asbestos polystyrene (aPS), the most common commercial PS, is an important thermoplastic material because of its ease of moulding, exceptional dimensional stability, well-balanced physical characteristics and transparency.[77] PS is a glassy polymer at room temperature and a viscous liquid above the glass-transition temperature (*T*g), thanks to the stiffening action of the pendant phenyl groups on the polymer chain.[78] Physical principles dictate that the PS's weight-average molecular weight should be around ten times greater than its chain entanglement molecular weight (*M*) for maximum strength. Since PS with a molecular weight (*M*w) below 150,000 is too brittle to be of any practical use, PS grades marketed commercially for general-purpose moulding and extrusion have an *M*w > 180,000 g/mol.[79] The melt viscosity rises as a consequence. The physical characteristics of PS are described in detail elsewhere. **Table 1** presents the impact of molecular weight on the melting point of polystyrene. It was concluded that the Tg values depend upon the molecular weight.[80–82]

Table 1. The effect of molecular weight on the Tg of polystyrene.

Sample	Mw		Tg (C)	
		Tig*1	Tmg*2	Teg*3
PS 1	1940	56.8	60.4	64.2
PS 2	4380	76.2	79.9	83.7
PS 3	5480	77.0	82.4	87.8
PS 4	12600	89.6	93.4	96.7
PS 5	35100	100.2	103.1	105.9
PS 6	65000	1006	104.0	107.3
PS7	275000	103.5	106.4	109.4
PS8	950000	103.9	106.7	109.7

**1 Onset temperature of Tg transition, *2 Mid-Point Temperature of Tg, *3 End temperature of Tg transition.*

The important characteristics of the polystyrenes are listed below:

- Polystyrene (PS) is being used as crystal clear, stiff, but brittle homopolymer 'general purpose polystyrene' (GPPS) or as impact modified, stiff but opaque 'high impact polystyrene' (HIPS).
- Expandable polystyrene (EPS): It is a foam based on GPPS beads containing pentane, which are expanded under heat. EPS is lightweight, strong, and offers excellent thermal insulation, making it ideal for packaging and construction.
- Styrene-acrylonitrile copolymer (SAN): It is a transparent, stiff, and thermoplastic polymer material based on styrene and acrylonitrile with enhanced stress cracking resistance.
- Styrene–methyl methacrylate copolymer (SMMA): It is a transparent and brittle polymer with enhanced scratch resistance compared to polystyrene (GPPS). It is often used in blends with styrene-butadiene copolymers (SBC) for clear and tough goods, which need enhanced scratch resistance.
- Acrylonitrile-butadiene-styrene copolymer (ABS): is an opaque, ductile, and stiff thermoplastic polymer with a broad processing window, which is strong and durable even at low temperatures, with good resistance to heat and chemicals.
- Methyl methacrylate-acrylonitrile-butadiene-styrene copolymers(MABS): are transparent, ABS-like materials with improved resistance against fats and oils compared to acrylonitrile-free styrene polymers.
- Acrylonitrile-styrene-acrylate copolymer (ASA): is a product similar to ABS. It is widely used for automotive exterior parts (mirror housings, grilles, and so on) and other outdoor applications in sports/leisure and durable electrical and electronics (E&E) housings.
- Blends: polystyrene blends homogeneously with polyphenylene (PPE) ether to yield high-temperature resistant, stiff, and tough materials (polyphenylene ether (PPE/HIPS). ABS and ASA blend well with polycarbonate (PC) and PA to yield PC/ABS, PC/ASA, PA/AB, S, and PA/ASA blends, combining the excellent thermal properties of the engineering thermoplastics PC and PA with those of ABS and ASA.
- Unsaturated polyester resins: these are durable, resinous polymers derived from styrene and used mainly in the construction, boat building, automotive and electrical industries.
- Styrene-butadiene copolymers (SBC) are transparent, stiff, and tough polystyrenes manufactured by a specific anionic process. SBCs are widely used in food packaging (beakers, multi-layer co-extruded and thermoformed 'modified atmosphere packaging' or shrink sleeves). They are different from styrene-butadiene rubber (SB) made by similar technologies, which have rubber-like properties. They also need to be differentiated from (crosslinked) styrene-butadiene latexes, which are used, for example, as paper sizing dispersions.
- Syndiotactic polystyrene is produced by a specific catalytic-polymerization process to yield a semi-crystalline, high temperature- resistant material.
- Other copolymers: styrene-maleic anhydride (SMA) copolymers, as well as styrene/*N*-phenyl maleimide copolymers, display high heat resistance and are often used as blend components in high-heat ABS and high-heat ASA.

Styrenic polymers offer various benefits in industries, including:

- Lightweight, water resistant, and excellent thermal insulation. Rigid, with a high strength-to-weight ratio that offers energy-saving benefits in transportation and excellent cost performance.
- Can be shatterproof and transparent if required.
- Good electrical insulation.
- Easy to process and produce in a range of attractive colors.
- Easy to recycle.

Styrene-based resins are used in applications such as toys, household appliances, consumer electronics, automobile parts, durable, lightweight packaging and insulation. They combine cost-effectiveness, outstanding performance, and simple processing, making them ideal for cutting-edge packaging, luxury home appliances, and electrical equipment.

2.13. Thermoplastic Elastomers

Thermoplastic elastomers (TPEs) are materials that can be processed through melting and exhibit elastomeric properties at ambient temperature. TPEs have features similar to rubber, such as softness, flexibility, and elasticity, but are melt processable due to their thermally reversible physical crosslinks. As the physical crosslinks are thermally reversible, TPEs can be melt-processed repeatedly.[83] The TPE industry is a developing sector of the polymer market, with a $10 billion revenue and 2.15 million metric tons expected to be consumed globally. Due to new applications and replacing traditional rubbers, the market is expected to increase by 7% annually. The industrialized nations of the US, Western Europe, and Japan dominate the market, but developing countries, especially those in Asia, are quickly growing their positions.[84]

The development of thermoplastic elastomers may be traced back to the discovery of plasticized poly(vinyl chloride) (PVC) in 1926.[85] In 1937, Otto Bayer's German company I.G.Farben Industrie developed polyurethane fibres that could compete with nylon by the reaction between isocyanates and alcohols.[86] Styrene tri-block copolymers (SBC) were first developed in the 1950s thanks to the advent of anionic polymerization and were first sold commercially by Shell Chemical Company in 1965. Polyether ester elastomers (TPE-E) first appeared on the market year 1970. In 1980, polyamide-based thermoplastic elastomers entered mass production. Styrenic tri-block copolymers (SBCs), thermoplastic elastomer blends (TPOs), and thermoplastic vulcanisates (TPVs) are the three primary categories into which TPEs fall. The market for TPEs was reported to grow at a CAGR of 6.3% in 2011, when it reached 3.7 million metric tonnes.[84,87] TPEs have various applications, including automotive, soft-touch materials, footwear, mattresses, and cushions. Multiple classes of TPEs, along with the application and advances in thermoplastic elastomers, macromolecular architectures and supramolecular chemistry, are shown in **Figure 3**.

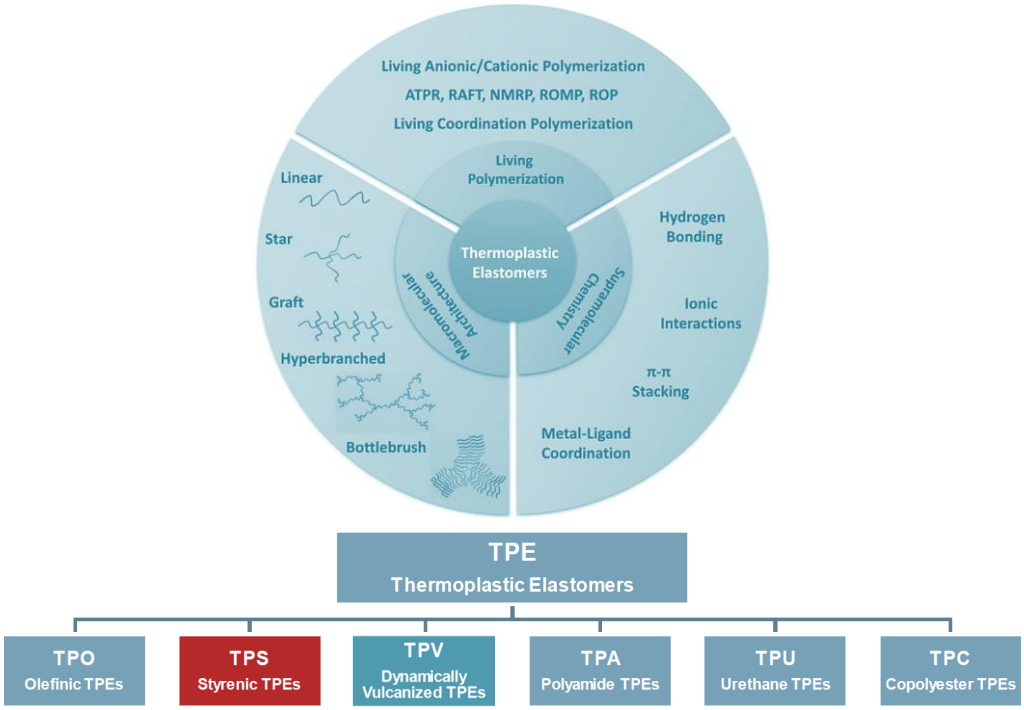

Figure 3. Application and advances in thermoplastic elastomers: macromolecular architectures and supramolecular chemistry.[88]

2.14. Application of polymers synthesized by ATRP

The use of polymers produced by ATRP is getting more attention and developing continuously as research progresses.[89,90] These polymers have shear stability, better thickening behaviour and temperature-independent viscosity, making them useful in various applications such as sealants, lubricants, and oil additives. Some current and forthcoming applications of polymers produced by ATRP are as follows:

- Telechelic, gradient, and block copolymers, comb polymers, and pigment stabilizers can be used as wetting agents, pigment dispersants, and surfactants. ATRP can be used to minimize the potential loss of transparency due to scattering from embedded particles.

- Chain end-functionalized polymers are highly applicable for blend compatibilization and thermosetting compositions, providing conductivity, surface hydrophilicity, andantibacterial properties.

- Star polymers prepared by ATRP are useful as viscosity index modifiers in the oil industry due to their smaller hydrodynamic radii and gyration, making them suitable for fluids that require low viscosity.

- Miktoam star-shaped polymers are thermoplastic elastomers and effective photoresist materials due to their lower chain entanglements and improved properties. They can decrease the unevenness of photoresist side walls by keeping the sensitivity or resolution intact.

- Star-shaped polymers are used as potential drug delivery agents. Core-shell-corona micellar structures can form hetero-armed star polymers that can uptake and release small molecules under different biological conditions. These molecules are attached to the arms of the star polymers and form the interior of the micellar structure during transport. They are also used to immobilise enzymes due to their increased functional groups in a small volume.

- Hydrogels for biomaterial applications can be developed from telechelic and semi-telechelic star-shaped polymers due to their lower gelation concentration and photo-cross-linkable functional groups. These gels can remove cholesterol from the blood and deliver drugs to specific areas in the body.

- Bottle-brush macromolecules have a long backbone and densely grafted side chains, making them super soft elastomers with low modulus and high mobility.

- ATRP can control the thickness of a tethered polymer brush by varying the grafting density. The surface properties of the brushes can be tailored by modifying the surfaces with thin polymer films and tethering block copolymers. The size and composition of each polymer segment affect the morphology and behaviour of the polymer brushes.

3. BIOMONOMERS: A NOVEL SUBSTITUTE FOR EXHAUSTIVE NATURAL RESOURCES

Renewable resources are increasingly important as an alternative to fossil-based energy sources, providing potential energy sources. The recent needs for high-speed aviation, radio engineering, rocket technology, extreme conditions in space, magnetic belts, and radiation fluxes demand new and heat-resistant materials. Polymer technology is now in search of novel materials which can withstand prolonged exposure to high temperatures. Biomonomers, derived from renewable sources, offer a sustainable alternative to traditional petroleum-based polymers, reducing environmental impact and creating a variety of polymers. Biomonomers promote circular economy principles by developing biodegradable and compostable materials, reducing waste accumulation, and promoting sustainable resource management.[91,92] It is a great challenge to find an alternative means of exhaustive resources. Petroleum stocks face exhaustion, leading to a focus on renewable resources. Laboratory explores preparing novel polymeric raw materials from forest products for environmental sustainability. Among various oil-bearing plants such as cashew, linseed, tung, vernonia, and castor, cashew nut shell liquid (CNSL) is utilized to obtain a phenolic monomer known as Cardanol through the distillation of the raw oil.[93] Phenolic monomers undergo chemical modifications to synthesize bio monomers like cardanyl acrylate and cardanyl methacrylate, potentially as a substitute for exhausted natural resources.[94]

3.1. Cashewnut shell liquid (CNSL)

Cashew nut shell liquid (CNSL) is a byproduct derived from the cashew processing industry, found in the soft honeycomb structure between the outer shell and the kernel of cashew nuts. These cashew trees (*Anacardium Occidentalelinn*) thrive in tropical regions and produce a dark reddish-brown multipurpose oil known as CNSO. The resin obtained from plants is used in a wide range of products. Petrochemical feedstock supplies have been strained due to a growing global population and a rising quality of life, and the world's supply of petroleum is rapidly depleting. Alternative fuels and petrochemical feedstock must be found to preserve the living standard and the continuation of the industrial sector. Cashew nut shells embody a chemical that may be used as a raw material for petrochemicals.[95]

The Anacardiales family comprises drought-resistant tree crops typically found within the geographical range between 23°N and 23°S of the equator. It is over 12 meters tall, has a diameter of 25 meters, and can thrive in various soils and moisture levels. In Nigeria, it is a vital tree crop with year-round, evergreen leaves. The cashew tree comprises cashew nuts, apples, leaves, and bark. Its edible seed has a honeycomb-like shell structure with an outer, inner, and kernel. The honeycomb matrix contains CNSL, a dark brown liquid.[96] Nigeria and other tropical nations rely heavily on the cashew plant for its lucrative goods, including food, pharmaceutical, chemical, and allied industries. It is also an aesthetic plant that prevents soil erosion, making it an ideal shade tree.[97]

The typical fruiting period of the cashew tree is around three to four years after planting, and the tree can continue to bear fruits for over 40 years. Unlike other tree nuts, the cashew nut is not found within the fruit, making the cashew fruit distinctive. The cashew apple is a pseudo-fruit, approximately 10 cm long, with a stem connecting it to the externally borne nut. It exhibits a range of colours from yellow to red and is abundant in vitamins A and C while also being fibrous and juicy. The cashew nut shell (CNS) is leathery and contains a blistering oily liquid in its raw state known as CNSL. The testa, a thin layer of skin covering the kernel, acts as a barrier between the shell and the kernel. Cold pressing or solvent extraction of Cashew Nut shells yields the raw Cashew Nut Shell Liquid (CNSL). Anacardic acid makes up 70%, cardol is 18%, and cardanol is 5% of the total, with the rest being various phenols and less polar compounds. Monohydroxy phenols are Anacardic acid and Cardanol. There are two dihydroxy phenols: cardol and cardanol (Detailed in **Figure 6**).[98]

3.1.1. Extraction of cashew oil

The cashew fruit has a nut. The fruit's nutlike receptacle is linked to its very end. The nut's pericarp comprises the epicarp, the mesocarp, and the endocarp. Cashew nut shell liquid is contained in a honeycomb-like network of shells in the mesocarp. Different processes are followed for the extraction of CNSL.

***Cold-Pressed Method*:** In the cold-pressed method, nuts are opened mechanically, and expellers extract CNSL. Solvent extraction and microwave heating are used to obtain CNSL.[99]

***Hot Oil Bath Method*:** In this method, the cashew nuts are first dipped in a bath of hot water at 25°C to achieve a moisture equilibrium between the shell and the kernel; the surface moisture is then removed by streaming the nuts, and the pores of the shells are opened. When most of the oil has been issued out of the shells, the cashew nuts have been properly conditioned. They are ready to be fed into a hopper and onwards via a feeder pipe by an electromagnetically vibrated feeder plate into the vat holding cashew nut shell liquid. After being drained from the water, the nuts pass through a vibrating screen and are centrifuged to remove any remaining oil. A steady oil bath volume is maintained by draining any excess via an overflow pipe.[95]

***Roasting Process*:** According to the method outlined by Hughes, nuts experience a rapid change in temperature and reach the point when charging is necessary. An explosive picture forms inside the cellular structure, pushing the liquid out of the shell. According to an Italian patent, the oil is extracted by first scraping the shells at 100°C–300°C with steel wool and sand in a revolving equipment and then roasting them at 400°C–700°C in an inert atmosphere.[100]

***Refining*:** Minerals, sulfides, nitrogenous compounds, and other contaminants can be found in cashew nut shell liquid. So, it requires refining. Numerous acid treatment techniques have been proposed to obtain better-quality CNSL. These techniques involve treating the raw CNSL with an aqueous solution of acids like hydrochloric, sulfuric, phosphoric, or sulfates such as sodium hydrogen sulfate. Under reduced pressure, the CNSL is distilled after being purified. A decolourized variant of CNSL is produced by allowing steam to flow through sulfuric acid-treated CNSL and then distilling it.[99] **Figure 4** shows the photographs of cashew processing technology in Vietnam.

Figure 4. Cashew processing technology in Vietnam.
https://www.mktech.vn/cnsl-processing-technology/

Cashew processing technology in Vietnam is increasingly developed because Vietnam has strengths in natural conditions for raw material production. Cashew processing technology has helped Vietnam become the world's No. 1 cashew exporter.[101]

3.2. Composition of CNSL

Anacardic acid, a hydroxybenzoic acid with an unsaturated side chain, makes up 90% of solvent-extracted CNSL. Upon heating, it undergoes decarboxylation to produce cardanol or 3-pentadecadienyl phenol, while the remaining portion is identified as 3-penta decadienyl resorcinol, commonly known as Cardol.[102] Although numerous R- groups can exist, all have m-substitution and consist of a 15-carbon alkyl chain. It has been determined that monoene (38.7%), diene (16.3%), and triene (45%) make up the majority of the anacardic acid from CNSL's unsaturated components. Anacardic acid will be decarboxylated upon heating, resulting in cardanol, a phenolic monomer. This natural-source monomer is known as a bio monomer and can be changed into various vinyl monomers to create a wide range of homopolymers, copolymers, resins, and IPNs.[103]

3.3. Availability of CNSL

About 15,000 MT of CNSL is produced in India, whereas the potential availability could be around 40,000 MT.[104] There is a great demand for the export of CNSL. But the export market is ever fluctuating and dwindling. The internal utilization of CNSL is restricted to only a few thousand metric tonnes since new avenues are not opening up. Thus, there is a great scope for fruitfully evolving newer methods and techniques to use this national resource.[105] The success in synthesizing high-temperature resistant plastics (ablative polymer) from CNSL and thermoplastic elastomers will open up a new era with tremendous market potential.

3.4. Application of CNSL

Cardanol, the main constituent of CNSL, which is separated after the vacuum distillation, is a substituted phenolic compound. It can be converted into different varieties of polymeric products which have a lot of industrial applications in the field of friction-resistant components, surface coating, rubber compounding ingredients, laminates, moulding materials, ion exchange membranes, lacquers, binder resins, paints, primers, varnishes, and adhesives. The ongoing saga of explosive high-tech advances ranging from electronics, computers, aerospace, bio-materials, and advanced composite materials takes the helping hand of polymeric products derived from CNSL.[104] CNSL is a primary raw material in various industrially imported chemicals and intermediates, including bactericides, fungicides, insecticides, and dyestuffs. It has been found to enhance processibility and hydrocarbon solubility in plastic moulding. CNSL-condensed with HCHO is used as a powder for plastic moulding, and its polyester alkyl resins are effective coatings and adhesives. Some resins are helpful as ion exchangers, dyes, pigments, and surface active agents.[106,107] It is possible to synthesize the metal salts of CNSL by sulfonating the CNSL derivatives. Hydrogenated cardanol may be directly nitrated to produce valuable nitro derivatives. The halogenation of CNSL is rather simple.[104] Chlorine gas in kerosene undergoes CNSL for 15% chlorination, achieving weight-for-weight conversion.[108] Cardanyl esters are produced by reacting cardanol with acid chlorides, using catalysts like epichlorohydrin and caustic soda. They can also etherify and polymerize CNSL into resin products, offering high hydrophobicity for various applications. Alkyl groups provide a desirable attribute for various applications.[109]

4. CARDANOL

It is a naturally occurring phenol produced by CNSL. Monohydroxy Phenol at the meta position has a lengthy hydrocarbon chain ($C_{15}H_{27}$). Distillation of technical CNSL at lower pressure yields cardanol.[110] More than seventy-two percent of Cardanol's composition is made up of cardol, eight percent polymeric material, less than one percent of 2-methyl cardanol, 2.3 percent of heptadecyl homolog triene, and the rest of the homologous phenols. Cardanol is made up of 90% cardanol and 10% cardol. The degree of side chain unsaturation varies across commercial Cardanol components; however, the following formula may be used to express it practically.[111] The unsaturated double bonds on the side chain in cardanol facilitate cross-linking and offer paints created from it with good progressive drying and baking qualities. Cardanol varnishes offer high electrical insulation, improved resistance to chemicals and water, and superior flexibility because of their unique structural design. Due to the extended hydrocarbon side chain, the solubility of cardanol aldehyde condensate increased in aliphatic hydrocarbons and drying oils like Linseed DCO or Tung Oil.[94] A significant benefit of Cardanol is that it may be chemically modified to achieve desired structural modifications to create tailor-made polymers with desirable qualities. Consequently, hydroxyl groups, aromatic rings, and side chains might all undergo structural modifications. Its unusual molecular structure facilitates polymerization cross-linking thanks partly to an unsaturated long hydrocarbon side chain. While the side chain influences the polymer's hydrophobic character, the coating provides water and weather resistance as an additional benefit.[112] Cardanol is a versatile coating material used in various industries, including epoxy curing agents, laminates, paints, varnishes, insecticides, mineral oils, rubber, brake linings, adhesives, electrical isolation putty, and ink printing. Its high electrical insulating qualities and thermal stability make it an excellent alternative to petroleum-based phenols. Cardanol is also used in polyurethane-based polymers, surfactants, epoxy resins, foundry chemicals, friction linings, laminating resins, paints, and varnishes.[112] Cardanol's amphiphilic properties enable responsive surfaces in smart coatings and sensor technologies. **Figure 5** shows the various stages of scraper wiped type industrial agitated thin film evaporator for the cardanol process line.

Figure 5. Cashew phenol cardanol process line.

Source:https://www.alibaba.com/product-detail/Scraper-wiped-type-industrial-agitated-hin_1600072397412.html

4.1. Properties and Reactivity of Cardanol

Cardanol has characteristic properties like low cost, renewable, versatility in polymerization, chemical modification, eco-friendly and can be easily functionalized through diverse chemical reactions. It has advantages over other phenolic resins like impact resistance, flexibility, faster heat dissipation, etc. Cardanol is used to develop automobile brake linings.[113] Conventional synthesis of cardanol is very difficult since the aliphatic side chain present in the meta position of the phenol group, leads to any subsequent substitution to ortho or para locations. The hydroxyl group, aromatic ring, and the side chain of cardanol may all be modified chemically to get desired characteristics needed to create high-value polymers tailored to the customer's specifications. Anacardic acid decarboxylates to cardanol when heated during extraction or refining operations.[114] Decarboxylation occurs when the crude CNSL is distilled due to its high cardanol content. Hydrogen with catalysts like copper, nickel, palladium, or platinum is often used in hydrogenation. Crude CNSL is separated by distillation, hydrogenated cardanol may be separated. $RuCl_3$-catalyzed transfer hydrogenation was used by Perdriau et al. to convert CNSL polyenes to monoenes.[115] **Figure 6** shows the isolation stages of cardanol from the cashew shell.

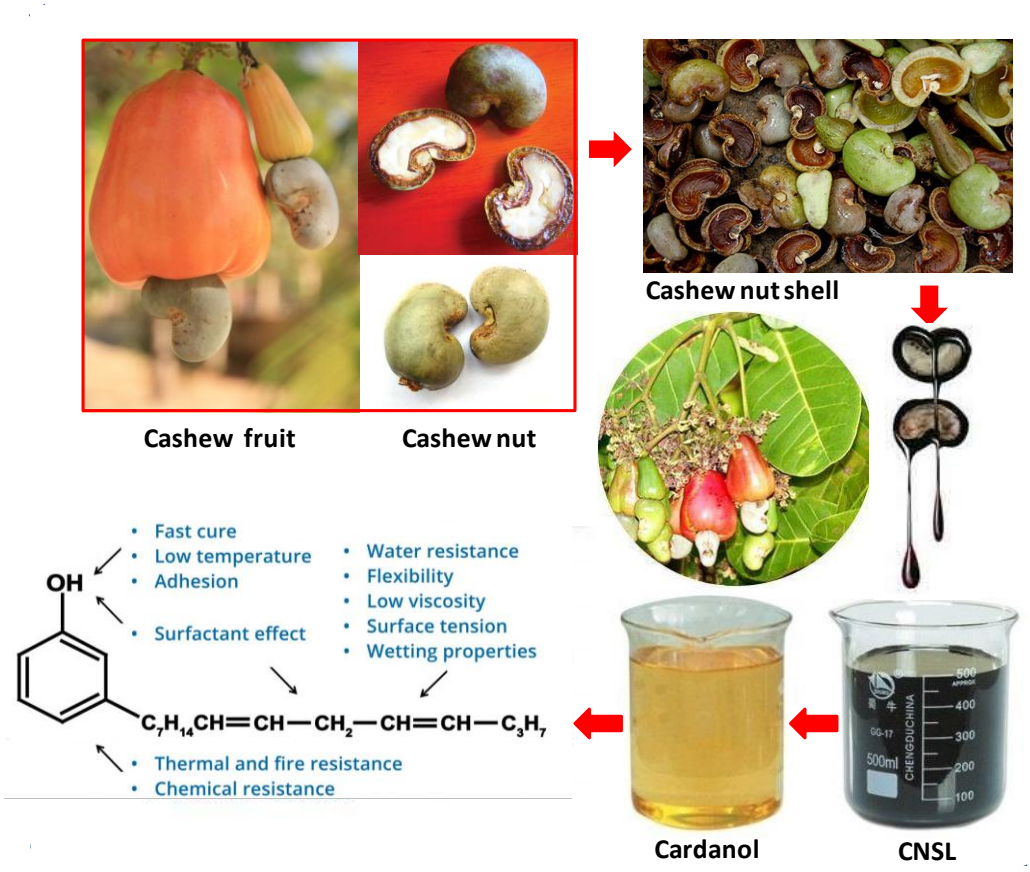

Figure 6. Isolation stages of cardanol from cashew shell.

4.2. Applications of cardanol in ATRP

Cardanol is a promising monomer for ATRP applications due to its unique molecular structure and functional groups.[117,118,119] Growing interest is focused on potential industrial applications of cardanol-based products, including but not limited to epoxy and acrylic monomers, as well as plasticizers and surfactants[116]. Cardanol-based ATRP polymers offer hydrophobic, internal plasticization, making them ideal for brake lining compositions[114]. ATRP incorporation of cardanol-based monomers in polymer chains creates advanced materials with favourable properties in coatings, including enhanced adhesion, durability, and corrosion resistance.[114] Cardanol-based ATRP produces tunable polymers with hydrophobicity and thermal stability, ideal for adhesives and high-performance materials.[120]

ATRP promotes sustainable, green chemistry principles and innovative materials for diverse applications. Reports show that comb-like polymer-graphene nanocomposites synthesized through surface-induced atom transfer radical polymerization. 0.6 wt% graphene is characterized by improved crystallization, melt temperatures, and rheological properties. Thesenanocomposites exhibit increased hydrophobicity, adhesive strength, and peel strength, making them potential for innovative adhesive applications.[121] Another study synthesized star-shaped polymers (SPCs) using PEG by ATRP. The SPCs were transformed from water-soluble to water-insoluble materials through UV-induced self-cross-linking. UV-cured membranes resisted bio- and oil-fouling due to PEG moieties on the cross-linked polymeric surface.[122] Synthesis ABA- triblock copolymers (PHCPMF#s) using ATRP, perfluoropolyether, and HCPM has also been reported. Cross-linked PHCPMF# films were formed on silicon wafers using spin coating and UV irradiation. The C-PHCPMF5 film demonstrated optimal biocidal/bacterial adhesion resistance and cell viability due to its biocidal and biocompatible units.[123] Six quaternaryammonium salts were synthesized using cardanol as a renewable resource, offering moderate to high yields. These salts are effective reactive surfactants, with gemini surfactants showing favorable surface-active properties.[124] PHCPMFs, synthesized via ATRP, are antifouling, bactericidal ABA tri-block copolymers with perfluoropolyether and cardanol segments, offeringhigh light transmittance, low water contact angle hysteresis and enhanced biocompatibility with human dermal fibroblasts.[125] Investigation of three polymerizable monomers derived fromcardanol by ATRP analyzes their structural characteristics, thermal behaviour, and the effects ofATRP ligands like PMDETA and bipyridine on polymer conversion, molecular weight, and polydispersity.[126] Cardanol can be functionalized with epoxy or (meth)acrylate groups to replace petroleum-based monomers. Combined with biobased reinforcements like microfibrillated cellulose (MFC) yields composites with improved mechanical strength. Photopolymerization of cardanol-based methacrylate monomers with MFC produces self-standing, flexible, and transparent films with high thermal stability in minutes.[127] A 57% yield reversible addition- fragmentation chain transfer agent and cardanol-based anionic surfactant was synthesized, resulting in a cardanol-terminated PMMA polymer. The material properties were enhanced through UV-curing, with an optimal irradiation time of 20 minutes determined based on resin behavior.[128] These reports show the potential applications and the promising future of cardanol by ATRP. **Table 2** details the applications of cardanol and its derivatives.

Table 2. Potential applications of cashew nut shell liquid and its derivatives.

Sl. No	Applications	Characteristics
1	As surface coatings andpaints	Cardanol-based resins are compatible with synthetic resins like alkyds, phenolics, and epoxies, making them suitable for various applications like paints, chlorinated rubber, and phenolic compounds. These applications benefit from the exceptional anti-corrosive properties exhibited by cardanol-based resins.
2	As binders	Cardanol replaced nearly 25% of phenolic compounds, which was used as a binding agent in plywood industries.
3	Cardanol-based resin-like Novolac &Resol resins and cardanol formaldehyde resins.	They possess insect resistance andantimicrobial properties.
4	Brake Lining applications	Cardanol derivatives are used as binders and forreducing fade in a better way because they can dissipate heat faster than Phenol-formaldehyde resins.
5	As a curing agent for Epoxy resin	When used as a curing agent it provides flexibilityand impact resistance better than commercial curing agents.
6	In rubber technology	Pure cardanol, when incorporated into rubber, acts as a deoxidant and plasticizer andsialso used to provide oxidative resistance to sulfur-cured natural rubber products.
7	In Bis-phenol basedepoxy	Cardanol can be used as a diluent, whichprovides excellent insulating properties
8	As an additive inlubricating oils	It lowers the pour point of lubricating oils dueto its antioxidant property.
9	All types of bondings	Alkylamine condensates cardanol used in metal-to-metal bonding because of its adhesive nature.
10	Laminates	Used to reduce brittleness and improve theflexibility of the laminates.
11	As surface active agents	Ethoxylated cardanol and sulfonated ethers ofcardanol are used as oil in water emulsifiers in pesticides and as wetting agents in textile industries. By the introduction of a sulphonic acid group on the phenolic ring of cardanol, itcan be used as ion exchange resins for oil-in-water and water-in-oil systems.
12	As Pesticide	Chlorinated Cardanol possesses good insecticidal,pesticidal, and germicidal properties.

CHAPTER-II.

MATERIALS, MONOMER SYNTHESIS AND CHARACTERIZATION TECHNIQUES

Millions of tons of vinyl-based homo/copolymers are synthesized each year for making radical polymerization an established process. Free radical polymerization is frequently utilized in industrial sectors and research labs for the wide spectrum production of polymeric materials. This extensive popularity is attributable to the adaptability of products, ease in synthetic processes, compatibility with other functional groups of monomers, and resistance to media and water. The techniques greatly simplify the experimental setup, leading to wide commercial adoption.[12,129] Numerous vinyls, acrylic, and methacrylic monomers, including functional monomers, have undergone successful polymerization or copolymerization via ATRP under controlled reaction conditions. The reactions can tolerate a wide range of solvents and other contaminants, and they take place at a consistent temperature range, usually between 0 and 100 °C. The lack of control over the polymer structure is one of the main limitations of controlled radical polymerizations. The production of polymers with high molecular weights and polydispersities typically involves relatively little architectural control because of the slow initiation, rapid propagation, and propensity to undergo various termination processes. These characteristics can be seen in the physical and mechanical characteristics of the synthesized polymers. As a result, precision polymer synthesis to create different topologies has been thought inappropriate for radical polymerization.[28,130,131]

Block copolymer synthesis is one of the potential methods for polymer modification since it offers unique physicochemical properties when the architecture of the copolymer is correctly designed with segments of different chemical compositions. Polystyrene (PS) is one of the hydrophilic polymers studied extensively because of its potential commercial applications in several fields, such as electrochemistry and surface chemistry. Surfactants, compatibilizers, dispersion stabilizers, etc. are some of the many uses for block copolymers containing hydrophilic and hydrophobic building units.[132] Since the macroinitiator may initiate the polymerization of a second monomer in the presence of a catalyst, ATRP is a helpful method for producing copolymers, namely block copolymers of the AB or ABA type.[133] The 2-halo propionate end group is one of the most efficient initiators for block copolymer production in controlled/"living" radical polymerizations. The use of mono and bifunctional poly(ethylene oxide) macroinitiators has been described for the synthesis of AB and ABA type block copolymers from tert-butyl acrylate, styrene, 2-hydroxyethyl methacrylate, methyl methacrylate, and other hydroxyl terminated oligomers.[134,135]

The goal of this chapter is to describe the detailed materials and characterization of styrene, PDPMA, and CA monomers for using varying number-average molecular weights of ethylbromo isobuterate in conjunction with a transition-metal catalyst (CuBr) in solution under ATRP conditions. All reagents, monomers, and solvents must be well purified before use in living radical polymerization techniques. In addition, an inert atmosphere devoid of contaminants and

moisture, oxygen, and other reactive gases is required for the reactions to be carried out. Special consideration must be given to purifying nitrogen/argon gas to obtain the ideal conditions for living/controlled polymerization under positive pressure. The overall purification processes, laboratory setups, manipulations, and characterization methods employed in this work are all explained in this chapter.

1. PURIFICATION OF CHEMICALS AND SYNTHESIS OF REACTANTS

1.1. Water

Water was obtained by redistilling it over alkaline permanganate in a glass quick-fit Pyrex setup and passing it through Biodeminrolit (permit Co. U.K.) mixed with ion exchange resin to remove any remaining ion traces, if any.

1.2. Nitrogen

Nitrogen was made free from oxygen traces by passing through five columns of Fieser's solution containing sodium hydrosulphite (15gm), sodium anthraquinone - sulphate (200 mg) per liter of a 5% NaOH solution followed by passage through wash bottles containing saturated lead acetate water respectively. The Fieser's solution was frequently renewed as the blood red coloration of the solution changed to dark brown with use. The organic solvents and other reagents used were of A.R, RDH grade and were either distilled or recrystallized before use.

1.3. Monomers

The monomers used for the research work were washed with 5% NaOH solution to remove the inhibitor. Then repeated washing was made to remove the alkali and the monomers were dried over anhydrous $CaCl_2$ and vacuum distilled in the presence of nitrogen under reduced pressure.

1.4. Purification of Copper (I) bromide

A chemical compound with the formula Cu(I)Br is copper (I) bromide. The pure solid is colorless, however, samples are frequently colored due to the impurities of copper (II) since the copper (I) ion readily oxidizes to form $CuBr_2$. Copper bromide is frequently used in ATRP reactions hence, purification of copper bromide is necessary.

***Procedure*:** Copper bromide (Cu(I)Br) was purified by stirring in glacial acetic acid until the color due to the presence of CuBr2 is removed. The washing liquid was replaced with fresh glacial acetic acid if necessary. Further, the white precipitate of Cu(I)Br was washed 3 times with ethanol ensuring no exposure to air. The white precipitate was then similarly rinsed with anhydrous diethyl ether 3–4 times, dried, and filtered. The precipitate was overnight vacuum-dried while being shielded from light. The purified Cu(I)Br was preserved in an airtight bottle.

1.5. Other Chemicals

Other chemicals like solvents and chemicals were of analytical grade. Before usage, they were either regularly recrystallized or vacuum distilled. The CNSL was obtained from Kerala Cashew Development Corporation, Quinol, India. It was then purified, and cardanol was extracted through a double vacuum distillation. The fraction obtained was distilled at 190-220 °C and 0.01 mmHg pressure and stored in an amber-colored container. Acrylic acid, metal catalyst Cu(I)Br, monomer styrene (St) bipyridine (dNBpy), initiator ethyl-2-bromo isobutyrate (EBriB), benzoyl chloride needed to produce acryloyl chloride, glacial acetic, ethanol was purchased from Sigma Aldrich, St. Louis, MO, USA and used as such. Acryloyl chloride used to produce acrylic acid and benzoyl chloride were purchased from Sigma-Aldrich, while triethylamine was provided St. Louis, Missouri, USA. LR-grade solvents methanol, dichloromethane and tetrahydrofuran were purchased from SD Fine Chem in Mumbai, India. Following a 5% aqueous sodium hydroxide solution wash, the styrene monomer was distilled under decreased pressure while maintained at -18 °C. Cu(I)Br was purified by mixing it with glacial acetic acid overnight, followed by washing with diethyl ether and ethanol and finally drying it at 50 °C under vacuum for 6 hours. Additional laboratory-grade reagents and solvents were utilized. All products were analyzed spectroscopically for their physicochemical properties. **Table 3** shows the materials used for the study along with their properties and sources.

Table 3. Materials: Properties and Sources

Sl. No	Materials	Description	Source	Code
1	CNSL	Density = 0.962 gm	KCDC, Quinol, India	CNSL
2	Cardanol	0.930 g/mL	refined from CNSL	--
3	Pentadecylphenol	-	Cardolite Specialty Chemical, Mangaluru	
4	Benzoyl chloride	1.21 g/cm³	Sigma-Aldrich, St. Louis, Missouri, USA.	--
5	Acrylic acid	1.05 g/cm³	Sigma-Aldrich, St. Louis, Missouri, USA.	AA
6	Triethylamine	726 kg/m³	Sigma-Aldrich, St. Louis, Missouri, USA	TEA
7	Methacrylic acid	1.02 g/cm³	Sigma-Aldrich, St. Louis, Missouri, USA	MAA
8	acryloyl chloride	Acrylicacid & Benzoyl Chloride.	Lab.	AC
9	Cardanyl Acrylate	-	Lab.	CA
10	Pentadecylphenylmethacrylate	-	Lab.	PDPMA
11	Bypyridine	982 kg/m³	Sigma-Aldrich, St. Louis, Missouri, USA.	dNBpy
12	Pentamethyldiethylenetriamine	830 kg/m³	Sigma-Aldrich, St. Louis, Missouri, USA.	PMDETA
13	Copper(I) bromide	4.71 g/cm³	Sigma-Aldrich, St. Louis, Missouri, USA.	Cu(I)Br
14	ethyl-2-bromo isobutyrate	1.329 g/mL	Sigma-Aldrich,St. Louis, Missouri, USA.	EBriB
15	Styrene	909 kg/m³	Sigma-Aldrich, St. Louis, Missouri, USA.	St
16	Toluene	867 kg/m³	SD Fine Chem in Mumbai, India.	--
17	Ethanol	789 kg/m³	SD Fine Chem in Mumbai, India.	--
18	Glacial acetic	1.05 g/cm³	SD Fine Chem in Mumbai, India.	GAA
19	Tetrahydrofuran	0.889 g/mL	SD Fine Chem in Mumbai, India.	THF
20	Methanol	792 kg/m³	SD Fine Chem in Mumbai, India.	--
21	Dichloromethane	1.33 g/cm³	SD Fine Chem in Mumbai, India.	DCM
22	Diethyl ether	713 kg/m³	SD Fine Chem in Mumbai, India.	--

1.6. Preparation of acryloyl/methacryloyl chloride

A mixture comprising 3 moles of acrylic acid (216 gm), 3 moles of methacrylic acid (258 gm), 6 moles of benzoyl chloride (84 gm), and 0.5 gm of hydroquinone was subjected to distillation using a highly efficient 25 cm distillation column. The distillation process was terminated when the column temperature, which fluctuated between 60 and 70 °C, reached 85 °C. The distillate was collected by a receiver containing 0.5 grams of hydroquinone dissolved in ice. After redistillation of the crude product through the same column, the fraction boiling at 72–74°C at 740 mm was collected, amounting to a final product quantity between 170–180 grams.

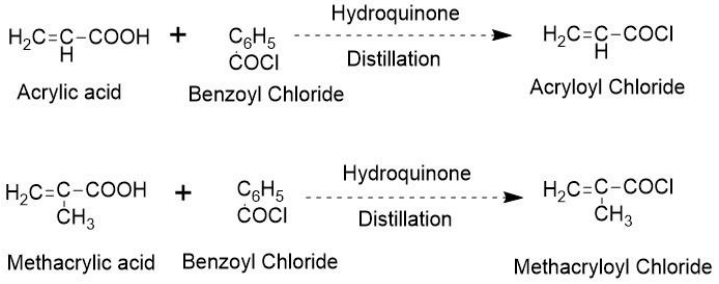

Scheme 4. Preparation of acryloyl/methacryloyl chloride

2. EXTRACTION OF CARDANOL AND MONOMER SYNTHESIS

2.1. Extraction of cardanol

Cashew nut shell liquid (CNSL) was sourced from Kerala Cashew Development Corporation, Quinol, India. CNSL was placed in a distillation flask fitted to a vacuum pump, thermometer, collecting flask, and condenser. The vacuum distillation was performed at 3-4mm of Hg, and the fraction distilled at 230 - 240° was cardanol. The distillate was redistilled to get the purest forms of cardanol. Its characteristic properties, including iodine value, saponification value and viscosity-specific gravity, were determined. The lesser viscosity of cardanol indicates lesser ash content. Cardanol and CNSL have high unsaturation, as shown by their higher iodine values. **Figure7** shows the route of isolation of cardanol with the percentage of contents. **Table 4 & 5** shows the characteristics of CNSL and Cardanol and the characteristic spectral data, respectively.

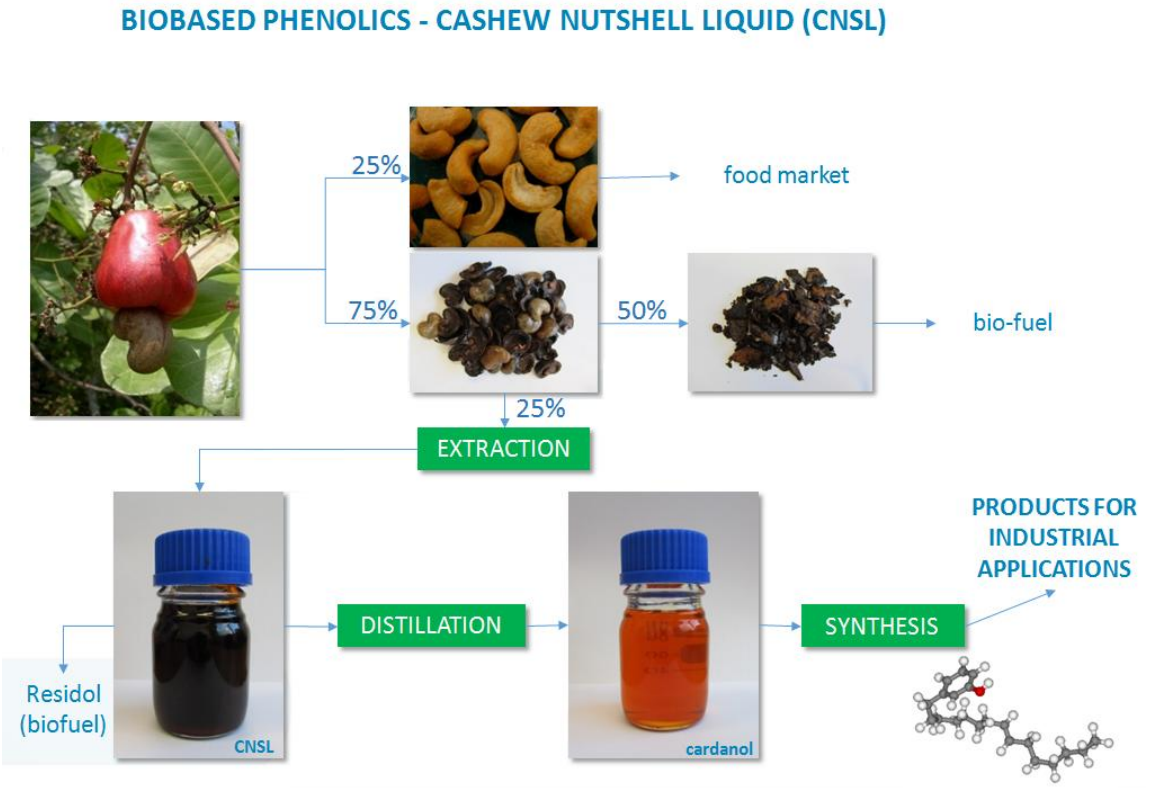

Figure 7. Isolation of cardanol with the percentage of contents.

Table 4. Characteristicsof CNSL and Cardanol

Sl. No.	Properties	Cardanol After Distillation	CNSL (ISI standard 840, 1964.)
1	Color	Dark brown	Dark brown.
2	Odour	Mild phenolic	Smoky and mild phenolic.
3	Specific gravity gm/cc at 30°C	0.868	0.960
4	Viscosity (CPS) at 30°C	38.5	55
5	Iodine Value	274.83	250
6	The moisture content at 100°C (%)	2.4	1.0
7	Saponification value	22.4	— —

Table 5. Characteristic spectral data of cardanol

Peak (cm^{-1})	Nature of peak	Probable assignment
3700- 3100 (centering at 3350)	Broad	- OH stretching vibration of phenolic - OH group (intermolecular H-bonded)
3170	Medium	Aromatic -C-H stretching vibration.
2920, 2852	Strong	-C-H stretching (asymmetric and symmetric) vibration of -CH2-linkages inside the chain.
1592, 1452	Strong	-C-C- stretching vibration of the aromatic nucleus.
920	Medium	Out of plane - C-H bending vibration in trans substituted C=C bond which indicates the presence of trans double bond in the aliphatic side chain.
1380	Weak	-C-H bending in -CH3 group of the side chain.

2.2. Pentadecyl phenol (PDP)

Cardanol can be hydrogenated to produce 3-pentadecylphenol (3-PDP), a chemically versatile byproduct that is used to synthesize various chemicals with potential applications. The class of phenolic lipids includes 3-pentadecylphenol (PDP). A large class of naturally occurring substances function as cytotoxic, fungicidal, and antibacterial agents and can interact with proteins, DNA, and biomembranes. One pentadecyl (C_{15}) chain makes up the phenol ring of the PDP compound. PDP chemicals are produced by hydrogenating unsaturated fractions of the alkyl phenolic oil, often termed as "cashew nut shell liquid" globally (CNSL). The CNSL oil contains a small amount of cardanol, primarily made up of PDP with very little saturated chain and an unsaturated C_{15} hydrocarbon chain. Both business and research are becoming more interested in this component due to the low cost of obtaining PDP from CNSL (the annual global production of cashew nuts is close to 500000 tons). By hydrogenating the side-chain double bonds of technical grade distilled cardanol, followed by further distillation and/or crystallization, it is simple to produce hydrogenated cardanol (3-n-pentadecylphenol) in its pure form. This prevents unfavourable side reactions attributed to the Olefinic moiety during the various functionalization of the aromatic ring or hydroxy group (also known as alkylation). **Scheme 5** shows the production processes of the cardanol-based precursors from CNSL.

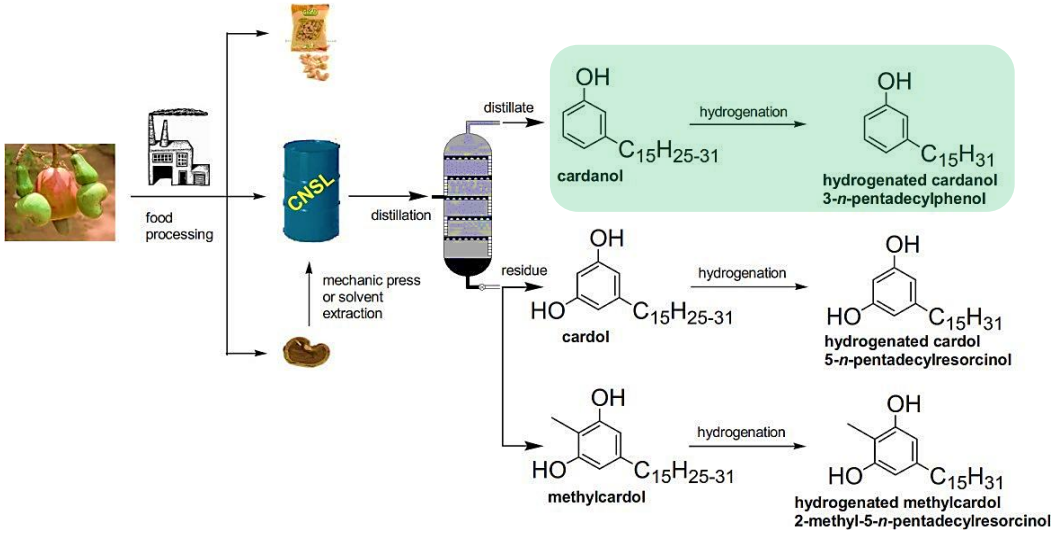

Scheme 5. Production processes of the cardanol-based precursors from CNSL.

2.2. Styrene

In the modern petrochemical industry, styrene (St) is one of the most significant monomers. Currently, there are about 20 million tons produced worldwide annually. DOW Chemical in the United States and BASF in Germany independently and simultaneously developed the

styrene method in the 1930s. The most significant polymeric compounds produced from styrene include polystyrene, styrene-acrylonitrile, and Acrylonitrile-butadiene-styrene. Making styrene-butadiene latex is another considerable application. Two techniques are primarily used in industry to create styrene.

- Dehydrogenation of ethyl benzene (EB) over iron oxide-based catalysts in the presence of steam **(Scheme 6)**.
- As a by-product of the epoxidation of propene using catalysts based on the Mo complex and ethyl benzene hydroperoxide.

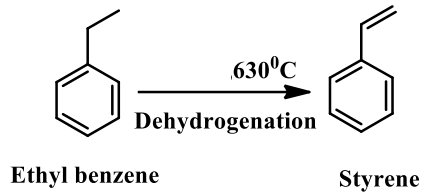

Scheme 6. Dehydrogenation of ethyl benzene (EB)

More than 90% of the global capacity is accounted for by the first process (1). The majority of the styrene is produced by the catalytic dehydrogenation process, which has traditionally used a potassium-assisted iron oxide catalyst since 1957.

3. PREPARATION OF MONOMERS

The biomonomers like cardanyl acrylate and Pentadecylphenyl methacrylate were prepared from cardanol with acryloyl chloride/ methacryloyl chloride using the following procedure.

3.1. Synthesis of Pentadecylphenyl methacrylate (PDPMA)

According to the method of Sitaramam and Chatterjee, PDPMA monomer was made from pentadecylphenol and methacryloyl chloride as per **Scheme 7.**[136]

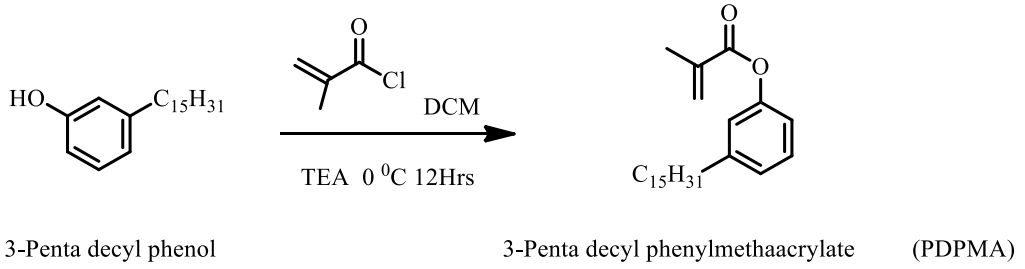

Scheme 7. Schematic representation of the synthesis PDPMA.

In a standard experimental setup, 250 ml three-neck round-bottom flasks were filled with 125 ml of dichloromethane and 50 gm (0.16 mol) of pentadecylphenol (PDP) under magnetic stirring. Gradually, triethyl amine was introduced into the homogeneous solution after cooling it to 0-5°C. Subsequently, a slow addition of 15.6 ml (0.16 mol) of methacryloyl chloride occurred for one hour at room temperature. The reaction continued for 12 hours. After the reaction, the mixture was neutralized with a 5% sodium bicarbonate solution and washed with distilled water. The resulting product was extracted with diethyl ether and dried using anhydrous sodium sulfate. A silica gel column (60-120 mesh) with a hexane-ethyl acetate mixture (98:2) was used to purify the product further. The monomer structure was confirmed using TLC, ^{1}H-NMR, and mass spectroscopy. The yield of the product obtained was 71%. The product was further purified on a silica gel column (60–120 mesh) using hexane-ethyl acetate (98:2) solvent system. The product yield obtained through column chromatography is presented in **Table 6**.

Table 6. Details of chromatographic separation of PDPMA.

Material	Material $_{wt}$	Product $_{wt}$	Purified M	Column yield
PDP	50g	42g	35.5 g	71 %

3.2. Synthesis of cardanyl acrylate (CA)

Cardanol and acryloyl chloride were reacted for 12 hours at room temperature with triethylamine to produce cardanyl acrylate. The reaction is depicted in **Scheme 8** according to the methodology proposed by Sitaramam and Chatterjee [137]. The synthesized monomer is purified using column chromatography.

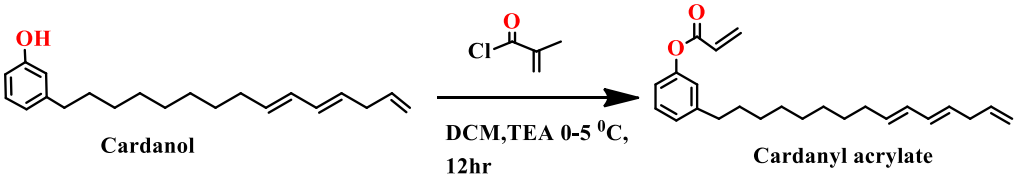

Scheme 8. Preparation of Cardanyl acrylate.

Following the standard procedure, a 250 mL three-neck round-bottom flask (RB) was charged with 125 mL of dichloromethane and 50 grams (0.16 mol) of cardanol. The mixture was then subjected to magnetic stirring. Triethyl amine was incrementally added dropwise in quantities of 23 mL (0.17 mol) once the solution attained homogeneity and was cooled to 0-5 °C. Afterwards, 15.6 mL (0.16 mol) of acryloyl chloride was gradually added within one hour. The reaction was left at room temperature (RT) for 12 hours. A 5 % sodium bicarbonate solution was employed to neutralise the reaction mixture, followed by washing with distilled water. The product was extracted with diethyl ether and dried using anhydrous sodium sulfate.

Further purification was carried out through a silica gel column using a solvent solution of hexane-ethyl acetate (98:2, 60-120 mesh). The monomer structure was confirmed through ^{1}H-NMR and mass spectroscopy analysis. The overall yield of the final product was 71%. **Figure 8** displays a photograph of the synthesized cardanol-based acrylate (CA), while **Table 7** provides detailed information on the chromatographic separation process.

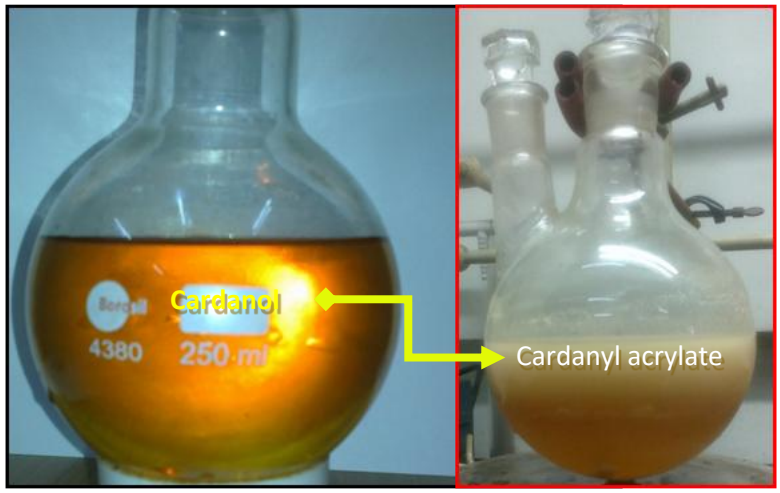

Figure 8. Synthesized Cardanyl acrylate from Cardanol.

Table 7. Details of chromatographic separation of CA.

Material	Material $_{wt}$	Product $_{wt}$	Purified M	Column yield
CA	50g	38g	32.2 g	64.4%

4. CHARACTERIZATION

Infra-Red Spectrometry (IR). FT-IR spectra were acquired using a Nicolet iS10 infrared spectrometer (Thermo-Fisher Corporation, USA) with a Smart ARK adapter specifically designed for liquid samples. The scanning range covered 650 to 4000 cm $^{-1}$ with 32 scans at a spectral resolution of 4 cm $^{-1}$. The OMNIC software (Thermo Electron Corporation, USA) was utilized to facilitate peak identification.

Nuclear Magnetic Resonance Spectroscopy (NMR). The ^{1}H and ^{13}C NMR spectra were acquired on a DRX-300 Advance NMR spectrometer (Bruker Corporation, Germany) using $CDCl_3$ as the solvent and tetramethylsilane (TMS) as the internal standard. The NMR data were processed using the MestReNova program from Mestrelab Research S. L. (Santiago de Compostela, Spain).

Mass spectroscopy (MS). Mass spectroscopy is a technique used to determine the mass of an object. Mass spectra were acquired in methanol using a FINNGAN LCQ Advance Max (California, USA).

Size Exclusion Chromatography (SEC). The high-pressure liquid chromatography (HPLC) system used for analyzing the SEC profiles of the synthesized copolymers consisted of equipment from Waters Corporation, USA. The experimental setup comprised a 1515 isocratic HPLC pump, a 717 plus automatic injector, and a column heater; all managed through Breeze software. For the separation columns, Waters Corporation Styragel HR1 and HR2 (300 mm x 7.8 mm) were employed and maintained at a constant temperature of 30 °C. The signals were detected using a Waters 2414 Refractive Index Detector. The eluent was 0.8 mL/min of HPLC-grade tetrahydrofuran (THF). THF solutions of 1525 mg/mL were used to dissolve the products, and the relative molar masses were determined using a set of closely spaced 1,4-Polyisoprene standards with a known molar mass of 31,400-10,500.

Thermogravimetric Analyses (TGA). Heat resistance testing was performed using a Netzsch STA 409PC. Samples weighing 3-5 mg were subjected to thermogravimetric analysis (TGA) at a heating rate of 10 °C/min. The analysis was conducted by ramping the oven temperature from 25 °C to 800 °C, with a nitrogen gas flow rate of 100 mL/min.

Differential Scanning Calorimeter (DSC). To investigate thermal transitions, DSC analysis was performed on 10 mg of samples using a Perkin-Elmer DSC instrument (USA). Two DSC analyses were performed on each sample. The specimen was analyzed in a nitrogen atmosphere, with scanning temperatures ranging from 25 to 220 °C. The heating rates used were 5, 10, 15, and 20 °C/min.

Transmission Electron Microscopy (TEM). TEM) analysis was performed on the samples using a 200 kV PHILIPS TECHNAI FE12 instrument from Philips, Holland.

Rheology. The rheological properties were analyzed using Anton Paar's MCR102 Dynamic Mechanical Analyzer (DMA) equipment in oscillatory shear mode.

5. PREPARATION OF ADHESION TEST SPECIMENS

The adhesion strength test specimen was made by applying a polymer solution in chloroform at a concentration of 20% (w/v) using a square applicator on carefully selected test pieces. After being air-dried for 6 hours, the coated sample was heated in an oven for 1 hour to speed up the drying process. After removing the samples and letting them cool to ambient temperature, they were bonded into the test pieces. For 48 hours before testing, a single 1-kilogram weight was placed on top of the bonded region. Four samples were made and tested for each combination, and the average was utilized in the final tally.

CHAPTER III.

ATR COPOLYMERIZATION OF STYRENE AND PENTADECYLPHENYL METHACRYLATE (PDPMA)

ABSTRACT: The study employed the ATRP technique to investigate the copolymerization behaviour of styrene and PDPMA at different monomer feed ratios. The compositional data obtained from ^{1}H NMR spectroscopy was analyzed using FR-KT methods to determine copolymer composition and reactivity ratios. The results showed a preference for styrene copolymerization with an alternation tendency, leading to copolymers rich in styrene at all feed compositions despite increasing PDPMA concentration. The reactivity ratio data indicated that the sequence length of PDPMA remained relatively constant, while the sequence length of styrene decreased with increasing PDPMA content in the feed. Size Exclusion Chromatography (SEC) characterization revealed that the molecular weight and polydispersity of the copolymers were influenced by the feed composition, ranging from 3,000 to 22,000 g/mole and 1.3 to 2.19, respectively. The copolymers exhibited varied glass transition behaviour and increased thermal stability with higher styrene content. Morphological analysis using Transmission Electron Microscopy (TEM) showed a phase-separated morphology. Rheological and adhesion tests suggested the potential use of styrene and PDPMA copolymers in hot melt adhesives, offering the flexibility to tailor adhesion properties.

1. INTRODUCTION

Bio-based materials significantly promote sustainability in various industries, including textiles, food, and plastic packaging, by reducing their environmental impact throughout the product's life cycle. Developing efficient processes is crucial for tailoring the physicochemical properties of bio-based materials to specific applications, such as enhancing mechanical strength through matrix cross-linking.[138] Research efforts are focused on sustainable, economically viable bio-based products balancing petroleum-based materials.

Cardanol, a phenolic renewable resource with a 15-carbon side chain with variable degrees of unsaturation, offers opportunities to develop value-added products.[75] Novel polymers with unique properties have been designed for industrial applications, such as adhesives, coatings, and lining materials based on cardanol-based monomers.[59,118] ATRP synthesized novel polymers with enhanced processability and performance, resulting in a nanocomposite with graphene for improved adhesion and surfactant capabilities.[126] Interestingly, the hydrogenated cardanol derivatives, including methacrylate and acrylate forms, exhibited superior potential and consistency. Ten Brinke et al. researched the interaction of PDP with block copolymers. They observed the creation of comb-like polymers due to the incompatibility between the alkyl side and the main chain.[139] The synthesis of a new reactive surfactant based on an acrylate derivative of polydimethylsiloxane resulted in improved hydrophobic characteristics in internally plasticized polystyrene.[140] The nanocomposite from combining PDPMA derivatives with graphene exhibited side-chain crystallization and improved adhesion characteristics.[121]

Besides, controlling adhesion properties can be achieved by copolymerizing with monomers such as MMA or styrene.[141]

In this context, an ATR copolymerization of styrene with PDPMA was investigated to explore the impact of styrene content on conversion, molecular weight, and polydispersity. Reactivity ratios were calculated from composition data using the FR-KT method. DSC and TGA were employed to study side chain crystallization and thermal stability, while morphology, rheological properties, and adhesion characteristics were also subjected to comprehensive analysis. This study seeks to optimize adhesion properties and expand the potential applications of bio-based polymers, enhancing their performance in diverse industries.

2. EXPERIMENTAL TECHNIQUES AND METHODOLOGIES

2.1. Materials

As described in Chapter 2, Table 3, page no. 58-68

2.2. Methods

2.2.1. Polymerization of Pentadecylphenylmethacrylate (PDPMA)

In a standard ATRP experiment (**Scheme 2**), a two-neck round-bottom flask was charged with PDPMA monomer (3 g, 0.008 mol), PMDETA ligand (33.51 L, 0.00016 mol), and CuBr catalyst (11.46 mg, 0.00008 mol), and the mixture was stirred magnetically until homogeneous. The reaction mixture was subjected to several freeze-thaw cycles and purged with argon. At 95 °C, ethyl-2-bromo-isobutyrate was added as an initiator (11.8 L, 0.00008 mol) using a syringe. Within 30 minutes, the reaction mixture turned viscous, and the catalyst was eliminated by diluting the product with THF (5 mL) and passing it through a silica gel column(100-200 mesh). The final product was dried under vacuum at 50 °C for 4 hours after repetitiveprecipitation with a 75:25 methanol-water mixture for purification. **Scheme 9** illustrates the homopolymerization of PDPMA.

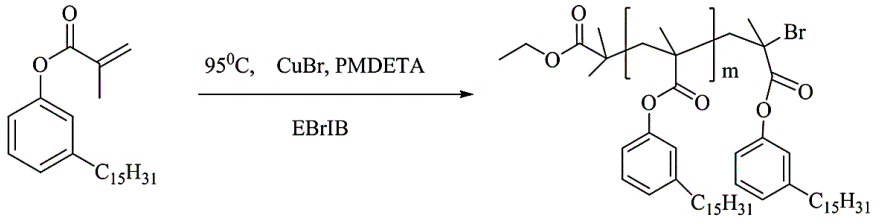

Pentadecylphenylmethacrylate (PDPMA) Poly pentadecylphenylmethacrylate (PPDPMA)

Scheme 9. Shows the homopolymerization of Pentadecylphenyl methacrylate.

2.2.2. Polymerization of Styrene

The styrene monomer underwent washing in a 5% aqueous NaOH solution and was distilled under low pressure. Cu(I)Br was purified by stirring in glacial acetic acid and then washed with ethanol and diethyl ether before being dried at 50 °C under a vacuum for 24 hours. Polystyrene (PS) was synthesized via ATRP using ethyl-2-bromo-isobutyrate as the initiator and a copper(I) bromide complexed PMDETA catalyst. **Schemes 11** and **12** depict thestructures of the resulting homopolymers, and **Scheme 10** provides a schematic representation of Polystyrene.

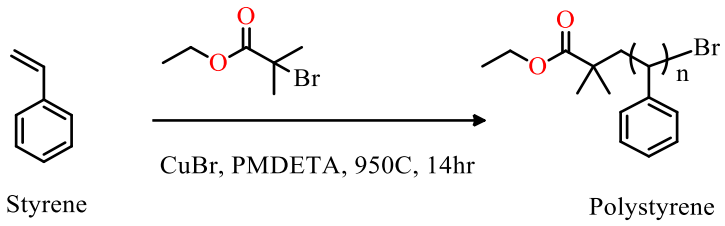

Scheme 10. Scheme of the homopolymerization of polystyrene via ATRP.

In a two-neck flask, CuBr (41.3 mg, 0.00028 mol), PMDETA (119 L, 0.000576 mol), and the monomer styrene (St) were combined and stirred magnetically until a homogeneous mixture was obtained. The reaction mixture underwent freeze-drying and was purged with argon gas for 15 minutes, followed by multiple freeze-thaw cycles. Ethyl-2-bromoisobutyrate initiator (43 L, 0.00028 mol) was introduced into the flask using a syringe, and the reaction was carried out at 95 °C in a thermostated bath. After the required reaction time, the product was diluted with THF (3 mL) and passed through a silica gel column to remove the catalyst. The polymer was then precipitated using a 75:25 mixture of methanol and water for recovery. This precipitation process was repeated three times, followed by six hours of drying at 60 °C under vacuum. Gravimetric conversions were performed, and the polymer structure was confirmed using ^{1}H NMR spectroscopy.

2.2.3. Copolymerization of Styrene-Co-PDPMA

Copolymerization investigations were conducted using a similar procedure with varying feed compositions. In a 50 mL round-bottom flask, CuBr catalyst (0.028 mol) and the appropriate monomers were initially introduced. Subsequently, the initiator ethyl-2-bromoisobutyrate (42 L, 0.0288 mol) and ligand PMDETA (119 L, 0.0288 mol) were added, and the flask was sealed under an argon atmosphere. The mixture underwent freeze-thaw cycles (3 times) and was then heated in an oil bath at 95 °C for 14 hours. Methanol was added to terminate the reaction, and the resulting product was dissolved in THF before being precipitated in a methanol-water solution. This precipitation process was repeated multiple times until the separated polymer was confirmed, through ^{1}H NMR spectroscopy, to be free of any remaining monomer.

3. RESULTS AND DISCUSSION

3.1. Structural Elucidation of PDPMA (FT-IR, ^{1}H-NMR, and mass spectroscopy)

The primary objective of this research was to examine the influence of copolymerization on adhesion and viscoelastic properties during the synthesis of cardanol copolymers. The PDPMA monomer was synthesized using hydrogenated cardanol, and its characterization was performed using FT-IR, ^{1}H-NMR, and mass spectrometry. The FT-IR analysis (**Figure 9**) revealed distinct C-H stretching vibrations at approximately 2926 cm^{-1}. The stretching of the -C=O- group occurred at 1756-1747 cm^{-1}. The -C=C- acrylic and aromatic vibrations were observed at 1645 cm^{-1} and 1629 cm^{-1}, respectively.

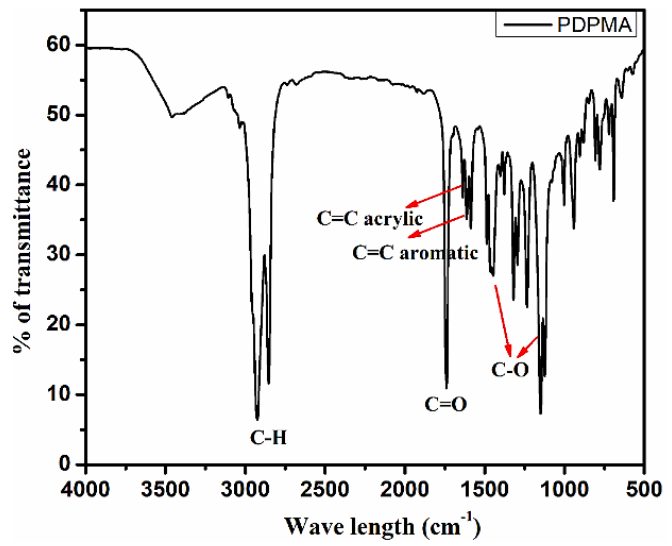

Figure 9. The FT-IR spectra of PDPMA.

The ^{1}H NMR spectrum of the PDPMA monomer (**Figure 10**) revealed critical structural details. Aromatic proton signals appeared at 6.9 and 7.2 ppm, while the alkyl side chain's terminal methyl (-CH3) protons were observed at δ 0.87 ppm. Resonance signals at 2.6 ppm were attributed to the α-CH_2 protons adjacent to the phenyl ring (Ph−**CH_2**−$(CH_2)_{13}$ CH_3 of PDPMA) in the aliphatic side chain. Vinyl proton signals were detected at 5.6 and 6.4 ppm (multiplet 2H, −$C(CH_3)=CH_2$). Notably, the characteristic peak at δ 1.25 ppm was assigned to the internal methylene protons ((−CH_2−$(CH_2)_{12}$−CH_3), while the singlet observed at 2.1 ppm was attributed to the methacrylate methyl group.

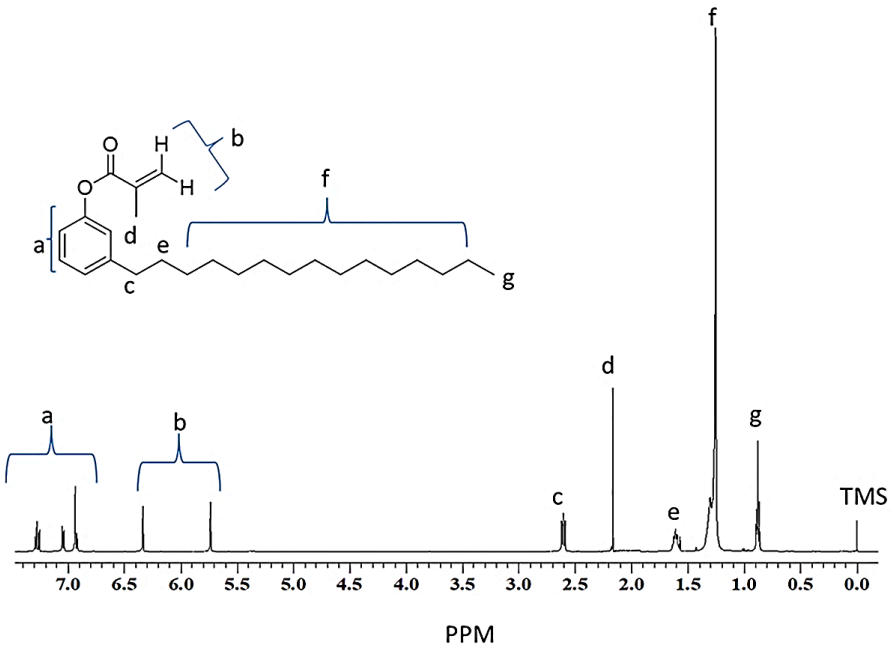

Figure 10. The ^{1}H NMR spectrum of PDPMA monomer.

Mass spectrometry was used further to confirm the monomer structure. (**Figure 11**). The molecular ion peak observed at 390.6 corresponds to the molar mass of the ammonium adduct (m/z + 18.039 g/mole), while the peak at 373.6 was attributed to the proton adduct (m/z + 1).

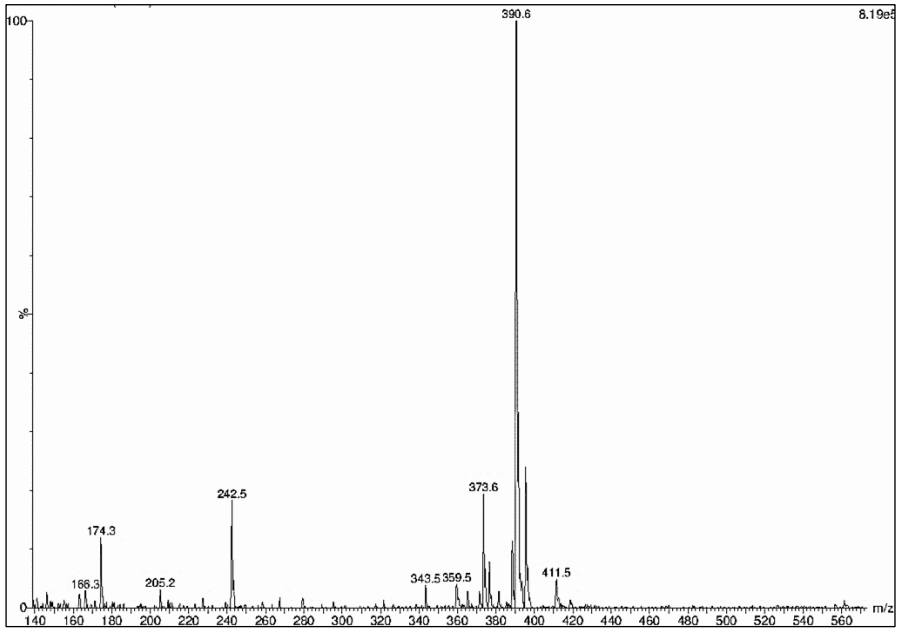

Figure 11. Established molecular weight of PDPMA by mass spectrometry.

3.2. Synthesis and Characterization polyPDPMA

The homopolymerization of PDPMA happened quite quickly, and the reaction mixture turned viscous in around 30 minutes. However, under the same circumstances, styrene homopolymerization only produced a 7% conversion rate. **Figure 12** depicts the typical ^{1}H NMR spectrum of the ATRP-produced PDPMA homopolymer. The notable deviation from Figure 1 was the elimination of the vinylic proton peaks in ^{1}H NMR after polymerization.

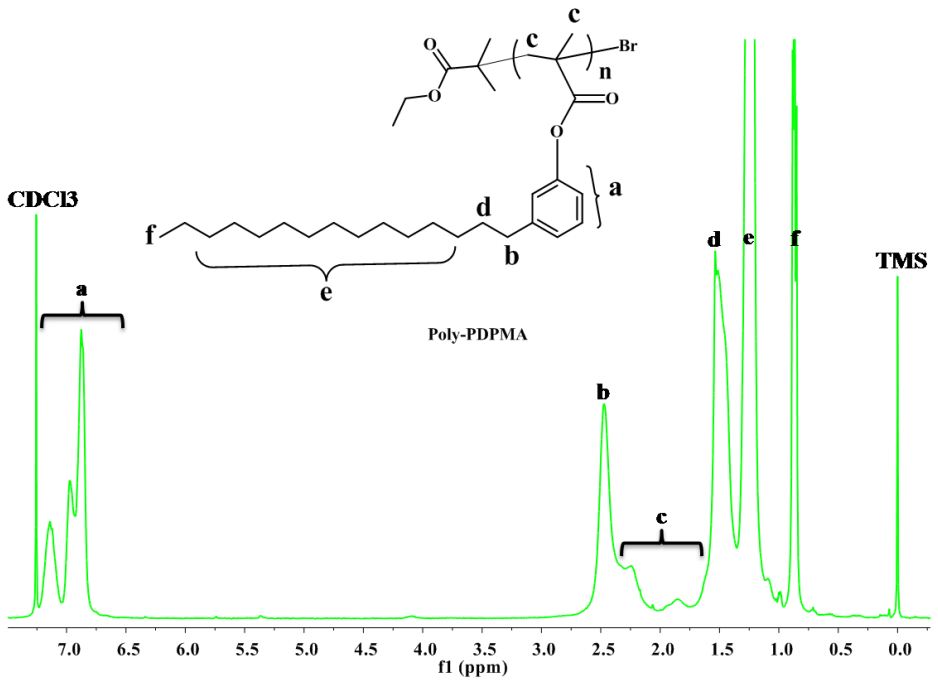

Figure 12. ^{1}H NMR spectrum of PDPMA homopolymer.

ATRP (ATRP) was used to polymerize the monomer PDPMA, and copolymers with styrene were also synthesized. **Scheme 11** depicts the bulk ATRP at 95 °C copolymerization process for styrene and PDPMA.

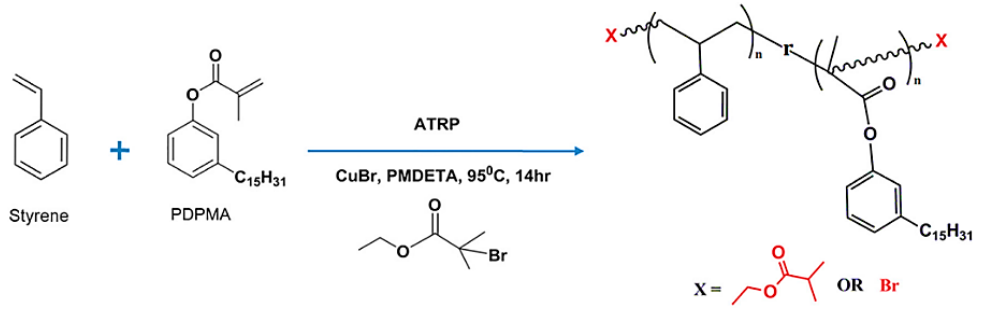

Scheme 11. Schematic of the copolymerization of styrene-PDPMA via ATRP.

Table 8 summarizes the styrene-PDPMA copolymer compositions and properties that were produced via ATRP, and **Table 9** details the yield of Styrene-PDPMA copolymer compositions. **Figure 13 & 14** shows the various stages of the ATRP procedure and the purified final product, respectively.

Table 8. Composition and characteristics of styrene Sty-co-PDPMA synthesized via ATRP

Sample Code	Composition				GPC		M_n Theory	PDI
	Feed		^{1}H NMR		M_w g/mole	M_n g/mole		
	St	PDPMA	St	PDPMA				
PS	100	0	100	-	3012	2551	3112	1.18
PDPMA	0	100	-	100	17,981	10,964	22,320	1.64
SPDPMA10	90	10	-	-	3758	2828	3338	1.33
SPDPMA30	70	30	75.35	24.65	31,923	23,047	36,521	1.38
SPDPMA50	50	50	65.5	35.5	29,068	13,896	37,378	2.09
SPDPMA70	30	70	57	43	21,325	7872	34,778	2.71
SPDPMA90	10	90	-	-	26,690	17,554	33,711	1.52

Note: $M_{n\ Theory}$ was calculated using the relation [M}o[I]o× conversion ×repeat unit mol. wt.

Figure 13. Photographs of various stages of ATRP

Table 9. The yield of Styrene-PDPMA copolymer compositions.

Sample code	[Styrene]: [PDPMA]	Yield (%)
Sty_{90}-co-$PDPMA_{10}$	90:10	70.1
Sty_{70}-co-$PDPMA_{30}$	70:30	76.7
Sty_{50}-co-$PDPMA_{50}$	50:50	78.5

1= [M]:[CuBr]:[PMDETA]:[I]= 100:1:2:1 and 20h at 95°C.

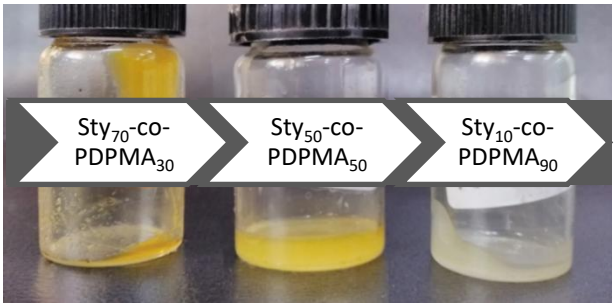

Figure 14. Photograph of the purified final product of styrene/PDPMA copolymer.

To examine the viscosity buildup and ensure that considerable conversion was achieved, the copolymerization tests were run for 14 hours. The ^{1}H NMR validated the copolymer's structure (**Figure 15**), and the composition was determined by integrating styrene and PDPMA peaks.

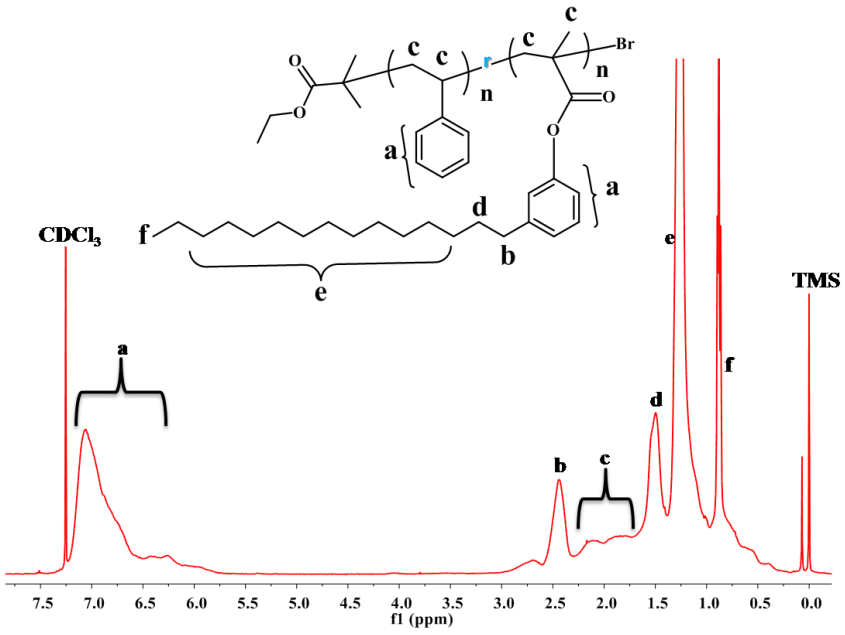

Figure 15. NMR spectrum of styrene-PDPMA copolymer (in the feed ratio 70:30) in CDCl3.

The phenyl ring protons were observed as a broad peak at δ 7–7.4 ppm (a). The characteristic peak of PDPMA, used to determine its composition, appeared at δ 2.5–2.6 ppm (b), corresponding to the protons α to the phenyl ring of PDPMA (Ph-CH_2-$(CH_2)_{13}$-CH_3). Other peaks observed include (c) the hydrogen on carbon β to the aromatic ring (Ph–CH2–CH2–) at δ 2.2 ppm, and (d), a broad peak, representing the –CH_2– and –CH– protons of the main chain, observed at δ 1.6–1.43 ppm. The internal methylene protons of the side chain of PDPMA were identified at δ 1.2 ppm (e), while the terminal -CH_3 protons of the alkyl side chain appeared at δ 0.83 ppm (f). Upon analyzing the composition data obtained from ^{1}H NMR and comparing it with the feed composition in **Table 8**, it was evident that the copolymers had lower PDPMA content than the feed. The reactivity ratios (r_1, r_2) were determined based on the composition data through the F-R and K-T methods. **Figure 16** illustrates the corresponding plot, and **Table 10** provides the tabulated values.

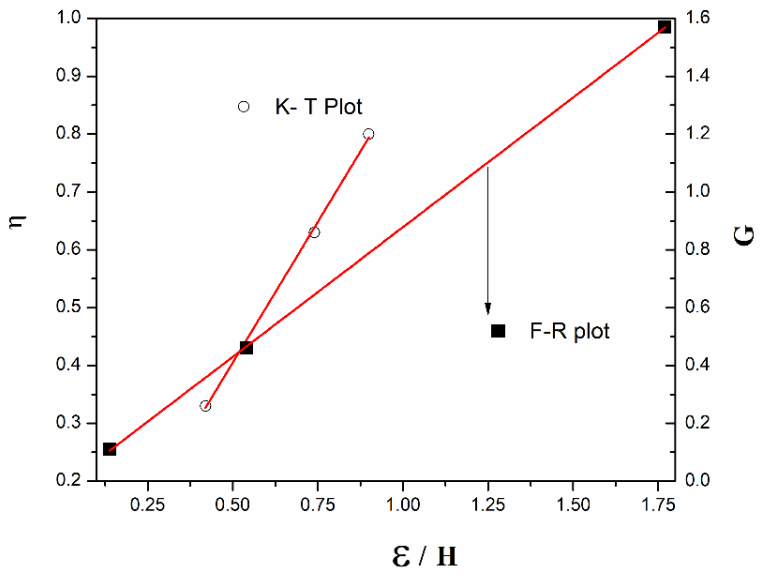

Figure 16. Fineman-Ross and Kelen-Tudos plot for styrene-co-PDPMA.

Table 10. Finemann-Ross (FR), and Kelen-Tudos (KT) parameters for styrene-co-PDPMA.

Styrene: PDPMA Composition		M= M_1/M_2	P= m_1/m_2	M/P	G	H	α + H	η	ξ
Sample	^{1}H NMR								
$StyPDPMA_{30}$	75.35:24.65	2.33	3.05	0.76	1.57	1.77	1.95	0.80	0.90
$StyPDPMA_{50}$	65.5:35.5	1	1.84	0.54	0.46	0.54	0.72	0.63	0.74
$StyPDPMA_{70}$	57:43	0.42	1.32	0.31	0.11	0.13	0.32	0.33	0.42

$(\alpha = H_{min} \times H_{max})^{1/2}$ i,e = 0.48, $G = M - M/P$, $H = M^2/P$, $\eta = G/(\alpha + H)$, $\xi = H/(\alpha + H)$.

Table 11. The reactivity ratio of styrene (r_1) and PDPMA (r_2) by FR-KT methods.

Methods Used	r_1 (Styrene)	r_2 (PDPMA)	r_1:r_2
FR	0.8965	0.0182	0.016
KT	0.9732	0.0816	0.073

The reactivity ratio of styrene (r_1) was identified as greater than that of PDPMA (r_2), and their product $r_1 \times r_2$ approached zero, falling within the range of zero to 1. These findings indicate a copolymerization behavior characterized as random, with a higher likelihood of styrene incorporation and a tendency toward alternation. The product $r_1 \times r_2$ being less than 1 and close to zero further supports this observation. By averaging the values obtained from both the Finemann-Ross (F-R) and Kelen-Tudos (K-T) methods, the reactivity ratio values were established as $r_1 = 0.93$ and $r_2 = 0.05$. These values suggest that the radical S* in styrene demonstrates a slightly stronger preference for copolymerization over homopolymerization. Conversely, the r_2 value suggests that PDPMA exhibits significantly lower preference for homopolymerization and instead favors copolymerization with the styrene monomer. Consequently, styrene is more prone to incorporating into the copolymer at a faster rate than PDPMA. This leads to the formation of extended sequences of styrene units across the entire composition range investigated. In consideration of the reactivity ratio, the sequence length was determined, with **Table 12** presenting values indicating a lengthier sequence of styrene (I_1) when the feed contains a higher styrene content. In contrast, the sequence length of PDPMA (I_2) remains relatively consistent, aligning with its tendency toward alternation or its limited capacity to form extensive sequences of PDPMA units.

Table 12. The monomer composition and sequence length ratio.

Monomer Feed Styrene: PDPMA	M_1/M_2	M_2/M_1	l_1	l_2	l_1:l_2
70:30	2.33	0.42	3.08	1.01	3.05
50:50	1	1	1.89	1.02	1.85
30:70	0.42	2.33	1.38	1.04	1.33

The values were calculated using $r_1 = 0.896$, and $r_2 = 0.018$ obtained by the FR method.

The compositional data obtained from ^{1}H NMR (**Table 8**) aligns with this discovery, as it demonstrates that despite an escalation in the feed concentration, the copolymer maintains a low PDPMA content. In the case of copolymerization between styrene and hydrogenated cardanyl acrylate (PDPA), the observed reactivity ratio diverged from the values reported in the literature. More specifically, previous reports indicated $r_1 = 0.34$ for styrene and $r_2 = 0.97$ for PDPMA. This discrepancy indicates that methacrylate has a lower photopolymerization tendency than PDPMA in the presence of styrene. The literature studies utilized a cobalt-based initiating system, which could explain the difference. Similar observations were made by Koiry

and Singha when polymerizing styrene with 2-ethylhexyl acrylate, attributing the influence of the starting system on reactivity[142]. It was hypothesized that ATRP and conventional radical polymerization may have distinct polymerization mechanisms, especially for monomers with non-polar side chains, making it challenging to form polar catalyst complexes. This hypothesis also applies to this case, given the 15-carbon alkyl side chain of the monomer, imparting hydrophobicity.

3.3. Molecular Characterization of Styrene-co-PDPMA by Size Exclusion Chromatography (SEC)

Size Exclusion Chromatography (SEC) was utilized to investigate the molecular characteristicsof the synthesized copolymers, and the corresponding data are presented in **Table 9**. Notably, deviations from the theoretically calculated molecular weight were observed in all cases except for styrene homopolymerization, with the extent of variation increasing as the PDPMA content in the feed increased. This observed discrepancy can be attributed to the influence of the 15-carbon alkyl chain present in PDPMA on the copolymer's hydrodynamic volume. The alkyl chain acts as short branches on each repeat unit, resulting in a more compact polymer structure and, reduced hydrodynamic volume and lower molecular weights. This relationship between branching, hydrodynamic radius, and intrinsic viscosity or molecular weight has been well-documented in previous studies[143]. Similar findings were reported in the case of styrene-ethylhexyl acrylate copolymers synthesized via ATRP[114]. **Figure 17** visually demonstrates the variations in molecular weight distribution of the different copolymers with increasing PDPMA concentration. The polydispersity values obtained from GPC showed variation with increasing PDPMA content in the copolymer.

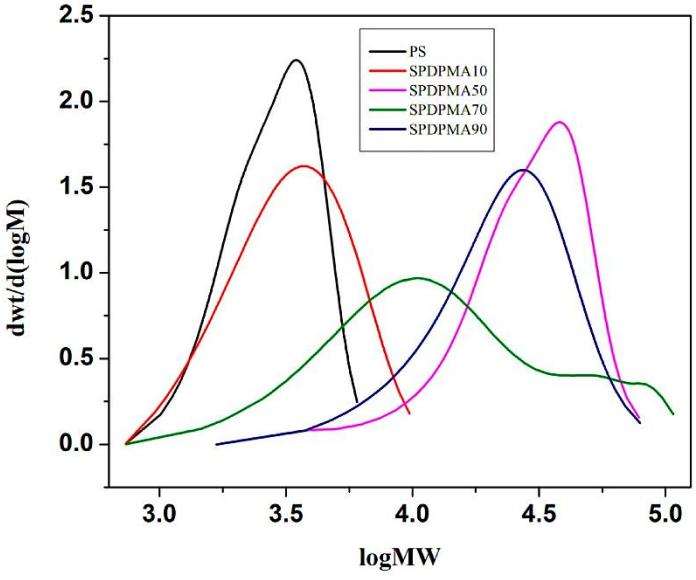

Figure17. dwt/dlogM vs. log Mwplots of styrene-PDPMA copolymers showing variation in mol. wt. distribution as a function of the feed composition.

The molecular weight distribution of the polystyrene homopolymer was the narrowest, whereas the polydispersity increased with higher levels of PDPMA. This observation indicates a potential loss of control over the polymerization process or indications of a branched structure with increased PDPMA content.

3.4. Glass Transition Behavior of Styrene-PDPMA Copolymers (DSC)

The glass transition behaviour of representative styrene-PDPMA copolymers studied by DSC is shown in **Figure 18**.

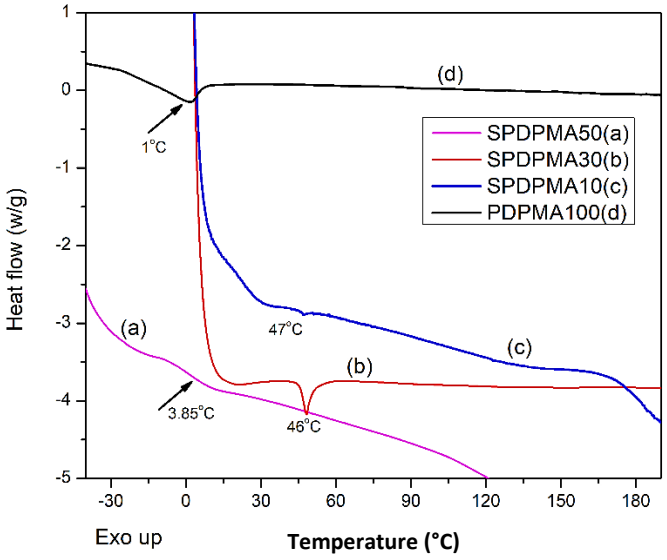

Figure 18. DSC curves of Styrene- PDPMA copolymers synthesized via one-pot ATRP copolymerization (The Tg of poly (PDPMA) was = 1 °C and poly (styrene) = 106 °C).

The homopolymer $PDPMA_{100}$ showed a small endothermic peak at approximately 1 °C. When the PDPMA content was at 10 wt%, the amorphous polymer's glass transition temperature (Tg) was observed at around 10 °C, along with a crystalline melting-like transition at about 47 °C, indicated by a baseline shift. The endothermic melting-like transition became clearer after increasing the PDPMA content to 30 wt%. The copolymer with 50 wt% PDPMA content displayed a broad glass transition centered at approximately 3.85 °C, without a distinct endothermic melting peak, despite the higher PDPMA content. The glass transition temperature decreased as the PDPMA concentration increased in the copolymer, in line with expectations. Previously reported melting transitions in comb-like polymers of n-alkyl acrylate polymers, characterized by crystallizable side chains like PDPMA, showed similar behaviour with distinct melting transitions alongside the glass transition. This indicates characteristic side chain crystallizable polymers, where the Tg aligns with the melting transition.

At 10 wt% PDPMA content, the primary observation was a softening effect in the material. However, at 30% PDPMA content, there was an increase in the crowding of alkyl chains, leading to enhanced crystallization. Surprisingly, with 50 wt% PDPMA, crystallization appeared less favoured, though the reasons for this observation remain unclear based on the current studies. A study by Sidney et al. explored side-chain crystallinity in polymethacrylates and polyacrylates containing n-alkyl groups ranging from 12 to 18 carbon atoms. These crystallites primarily consist of the n-alkyl groups extending from the molecular backbone rather than segments of the backbone itself, with overlap or interdigitation of alkyl chains on different polymer chains. When crystallization is favoured in the copolymer, a two-phase structure emerges, consisting of packed alkyl crystalline domains (on the left-hand side of Scheme 12) distributed in the amorphous matrix. The interdigitation of alkyl chains on different chains is illustrated on the other side of scheme 12. The observed phase separation or crowding of alkyl chains in $SPDPMA_{30}$ can be depicted schematically, as shown in **Scheme 12** below.

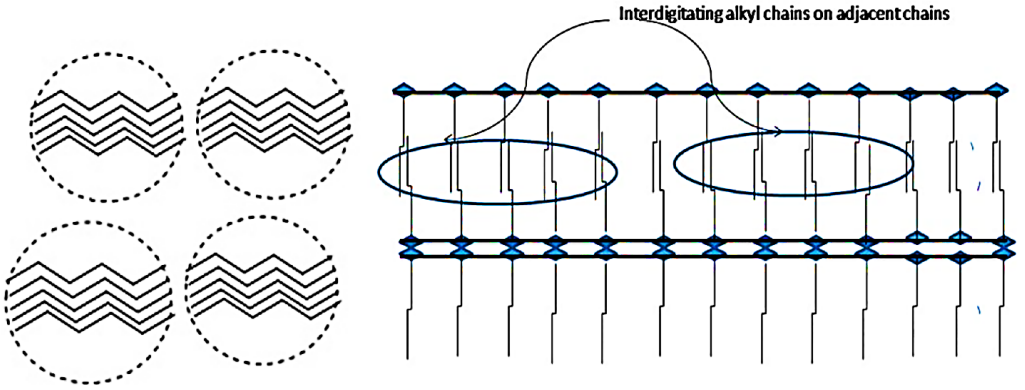

Scheme 12. Schematic of the crystalline alkyl chain domains (LHS) formed due to aggregation behavior of alkyl chains on alternate repeat units (RHS of the scheme).

Transmission electron microscopy (TEM) analysis reveals nanoparticle size, shape, distribution, phases, and domains in copolymers, revealing phase separation, crystalline regions, and specific nanostructure formation. The TEM image of $SPDPMA_{70}$ further confirmed the formation of this phase-separated domain structure. **Figure 19** shows TEM images of SPDPMA70, which reveal the formation of a core-shell type structure with crystalline (light color) domains and aromatic, electron-rich styrene domains due to phase separation. Visualizing the microstructure copolymer provided valuable insights into properties and behaviour, aiding in understanding the potential applications and optimizing performance in the synthesised copolymer's adhesives, coatings, and industrial fields.

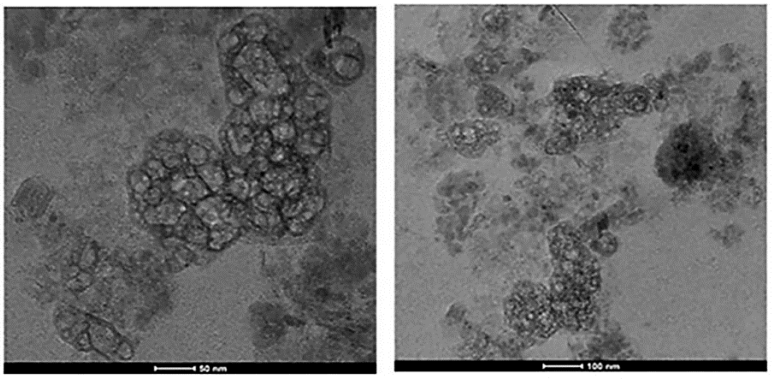

Figure 19. TEM Images of $SPDPMA_{70}$ show the presence of a phase-separated domain structure, where the light-colored domains are from the PDPMA segments.

3.5. Thermal Stability of Copolymers (TGA)

The thermal stability of the copolymers was evaluated by thermogravimetric analysis (TGA) at temperatures ranging from 50 °C to 200 °C at 10 °C min^{1}. **Figure 20** depicts typical plots.

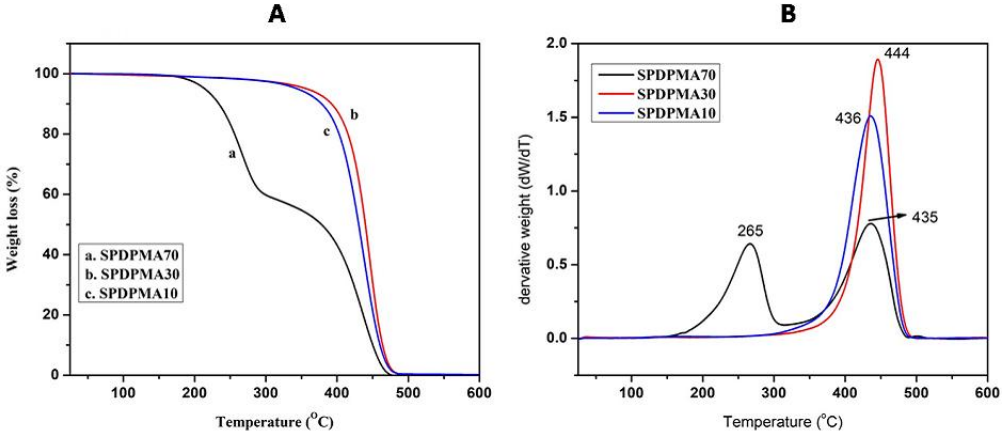

Figure 20. Thermal degradation properties of styrene-PDPMA copolymers (A) weight loss curve and (B) derivative plot.

The copolymers with higher styrene content (90% and 70% wt%) exhibited maximum thermal stability. The copolymer with the lowest styrene concentration (30 wt%) showed decomposition in two stages at 265 °C and 435 °C, as depicted in the derivative thermogram (**Figure 8B**). The copolymer with 50% and 70% styrene content decomposed in a single stage. The decrease in thermal stability at higher PDPMA concentrations may be attributed to the presence of polar carbonyl groups, which increase its susceptibility to degradation. At higher styrene concentrations, the thermal stability of the phenyl group contributes.

3.6. Rheological Properties

The rheological properties were investigated using the oscillatory shear mode, and the changes in storage modulus (G′), loss modulus (G″), and complex viscosity (η*) were measured as functions of frequency and temperature. The data obtained from the analysis are presented in **Tables 13 & 14**, and typical results are illustrated in **Figure 21**. The measurements were conducted at various temperatures, employing a strain rate of 0.5%.

Table 13. Storage and loss modulus of copolymers at different temperatures at 100 (rad/s) frequency (ω).

Sample code	Temp(0^0C)	30	40	50	60	70	80	90	100	110	120	130
Sty_{30}-co-$PDPMA_{70}$	G' (Pa)	8.4857 $\times10^2$	8.024 $\times10^3$	5.931 $\times10^3$	5.676 $\times10^3$	5.015 $\times10^3$	4.135 $\times10^3$					
	G" (Pa)	169.71	160.48	118.64	113.53	100.31	82.709					
Sty_{50}-co-$PDPMA_{50}$	G' (Pa)	87466	51509	5388.5	3884.1	1609.7	414.41					
	G" (Pa)	1.87 $\times10^5$	98154	7124	6850.2	4124.4	2172.8					
Sty_{70}-co-$PDPMA_{30}$	G' (Pa)			92494	92096	55194	12289	8231.6	1879.1	426.53	8.8104 $\times10^2$	9.7288 $\times10^2$
	G" (Pa)			1.66 $\times10^5$	1.41 $\times10^5$	92092	37303	30292	14209	6964.8	1762.1	1945.8

Table 14. Complex viscosity of copolymers at different temperatures at 100 (rad/s) frequency. (ω)

Sample code	Temp(0^0C)	30	40	50	60	70	80	90	100	110	120	130
Sty_{30}-co-$PDPMA_{70}$	η*(Pa.s)	16971	16048	1186.4	1135.3	1 003.1	827.09					
Sty_{50}-co-$PDPMA_{50}$	η*(Pa.s)	2.07 $\times10^6$	1.11 $\times10^6$	89323	78748	44274	22120					
Sty_{70}-co-$PDPMA_{30}$	η*(Pa.s)			1.90 $\times10^6$	1.68 $\times10^6$	1.07 $\times10^6$	3.93 $\times10^5$	3.14 $\times10^5$	1.43	69778 $\times10^5$	17621	19458

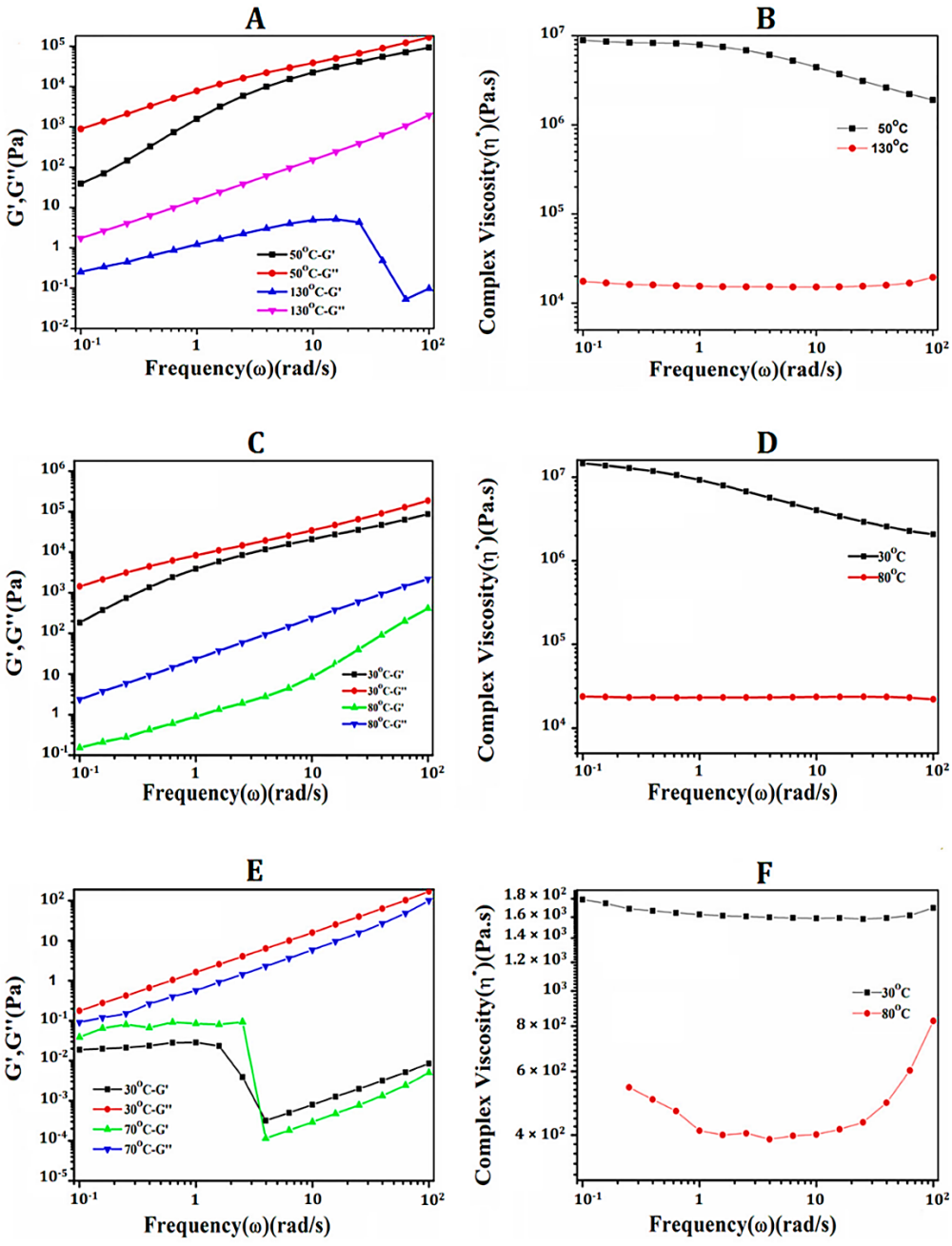

Figure 21. Variation in storage modulus (G′), loss modulus (G″), and complex viscosity (η*) of styrene-PDPMA copolymers of varying styrene content at different temperatures. (Strain rate: 0.5%). Feed ratios for figures are, (A, B)—Styrene $_{70}$–PDPMA $_{30}$, (C, D)—Styrene $_{50}$–PDPMA $_{50,}$ and (E, F)—Styrene$_{30}$–PDPMA $_{70}$.

With increased PDPMA content in the copolymer feed, the resulting copolymers' storage modulus (G') and complex viscosity (η*) decreased. The copolymer containing 70 wt% PDPMA had a maximum measurement temperature of 80 °C, while the copolymer with 30 wt% PDPMA could be measured up to 130 °C. This difference in maximum measurement temperature was attributed to the copolymer with 70 wt% PDPMA showing a significantly lower modulus at elevated temperatures, which made data collection challenging beyond 80 °C. Conversely, with increased styrene concentration, the viscoelastic properties were better maintained at elevated temperatures, allowing data measurement up to 130 °C. Similarly, the copolymer with 70% styrene content had a minimum measurement temperature of 50 °C because the high styrene content resulted in a hard resin at lower temperatures, making data collection more feasible. Based on these observations, copolymers with higher styrene content are suitable candidates for hot melt adhesives.

3.7. Adhesion Behavior Styrene- PDPMA copolymer

The copolymers' lap shear strength (LSS) and peel strength (PS) adhesion properties were assessed using ASTM standards D1002-10 and D903-98, respectively. The investigated copolymers contained 70%, 50%, and 30% wt% styrene. Test specimens were prepared using kraft paper and polyethylene terephthalate (PET) as substrates. However, the 30% wt styrene sample showed inadequate adhesive strength on all substrates, rendering it unsuitable for further testing. Table 15 summarises the results obtained for copolymers with 70% and 50% styrene content.

Table 15. Adhesion properties of styrene-PDPMA copolymers on different substrates.

	S_{70} $PDPMA_{30}$		S_{50}-$PDPMA_{50}$	
Substrate Tested	Lap Shear Strength (Pa)[a]	Peel Strength (Pa) [a]	Lap Shear Strength (Pa) [a]	Peel Strength (Pa) [a]
Paper-Paper	3.93×10^5	1.75×10^4	1.5×10^5	2.5×10^3
PET-PET	6.0×10^4	2.25×10^3	2.91×10^4	2.22×10^3
Paper-PET	3.67×10^5	2.25×10^3	3.23×10^5	1.3×10^3

a = peel strength or lap shear = load (N)/bonded area (mm2) and in both case adhesion area is 25 × 25 mm2.

Table 15 illustrates the impact of varying styrene concentration on lap shear strength (LSS) and peel strength (PS) for different substrates. When the styrene concentration decreased from 70% to 50% wt%, the LSS on the paper substrate decreased by approximately half, while the PS increased by six times. At 70% styrene concentration, the LSS on the mixed substrate (paper-PET) was 367,000 Pa, and it showed only a minor decrease at 50% styrene content, with the PS values decreasing by about half. As a result, the highest lap shear strength values were achieved at 70% styrene content for both paper-paper and mixed substrates (paper-PET). On the paper substrate, the maximum peel strength was attained at 70% styrene content, and it decreased at

50% styrene content, with minimal variation on other substrates. For the copolymer with 70% styrene content, the lap shear strength consistently surpassed the peel strength in all cases. In conclusion, the adhesion properties were composition-dependent, indicating that the adhesion characteristics can be tailored through the styrene-co-PDPMA process.

4. CONCLUSION

The ATRP behaviour of styrene and PDPMA at varying monomer feed ratios was investigated in this study. The reactivity ratios of copolymers were determined using ^{1}H NMR composition data and the copolymer composition data obtained from FR-KT methods. The results indicate a preference for styrene copolymerization with an alternation tendency, and the resulting copolymer was highly styrene-rich regardless of the feed composition. Based on the reactivity ratio values, it is suggested that the sequence length of the PDPMA is inconsistent and that the styrene sequence's length decreases with the rise in PDPMA feed content. GPC molecular analysis reveals copolymer weight and polydispersity variations based on feed composition, indicating variations in copolymer properties. Depending on the feed composition, the molecular weight of the copolymer varied between 3000–32,000 g/mole and its polydispersity between 1,319 - 2,19. Variations in glass transition behaviour and improved thermal stability with increasing styrene concentration were seen in copolymers prepared from different feed compositions. TEM morphological analysis hinted at a phase-separated structure. Rheological tests show styrene and PDPMA copolymerization suggest tunability in adhesion properties, making them useful in hot melt adhesives.

CHAPTER IV.

ATR COPOLYMERIZATION OF STYRENE AND CARDANYL ACRYLATE (CA)

ABSTRACT: The present study deals with the copolymerization of styrene and cardanyl acrylate (CA) using Atom Transfer Radical Polymerization (ATRP) at different monomer feed ratios. The CA monomer synthesized from cardanol underwent structural characterization using ^{1}H-NMR, ^{13}C, and mass spectrometry. The reactivity ratios of the copolymers were determined based on ^{1}H NMR composition data and copolymer composition data obtained from the FR-KT methods. The findings reveal that, despite an increase in CA percentage in the feed, styrene preferentially copolymerizes with an alternation tendency, resulting in a styrene-rich copolymer at all feed compositions. Sequence length calculations, utilizing reactivity ratio data, indicate that while CA's sequence length remains constant, styrene's sequence length decreases with rising CA concentration in the feed. Gel permeation chromatography (GPC) analyses demonstrate that the molecular weight and polydispersity of the copolymers are influenced by the feed content, with molecular weights varied from 2551 g/mol to 6934 g/mol and polydispersity values ranging from 1.18 to 3.45 based on monomer feed ratios. The copolymer's glass transition behaviour varied with the feed composition, with increased styrene content leading to enhanced thermal stability. Thermogravimetric analysis (TGA) was conducted from -50 °C to 200 °C at a heating rate of 10 °C/min, showing maximal stability in copolymers with high styrene contents (90, 70, and 50 wt %). Transmission electron microscopy (TEM) analysis shows a phase-separated core-shell morphology consisting of aromatic, electron-rich styrene and crystalline CA-derived domains. Adhesion studies demonstrated that load-bearing capacity increased proportionately with higher styrene concentration. In conclusion, the ability to tune adhesion properties through styrene-CA copolymerization suggests potential applications. The comprehensive structural characterization presented herein is crucial for developing environmentally friendly methods that leverage the unique properties of stiff benzene rings and the flexible C_{15} alkyl chains in the cardanol. Thus, CA presents an environmentally friendly alternative to petroleum-based monomers for producing curable coatings with a substantial proportion of bio-based material.

1. INTRODUCTION

Bio-based materials are essential in promoting sustainability across industries like textiles, food, and plastic packaging because they reduce environmental impact throughout the product life cycle. Developing efficient processes is paramount to optimize the physicochemical properties of these materials for specific applications, with a particular focus on enhancing mechanical strength through matrix cross-linking.[138] Recent research efforts are dedicated to creating bio-based products that are both sustainable and economically viable while also striking a balance with petroleum-based materials. This research direction aims to harmonize the utilization of renewable resources with the existing landscape of petroleum-derived materials, thus fostering a dynamic equilibrium between environmental responsibility and industrial viability.

Various techniques synthesize controlled molecular weight and polydispersity cardanyl acrylate prepolymers and copolymers with styrene or other acrylates. These polymers offer excellent adhesion and gloss, making them suitable for inks, coatings, and adhesives.[144,145] ATRP chemistry is compatible with several functional groups, enabling the controlled synthesis of diverse functional polymers. The mechanism of reactions involves a rapid exchange between propagating radicals and dormant species, maintaining low concentrations and inhibiting termination and transfer processes.[52] The versatility of ATRP has been demonstrated through the successful production of various block copolymers and functional polymers (e.g.; styrene-allyl methacrylate) and other well-defined acrylic polymers for coatings, garnering attention for their potential applications.[146]

This study aims to prepare CA monomer from cardanol and demonstrate the synthesis of cross-linkable polycardanyl acrylate (PCA) and styrene-CA copolymers using an ATRP method. The study involves ATRP of styrene and CA at different feed ratios, resulting in the production of copolymer (sty-co-CA) with controlled molecular weight (M_W) and narrow polydispersity index (PDI). The chemical structure of the CA monomer was confirmed through FT-IR, ^{1}H NMR, and ^{13}C NMR spectroscopy. Structural characterization of the copolymers was conducted using ^{1}H NMR spectroscopy, and molecular weight determination was performed using size exclusion chromatography (SEC). The thermal properties of the copolymers were assessed using differential scanning calorimetry (DSC) and thermogravimetric analysis (TGA). The adhesive qualities of the copolymers on two different substrates, Kraft paper and polyethylene terephthalate (PET) sheet, were evaluated. Adhesion parameters were assessed using ASTM standards (D1002-10 and D903-98). Thus, in this investigation, a CA monomer was successfully synthesized and employed as a reactive diluent in the formulation of UV-curable coatings with a substantial proportion of bio-renewable content. This approach was adopted to address the drawbacks mentioned earlier.

2. EXPERIMENTAL TECHNIQUES AND METHODOLOGIES

2.1. Materials

As described in Chapter 2, Table 3, page no. 58-68

2.2. Methods

2.2.1. Polymerization of Cardanyl acrylate (CA)

A typical ATRP procedure, as previously described in Chapter 3, was used to homopolymerize cardanyl acrylates, as indicated in **Scheme 13**. Using the ATRP technique, the initiator ethyl-2-bromo-isobutyrate, and a copper (I) bromide complexed PMDETA catalyst, the poly cardanyl acrylate was created. The structures of the homopolymers are displayed in **Schemes 13**.

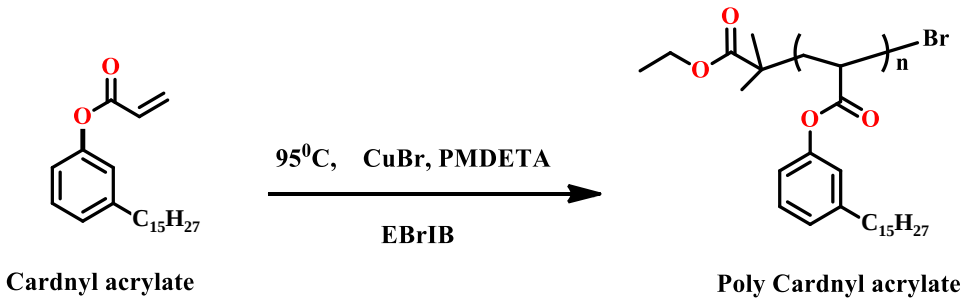

Cardnyl acrylate

Poly Cardnyl acrylate

Scheme 13. Scheme of the homopolymerization of cardanyl acrylate via ATRP.

In a typical experiment, 10 g (0.03 mol) of cardanol is dissolved in 25 ml of dimethylformamide (DCM) in a 250 ml double-necked R.B. flask equipped with a dropping funnel and the mixture is stirred to produce a homogenous solution. The previously indicated homogenous mixture was now given 4.6 ml of T.E.A at a temperature of 0-5°C, and then 2.7 ml (0.03 mmol) of acryloyl chloride was added to the flask dropwise using a funnel, all while stirring constantly and maintaining a temperature of 0-5°C. Three hours were allowed for the reaction to be at a temperature range of 0-5°C, and then the reaction continued for 12 hours to proceed at the same temperature. Excess water was used to wash the product until the washings were neutral when tested with litmus paper. The product was dried over anhydrous sodium sulphate after being extracted with DCM and diethyl ether, and the solvent was then evaporated at low temperature and pressure. Hexane was used as the eluent for column chromatography to purify the residue. The ^{1}HNMR study confirmed the presence of the synthesized monomer, and the yield was attained at 60.3%.

2.2.2. Synthesis of Styrene-Co-CA

In a one-step polymerization, both monomers are introduced sequentially and the polymerization is carried out. Styrene and Cardanyl acrylate have mole ratios of (90:10), 70:30, and 50:50, respectively. CuBr (0.00028 mol), PMDETA (0.00057 mol), and the monomers Styrene and Cardanyl acrylate were used in a 90:10 mol ratio for the standard ATRP experiment. Styrene (0.0259 mol) and Cardanyl acrylate (0.00288 mol) were added to a two-neck R.B. flask and swirled magnetically until homogenous. The flask was then purged with argon gas for 15 minutes and expelled the gas before being sealed using multiple freeze-thaw cycles. Then, inject the ethyl-2-bromo-isobutyrate (0.00028 mol) initiator using a syringe. Polymerization was performed for 14 hours at 95ºC. Similarly, the remaining three-mole ratios of 70:30 and 50:50 were maintained. The obtained viscous solution was diluted with THF (3 ml). Subsequently, the catalyst was removed by column chromatography and the polymer was recovered through precipitation in a methanol and water mixture (75:25). The procedure was repeated thrice and then the product was dried at 60 °C under vacuum for 6 hours. The polymer structure was verified using NMR.

3. RESULTS AND DISCUSSION

3.1. Structural Elucidation of CA monomer (^{1}H-NMR, ^{13} C NMR & mass spectroscopy)

The primary objectives of this study were twofold: to develop copolymers derived from cardanol and to evaluate how copolymerization influences adhesion and viscoelastic properties. The successful synthesis of the CA monomer from cardanol was achieved, and its characterization was carried out using ^{1}H-NMR, ^{13}C NMR, and mass spectroscopy. The ^{1}H NMR spectrum of the CA monomer (**Figure 22**) unveiled crucial insights into its chemical structure. All the observed peaks for cardanol and CA corresponded to their respective chemical structures. In the cardanol spectrum, the chemical shifts at 6.7–7.3 ppm were attributed to the protons on the benzene ring, while the peak at 5.46 ppm was indicative of the protons associated with C=C in the side chains. Notably, in the CA spectrum, new peaks emerged at 5.99, 6.31, and 6.57 ppm, and these were assigned to the protons originating from the acrylic groups introduced during the synthesis.

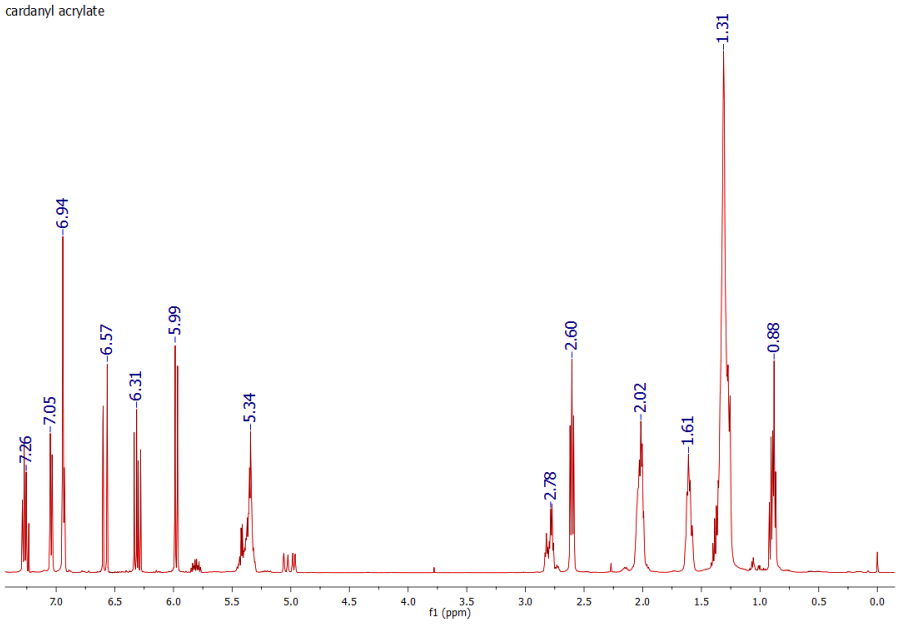

Figure 22. The ^{1}H NMR spectrum of CA monomer.

The ^{13}C NMR spectra of CA are depicted in **Figure 23**. In the cardanol spectrum, the peaks ranging from 112.9 to 156.3 ppm were associated with the unsaturated carbons located on the benzene ring and the aliphatic section of cardanol. The presence of the $CDCl_3$ solvent used in the NMR measurement was indicated by the peak at 77.2 ppm. Furthermore, the peaks at 25.5–35.7 ppm and 13.2 ppm corresponded to the methylene and methyl carbons present in the aliphatic segment, respectively. In the CA spectrum, new shifts at 164.4 and 132.3/125.6 ppm were conspicuous, signifying the existence of carbonyl carbons and unsaturated carbons attributed to the incorporated acrylate structure. These findings collectively support the successful introduction of the acrylic structure onto the cardanol molecule.

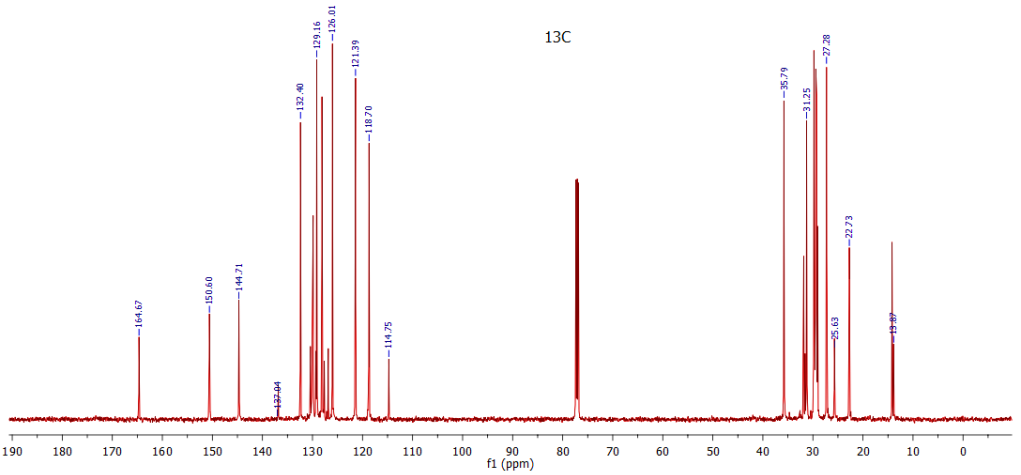

Figure 23. The ^{13}C NMR spectrum of CA monomer

Mass spectrometry further confirmed the monomer molecular mass (**Figure 24**). The molecular ion peak at 390.6 corresponds to the molar mass of the ammonium adduct (m/z +18.039 g/mole), while the peak at 375 was assigned to the proton adduct (m/z+1).

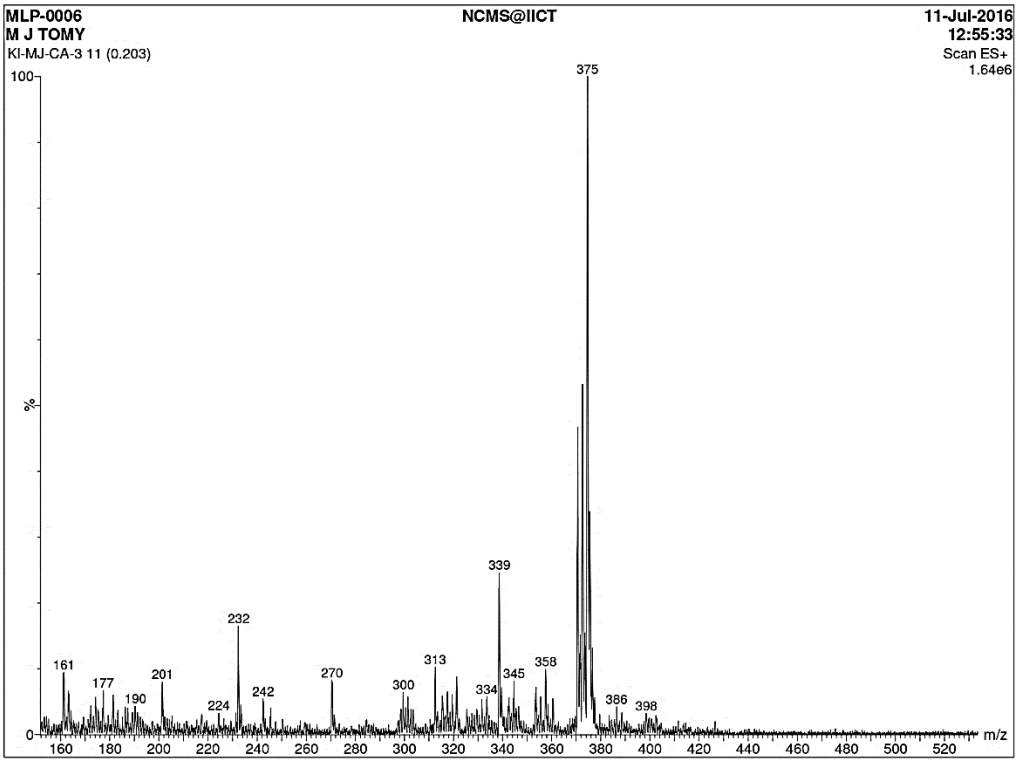

Figure 24. The mass spectrum of CA monomer.

3.2. Synthesis and Characterization poly-CA

Since CA did not homopolymerize quickly, the reaction mixture took 14 hours to become completely viscous. However, under the same circumstances, styrene homopolymerization produced an approximate 7% conversion in less than 30 minutes. **Figure 25** depicts the typical ^{1}HNMR spectrum of the CA homopolymer produced by ATRP. The elimination of the acrylic proton peaks was the main variation in ^{1}HNMR following polymerization compared to **Figure 22**. The characteristic resonance signals observed for the homo polymer are seen at δ = 6.8–7.14 ppm as the broad peak for the phenyl protons, δ 2.3 ppm for –CH_2–Ph of C_{15} alkyl side chain, δ 5.4 ppm for Olefinic protons on the side chain of the aromatic ring (Ph–CH_2–CH_2–), the internal protons of the alkyl side chain appear at δ 1.2 ppm as a broad peak, and the peak at δ 0.83 ppm is attributed to the terminal -CH_3 protons of the alkyl side chain.

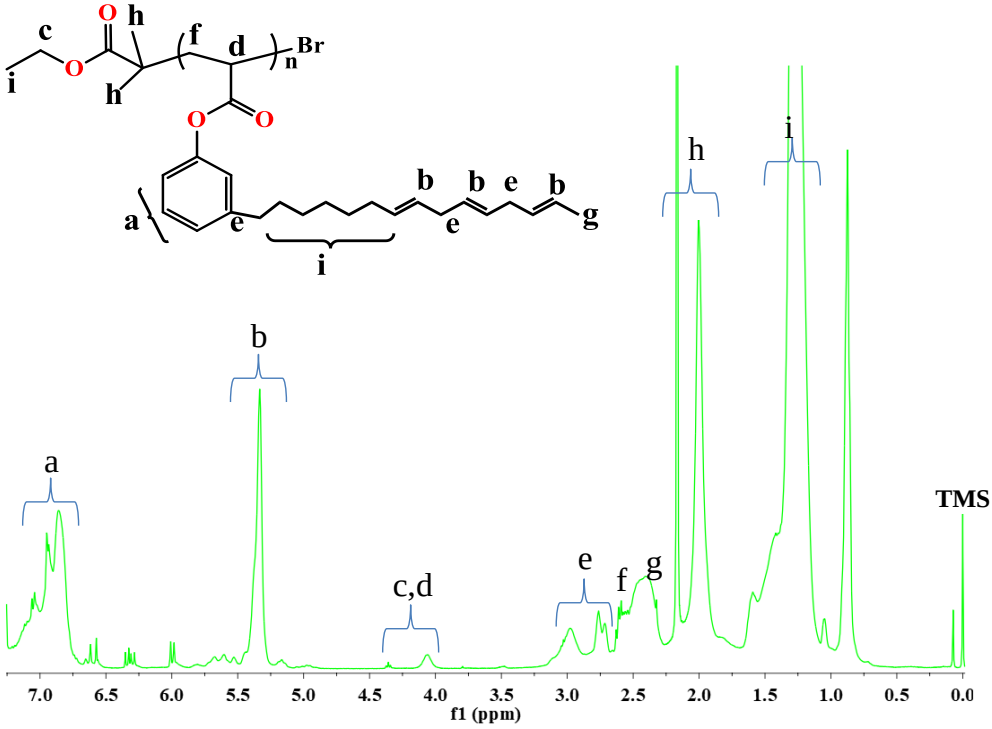

Figure 25. ^{1}H NMR spectrum of polycardanyl acrylate (poly CA).

Styrene-co-cardanol acrylates, were synthesized with different monomer ratios using ethyl-2-bromo-isobutyrate as the initiator and a copper (I) bromide complexed PMDETA catalyst. The copolymerization process was conducted through bulk ATRP at a temperature of 95 °C. **Scheme 14** depicts the structures of the copolymers that were successfully synthesized during this process. **Tables 16 & 17** provide an overview of the styrene-CA copolymer composition, properties produced via ATRP, and the corresponding yield.

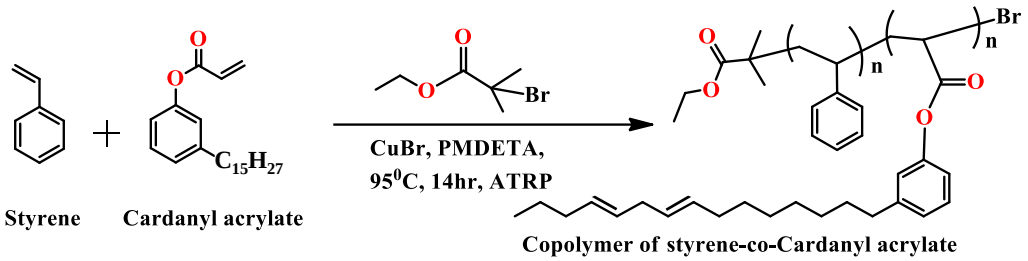

Scheme 14. Schematic of the copolymerization of styrene-cardinal acrylate via ATRP.

Table 16: Composition and characteristics of styrene (St)-CA copolymers synthesized via ATRP.

Sample Code	Composition				SEC		M_n Theory	PDI
	Feed		^{1}H NMR		M_w g/mole	M_n g/mole		
	St	CA	St	CA				
PS	100	0	100	-	3012	2551	3112	1.18
CA	0	100	-	100	10846	4562	7,617	2.37
$StyCA_{10}$	90	10	-	-	23467	16818	24780	1.39
$StyCA_{30}$	70	30	77.05	22.95	80044	62588	25204	1.27
$StyCA_{50}$	50	50	54.32	45.68	25983	16963	18024	1.53
$StyCA_{70}$	30	70	38.64	61.36	25436	9257	19142	2.74
$StyCA_{90}$	10	90	24.17	75.83	23944	6934	16,970	3.45

Note: $M_{n\ Theory}$ was calculated using the relation $\frac{[M]o}{[I]o}$×conversion × repeat unit mol. wt.

Table 17. The yield of Styrene-cardanol acrylate copolymer composition.

Sample code	[Styrene]: [CA]	Conversion (%)
Sty_{90}-co- CA_{10}	90:10	70.2
Sty_{70}-co- CA_{30}	70:30	71.4
Sty_{50}-co- CA_{50}	50:50	51.06
Sty_{30}-co- CA_{70}	30:70	38
Sty_{10}-co- CA_{90}	10:90	33
CA	100	24.5

1= [M]: [CuBr]: [PMDETA]: [I] = 100:1:2:1 and 20h at 95°C.

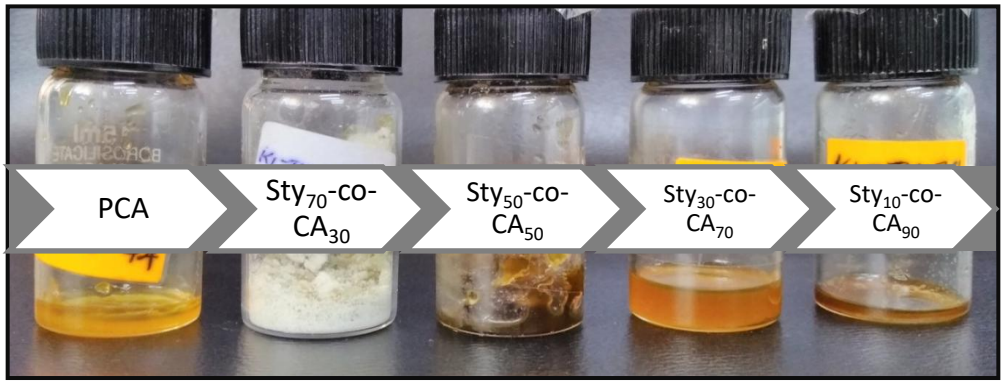

Figure 26. Photographs provide visual confirmation of the synthesis of essentially colored sty-CA copolymers with varying monomer feed ratios.

To examine the viscosity buildup and ensure that considerable conversion was achieved, the copolymerization tests were run for 14 hours. By integrating the peaks indicative of styrene and cardanyl acrylate, the composition of the copolymer was determined and the copolymer structure was validated by ^{1}H NMR (**Figure 27**).

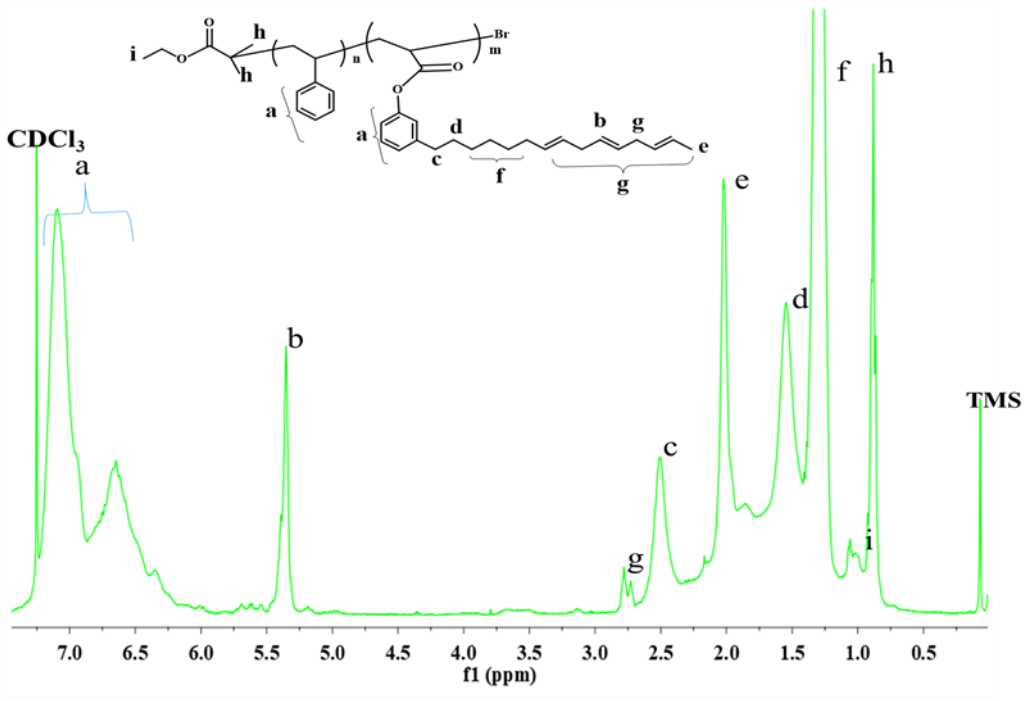

Figure 27. ^{1}H-NMR spectrum of styrene-CA copolymer (in the feed ratio 70:30) in $CDCl_3$.

The NMR spectrum revealed broad peaks between δ 7 and 7.4 ppm, corresponding to the phenyl ring protons of both monomers. A peak at δ 5.4 ppm indicated the presence of olefinic protons in the aliphatic side chain adjacent to the phenyl ring of cardanyl acrylate. The internal protons of the alkyl side chain appeared as a broad peak at δ 1.2 ppm, while the peak at δ 0.83 ppm was attributed to the terminal -CH_3 protons of the alkyl side chain. Copolymers synthesized with cardanol showed peaks due to unsaturation in the side chain of cardanol [δ 4.9–5.4 ppm]. The composition data obtained from ^{1}H NMR and the feed composition presented in **Table 16** indicated that the copolymers had lower cardanyl acrylate content than the feed. The reactivity ratios (r_1, r_2) were calculated using the F-R and K-T methods based on the composition data, and the corresponding plot is depicted in **Figure 28**, with the values tabulated in **Tables 18 & 19.**

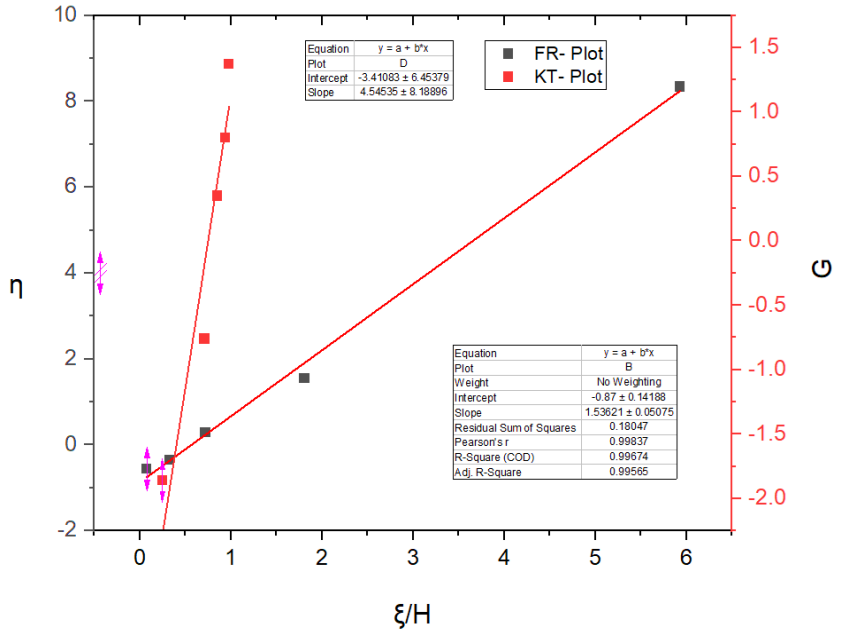

Figure 28. Fineman-Ross and Kelen-Tudos plot to determine reactivity ratio in the copolymerization of styrene and CA.

Table 18. Finemann-Ross (FR), and Kelen-Tudos (KT) parameters for styrene-co-CA.

Styrene: CA Composition		M=	P=	M/P	G	H	α + H	η	Ξ
Sample	^{1}H NMR	M_1/M_2	m_1/m_2						
$StyCA_{10}$	93.17: 06.83	9.00	13.64	0.66	8.34	5.93	6.05	1.37	0.98
$StyCA_{30}$	75.05: 24.95	2.33	3.00	0.776	1.55	1.81	1.93	0.80	0.94
$StyCA_{50}$	58.32: 41.68	1.00	01.39	0.71	0.29	0.72	0.84	0.35	0.85
$StyCA_{70}$	35.64: 64.36	0.43	0.55	0.78	-0.35	0.33	0.46	-.76	0.71
$StyCA_{90}$	14.17: 85.83	0.11	0.16	0.67	-0.56	0.076	0.30	-1.86	0.25

$(\alpha = H_{min} \times H_{max})^{1/2}$ i,e = 0.48, $G = M - M/P$, $H = M^2/P$, $\eta = G/(\alpha + H)$, $\xi = H/(\alpha + H)$.

Table 19. The reactivity ratio of styrene (r_1) and CA (r_2) was determined by different methods.

Methods Used	r_1 (Styrene)	r_2 (CA)	r_1:r_2
FR	1.5462	0.87	1.3451
KT	4.1712	-2.1317	-7. 0629

The reactivity ratio for styrene (r_1) was higher than that of CA (r_2), indicating a tendency towards random copolymerization. The product of $r_1 \times r_2$ was close to zero and less than 1, suggesting a higher chance of styrene incorporation with a tendency to alternate. The F-R and K-T methods determined the average values of r1 and r_2 as r_1=2.63 and r_2=-6.7178, respectively. These values imply that the styrene-type radical (S*) slightly prefers homopolymerization over copolymerization. On the other hand, the r2 value indicates that CA has a very low preference for homopolymerization.

Consequently, styrene tends to enter the copolymer more easily than CA, resulting in long sequences of styrene units throughout the entire composition range studied. The sequence length analysis based on the reactivity ratio (as shown in **Table 20**) suggested a higher styrene sequence length (I_1) when the styrene content in the feed was high. In contrast, the CA sequence length (I_2) remained relatively constant, indicating its reduced tendency for copolymerization or homopolymerization, resulting in an inability to form long sequences of CA units.

Table 20. The monomer composition and sequence length ratio.

Monomer Feed Styrene: CA	M_1/M_2	M_2/M_1	l_1	l_2	l_1:l_2
70:30	2.33	0.43	3.00	2.01	4.05
50:50	1.00	1.00	01.39	2.44	2.82
30:70	0.43	2.33	0.55	1.40	2.22

The values were calculated using r_1=0.896, and r_2=0.018 obtained by the FR method.

The composition data obtained from ^{1}HNMR (as shown in **Table 16**) further corroborates this finding, indicating that the content of cardanyl acrylate (CA) in the copolymer remained relatively low, even with an increase in the feed concentration. This observation suggests that cardanyl acrylate has a reduced tendency for homopolymerization when co-polymerized with styrene. The difference in behaviour could also be attributed to the use of different initiating systems. It is known from the literature that mechanisms of conventional radical polymerization and ATRP differ due to the challenges in forming the polar catalyst complex with monomers possessing a non-polar side chain. This circumstance is relevant to the current instance due to the hydrophobicity of monomer due to its 15-carbon alkyl side chain.

3.3. Molecular Characterization of Sty-co-CA by size exclusion chromatography (SEC)

Table 16 lists the molecular weights and polydispersity values of the synthesized homopolymer and copolymer obtained from SEC curves. A mobile phase made of polystyrene standards in THF was used for the study. The molecular weight of the copolymers ranged from 3012 to 23944, and the values for polydispersity were 1.18 to 3.45. Except for styrene homopolymerization, all cases exhibited deviations from the theoretically calculated molecular weights. These deviations increased with higher CA content in the feed. The observed variations in the characteristics of Sty-co-CA can be attributed to the presence of the 15-carbon alkyl chain in CA, which acts as short branches. This leads to a more compact polymer structure, resulting in a smaller hydrodynamic volume and reduced molecular weight. The relationship between hydrodynamic radius, branching and molecular weight or intrinsic viscosity has been previously documented[143]. Similar findings can be seen in the synthesis of styrene-ethyl hexyl acrylate copolymers by the ATRP method[114]. **Figure 29** illustrates the changes in molecular weight distribution as CA concentration increases. SEC also showed variations in the polydispersity values obtained with increased CA content in the copolymer. Similar results were obtained in a recent copolymerization investigation of Styrene-co-PDPMA that was previously reported. The copolymers synthesized exhibit narrow polydispersity and controlled molecular weights.

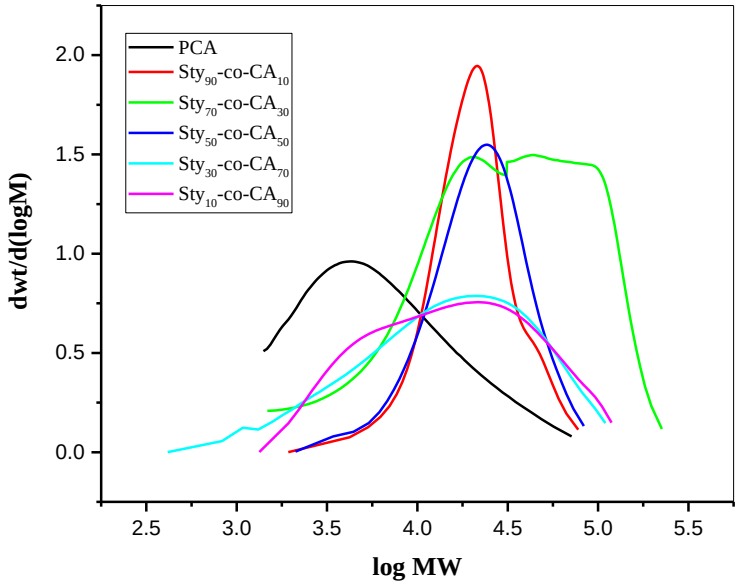

Figure 29. dwt/dlogM vs. log $M_w$plots of styrene-CA copolymers showing variation in mol.wt.distribution as a function of the feed composition.

The distribution was narrowest for the homopolymer of polystyrene, and it became more so with increasing CA concentration, suggesting either a lack of control over the polymerization or the presence of branched structure.

3.4. Glass Transition Behavior of Styrene-CA Copolymers

The DSC results for styrene-CA copolymers at the glass transition are shown in **Figure 30**. A small endotherm at 94 °C was visible at 50 weight percent CA concentration. An enhanced side chain melting transition was anticipated upon increasing the CA content, but the copolymer exhibited a broad glass transition without a distinct endothermic melting peak. The glass transition was evident as a baseline shift at approximately 10 °C, although crystalline melting-like transitions were not observable. As expected, the glass transition temperature (Tg) decreased with increased CA concentration within the copolymer. Previous studies have indicated that the presence of crystallizable side chains, as in the case of CA, can result in additional melting transitions, distinct from the glass transition, as in comb-like polymers of n-alkyl acrylate polymers. The Tg generally coincides with the melting transition, characteristic of side-chain crystallizable polymers. Overall, a softening effect was observed at 50 wt% CA, whereas at 70 wt% CA, the crowding of alkyl chains promoted crystallization.

Interestingly, at 70 wt% CA, crystallization was less favoured, although the exact cause for this phenomenon could not be elucidated in the current investigation. Notably, these crystallites comprisen-alkyl groups extending from the molecules' backbones, rather than individual backbone segments. A two-phase structure resembling packed alkyl crystalline domains (Similar phase separation to the LHS of **Scheme 12**, **CHAPTER 3**) dispersed in the amorphous matrix is created if crystallization is encouraged in the copolymer. Alkyl chains on two distinct chains are interdigitated, as seen on the RHS of **Scheme 12**.

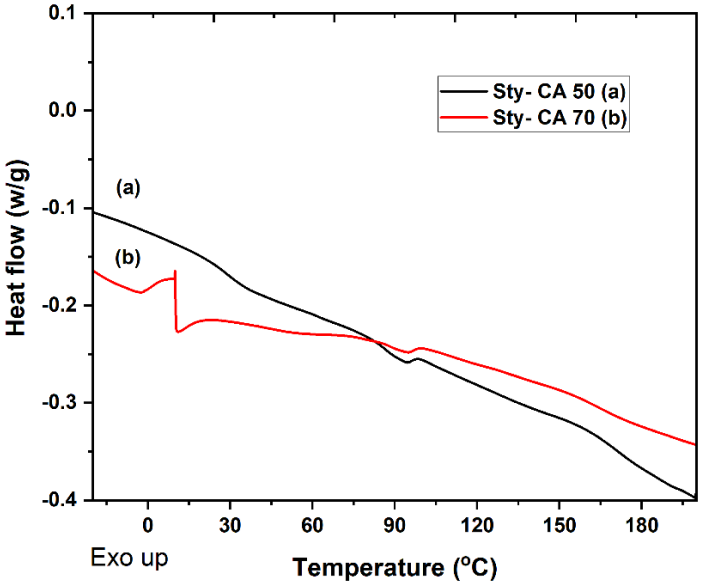

Figure 30. DSC curves of Styrene-CA copolymers synthesized via one-pot ATRP copolymerization (The T_g of poly (CA) was =1 °C and polystyrene = 106 °C).

Transmission electron microscopy (TEM) was used further to confirm this phase-separated domain structure noticed. TEM analysis reveals nanoparticle size, shape, distribution, phases, and domains in copolymers, revealing phase separation, crystalline regions, and specific nanostructure formation. A phase-separated core-shell structure composed of aromatic, electron-rich styrene domains and crystalline (light colour) domains is confirmed by TEM images of Sty-CA_{70} (**Figure 31**). Visualizing the microstructure copolymer provided valuable insights into properties and behaviour, aiding in understanding the potential applications and optimizing performance in the synthesised copolymer's adhesives, coatings, and industrial fields.

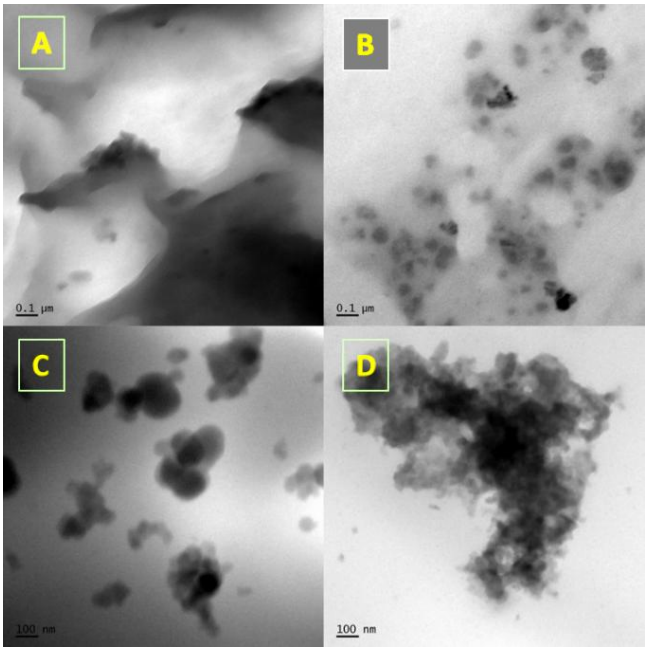

Figure 31. TEM images of Sty-CA-70 demonstrate the presence of a phase-separated domain structure, with the light-colored domains derived from the CA segments.

3.5. Thermal Stability of Copolymers

Thermogravimetric analysis (TGA) was performed to evaluate the thermal stability of the copolymers within the temperature range of 50 °C to 200 °C, with a heating rate of 10 °C min^{-1}. **Figure 32** shows representative weight loss curves and derivative thermograms for copolymer samples with different monomer feed ratios (90, 70, 50, 30, and 10 wt%). Copolymers with higher styrene concentrations (90, 70, and 50 wt%) exhibited superior thermal stability. However, at elevated CA concentrations, a decrease in thermal stability was observed, likely attributed to the presence of polar carbonyl groups that render the copolymer more susceptible to degradation. Conversely, at higher styrene concentrations, the thermal stability was enhanced, likely due to the contribution of the phenyl group.

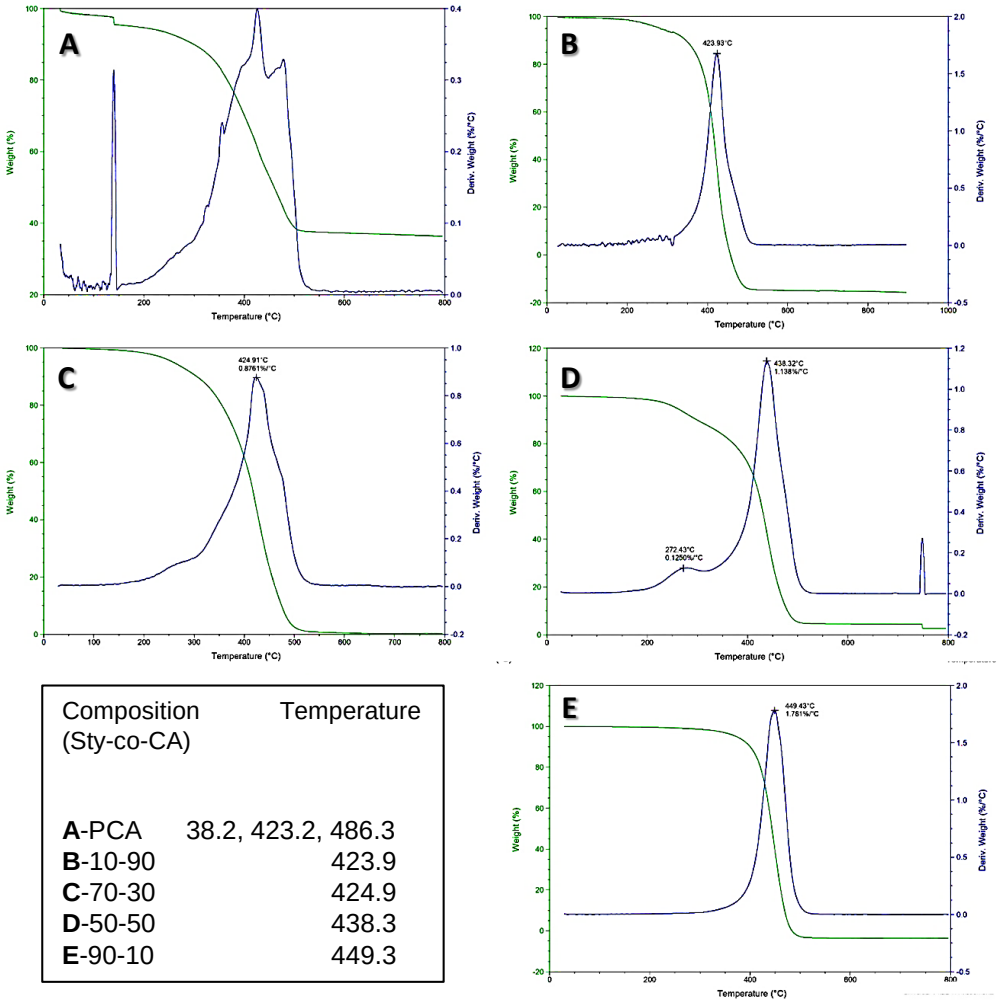

Composition (Sty-co-CA)	Temperature
A-PCA	38.2, 423.2, 486.3
B-10-90	423.9
C-70-30	424.9
D-50-50	438.3
E-90-10	449.3

Figure 32. Thermal degradation properties of styrene-CA copolymers (**A**) weight loss curve and (B) derivative plot.

3.6. Adhesion Behavior of Styrene- CA copolymer

After noticing an increase in the tack and modulus values, the study looked into the adhesion properties of the sty-CA copolymer. The adhesive performance on two different substrates, Kraft paper, and polyethylene terepthalate (PET) sheet, were examined. The adhesion characteristics, including lap shear strength (LSS) and peel strength (PS), were assessed based on the ASTM standards (D1002-10 and D903-98) on different substrates. In addition to identical substrates like paper-paper and PET-PET, the bonding of PET to paper was studied. Styrene concentrations of 70%, 50%, and 30% in the copolymers were tested. The sample with 30% styrene showed minimal adhesive strength, making it impossible to analyze. **Table 21** below summarizes the findings for copolymers with 70 wt% and 50 wt% styrene content.

Table 21. Styrene and CA copolymer adhesion characteristics on various substrates. Results of peel strength and lap shear strength on paper-paper, PET-paper, and PET-PET substrates as a function of various monomer concentrations.

	S_{70} CA_{30}		S_{50}-CA_{50}	
Substrate Tested	Lap Shear Strength (Pa)[a]	Peel Strength (Pa)[a]	Lap Shear Strength (Pa) [a]	Peel Strength (Pa)[a]
Paper-Paper	2.47×10^5	1.15×10^4	1.3×10^5	2.13×10^3
PET-PET	5.72×10^4	2.17×10^3	2.77×10^4	1.90×10^3
Paper-PET	2.22×10^5	1.95×10^3	2.65×10^5	1.16×10^3

[a] = peel strength or lap shear = load (N)/bonded area (mm^2) and in both case adhesion area is 25×25 mm^2.

In general, the lap shear and peel strength of polyester (PET) substrates were greater than those of Kraft paper, and the copolymer demonstrated an increase in adhesion strength when the weight percent styrene content was increased. The increase in lap shear strength is almost tenfold on paper substrates, whereas, on PET substrates, the increase is approximately four times at the same styrene loading. The peel strength significantly decreased by approximately six times as the styrene concentration was reduced from 70% to 50% wt (**Table 21)**. The lap shear strength on paper substrate decreased from 247,000 Pa to nearly half. At 70% styrene, the lap shear strength was 222,000 Pa on the combined substrate (paper-PET), and there was a minimal change at 50% styrene, but the peel strength values decreased by almost half. The study determined themaximum lap shear strengths on paper-paper and mixed substrates (paper-PET) containing 70%styrene. On paper substrates, the maximum peel strength was attained at a styrene concentration of 70% weight, and on other substrates, the value was reduced to 50% weight without noticeablychanging the peel strength. In all cases, the lap shear strength was greater than the peel strength for the copolymer with 70% styrene content. Due to bonding failure, the peak strength tests withthe homopolymer (styrene and CA) were unsuccessful. Thus, the value is set to zero for styrene and CA. When the styrene content rises, the load-bearing capacity increased proportionately. In conclusion, the observed changes in adhesion properties with varying compositions highlight the tunability of adhesion characteristics achieved through the copolymerization of styrene and CA.

4. CONCLUSIONS

This research centres on cardanol, a sustainable organic resource derived from the cashew industry. The study devised a unique and synergistic approach by grafting acrylic groups onto styrene via ATR polymerization to develop oil-based copolymers with enhanced properties. This polymerization process offers the potential to create polymeric materials from renewable sources in an environmentally friendly and straightforward manner, aligning with "green" chemical principles. The resulting styrene-co-cardanol copolymers exhibit stiff bioplastic characteristics, high crosslink densities and exceptional properties. ATRP was used at different monomer feed ratios to study styrene-co-CA behaviour. The copolymer reactivity ratios were calculated using ^{1}H NMR composition data and the copolymer composition data obtained from FR-KT methods. Findings show that styrene copolymerizes preferentially with an alternation tendency regardless of feed content. Besides, the resultant copolymer is rich in styrene content. Based on the reactivity ratio data, it can be concluded that the sequence length of CA remains relatively constant. Still, the sequence length of styrene decreases as the concentration of CA in the feed increases. SEC analysis reveals that the molecular weight and polydispersity of the copolymers vary with the feed content. Depending on the composition of the feed mix, the molecular weight and polydispersity of the resulting copolymer ranged from about 3,000 to 32,000 g/mole and from about 1.18 to 3.45, respectively. Enhanced thermal stability of the copolymer has been achieved with increasing styrene content, while glass transition behaviour varied with feed composition. A phase-separated morphology was found by TEM examination. Studies of rheology and adhesion suggest that styrene and CA copolymers may be effective in hot melt adhesives by modifying their adherence qualities. The structural characterization of cardanol is crucial for eco-friendly processes in the sustainable chemical industry. With its diverse unsaturation degrees, CA can create curable coatings with high biobased content, replacing petroleum-based monomers.

CHAPTER-V

DISCUSSION ON STUDY OUTCOME - EVALUATION ON ATRP SYNTHESIS OF CARDANOL-BASED MONOMERS AND POLYMERS SYNTHESIZED VIA ATRP

1. STRUCTURAL, MOLECULAR AND THERMAL PROPERTIES

We previously reported the synthesis of three polymerizable monomers from cardanol using ATRP. These monomers, CA (cardanyl acrylate), PA (pentadecylphenylacrylate), and PMA (pentadecylphenylmethacrylate/PDPMA), were prepared using established protocols[144,147,148] from various sources, including author group. The study used differential scanning calorimetry (DSC) for structural characterization and thermal analysis (**Figure 33 A**). The PA monomer showed melting (T_m) at 35°C and crystallization (T_c) at 3.27°C, while the synthesized polymer had a T_m of 16.5°C and increased Tc of 7.2°C. The PMA monomer had T_m and T_c at 15.21°C and 11°C, respectively which were decreased to 1 °C and 18 °C in the corresponding polymer. The CA monomer and its polymer transitions were broader and less distinct, and high conversions were obtained through homopolymerization of both CA and PMA monomers. This outcome is likely attributed to the greater crystallinity of the PA monomer, hindering polymerization efficiency. The study aimed to analyze the polymerization of cardanol-derived monomers using ATRP, focusing on structural characterization and crystallization behavior using differential scanning calorimetry. Factors like main chain flexibility and side chain confinement were explored to understand the impact of these factors on acrylate and methacrylate monomers and polymers.[149–151] The study investigated the impact of ATRP ligands, specifically PMDETA and dNbpy, on conversion, molecular weight, and polydispersity, and the influence of monomer structure on thermal transitions in monomers and polymers.

1.1. Synthesis and characterization of monomers

Comparative analysis of spectral data was performed, corroborating the findings with literature values.[144,148,152] The study analyzed comparative ^{1}H-NMR spectral data of CA, PA, and PMA monomers, revealing characteristic proton resonances related to the phenyl ring and alkyl side chain to PDPMA **Figure 34 A**. It was noted that, the structural arrangement of the 15-carbon side chain in the meta position of the phenolic ring distinguishes conventional acrylate monomers from cardanol-based ones. Proton resonances typical of methyl-substituted acrylate and olefinic unsaturation were also observed in the ^{1}H-NMR spectra of PMA and CA (**Figure 12 & 25** respectively). The study confirmed monomer structures through ESI mass spectrometry, (**Figure 11 & 24** respectively), revealing characteristic molecular ion peaks. Thermal analysis using Differential scanning calorimetry (DSC) confirmed the alignment of alkyl side chains in cardanol-based monomers, aligning with previous literature.[153–155]

The thermal analysis of PA monomer was conducted in two cycles: heating from 50 to 150°C, cooling to 50°C, and reheating to 150°C. The thermograms showed endothermic transitions

during heating and exothermic transitions during cooling, attributed to alkyl side chain crystallization similar to n-alkyl acrylate and methacrylate monomers reported in literature.[153–155] The study found an endothermic melting peak at 35°C and a crystallization peak at 3°C. PMA is influenced by bulky methyl substituents, resulting in a shifted melting transition (T_m) at 15.21°C and a corresponding shift in crystallization transition (T_c) to 11°C, possibly due to different domain sizes of crystallites. The multiplicity in the crystallization peak of PMA might arise from crystallites with different domain sizes. The DSC analysis of CA showed a broad Tm range of -16°C to -10°C, with Tc at -40°C, confirming the organized alignment of alkyl side chains in cardanol-based monomers. Previous reports.[149,156] highlighted the self-assembly of alkyl side chains in pentadecyl phenol, a precursor in this study, forming crystalline nanodomains. CA transition temperatures were lower compared to PA or PMA. The difference in thermal transitions between PA and PMA can be attributed to the elongated conformation of alkyl side chains, promoting greater ordering and higher transition temperatures. Conversely, the unsaturated structure of CA led to chain bending, hindering orderly packing into crystallites and resulting in a broader melting peak and lower T_c value. Crystallinity and thermal behavior variations among extended-chain acrylate monomers may affect their polymerizability in controlled radical polymerization, crucial for establishing a dynamic equilibrium involving catalyst-monomer complexes, as observed in other ATRPs.[24]

1.2. Polymerization behaviour and thermomolecular properties

The study discussed on ATRP behaviour process for CA, PA, and PMA using a CuBr/amine ligand system at 95°C (**Figure 33. B**). The results show that CA achieved better conversion than PMA which showed the highest conversion within 10 hours. PA polymerization was slower, with 43% conversion. Modifying ligand concentration improved conversion rates, while increased PMDETA ligand concentration led to 87% conversion for methacrylate (PMA) and lower polydispersity. Bypyridine ligand also improved conversion rates. PMA's improved conversion was due to its reduced monomer crystallinity, facilitating interactions between monomer, ligand, and metal halide during ATRP. This is crucial for successful ATRP of extended-chain acrylates, as highlighted in existing literature. The addition of small quantity of Cu^{2+} (0.1 wt% $CuBr_2$) to ATRP led to a favourable dynamic equilibrium between catalyst-ligand and monomer, resulting in nearly complete conversion within 1-2 hours for all monomers. In terms of the ligand effect, dN showed favourable conversions and homogenous reaction mixtures, indicating enhanced complexation between monomer, ligand, and CuBr compared to PMDETA ligand. The synthesized polymers underwent purification and ^{1}H-NMR analysis, revealing unique side chain functionalities for each monomer (**Figure 34 A**). The PCA spectrum showed resonance peaks for saturated, methacrylate, and olefinic side chain moieties, depending on the monomer. The study found that monomer residual peaks in the 5.9 to 6.5 ppm range disappeared in polymers after precipitation and purification. Olefinic unsaturation of CA remained unaffected during ATRP, suggesting potential for cross-linking in photocurable systems. Previous research also demonstrated the copolymerization of CA with MMA, leading to the development of cross-linkable resins.[144] The polymerization experiments revealed significant differences in conversion and yield, while thermal analysis using DSC revealed distinct melting and crystalline transitions, distinct from monomers due to side chain crystallization.

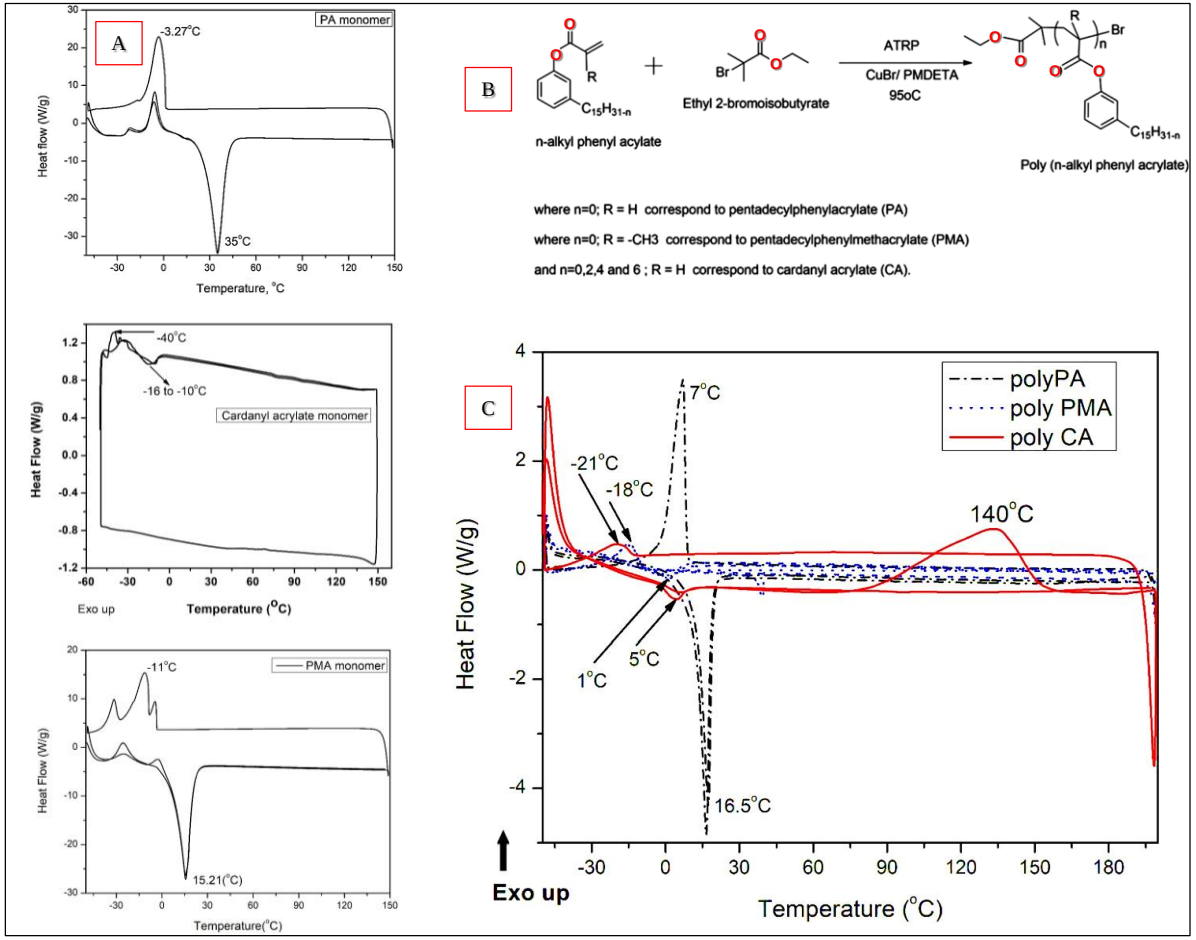

Figure 33. A. Typical thermogram of the cardanol based monomer, PA, showing endothermic melting (Tm) and crystallization (Tc) transitions of the alkyl side chain. **B.** Schematic of the synthesis of different cardanol based polymers via atom transfer radical polymerization (ATRP). **C.** The thermogram of polyPA shows endothermic melting transition and exothermic side chain crystallization peak.

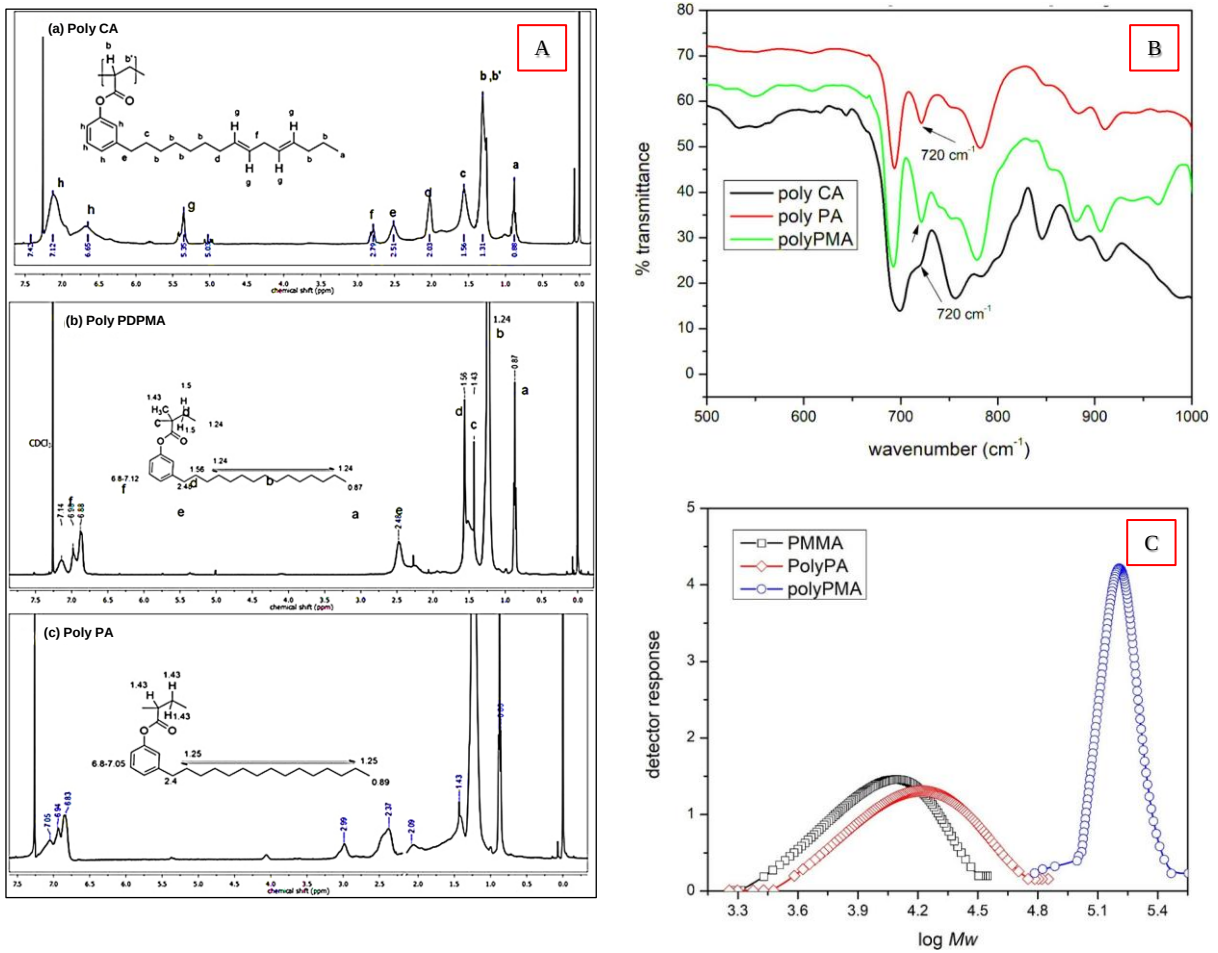

Figure 34. A ^{1}H-NMR spectrum of homopolymers of (a) cardanyl acrylate (CA) (b) pentadecyl phenyl methacrylate (PMA) and (c) pentadecyl phenyl acrylate (PA) (ATRP in bulk at 95 ˚C, using ethyl-2-bromisobutyrate initiator). **B**. Expanded portion of the IR spectra of cardanol based polymers in the region 500- 1000cm^{-1}showing characteristic band at 720 cm-1 due to crystallizing aliphatic segments. **C**. Molecular weight distribution curves of cardanol based homopolymers PA and PMA compared with PMMA homopolymer (ATRP using PMDETA ligand with M:L ratio ¼1:2).

There was lack of comparative studies on cardanol-based monomer polymerization via ATRP. Initiator efficiency was inferred from molecular weight data, with the extended conformation of side chains in PA and PMA causing greater deviations and diminishing initiator efficiency. DSC analysis was conducted to understand polymerization's impact on melting and crystallization transitions, with results shown in **Figure 33 C**. Post-polymerization, thermal transitions were observed, with PA polymer's T_m peak changing to 16.5°C and a T_c peak at 7.2°C upon cooling, while PMA polymer's endothermic Tm transition occurred at 1°C and crystallization transition at 18°C. The polycardanyl acrylate polymer (polyCA) showed a crystallization peak at 21°C and a melting/glass transition around 5-6°C. The DSC spectrum showed an exothermic transition around 140°C during the initial heating cycle likely attributed to polymerization through the side chain unsaturation of cardanyl acrylate. The DSC analysis was supported by IR spectroscopy, which detected vibration bands of aliphatic chains within crystalline domains consistent with established literature **(Figure 33 B)**.[157–159] Further analysis revealed a distinct vibration band at 720 cm^{-1}, indicating crystallizing aliphatic chains, a feature previously found in n-alkane segments.[160] The molecular weights of the polymers (as presented in Table 1.[126]) were slightly lower than theoretically calculated, likely due to the branched structure of the polymers, as linear standards were used in the SEC analysis. The molecular weight distribution (PDI) of homopolymers showed higher values for CA polymer, while PA and PMA showed narrower distributions, especially with a 1:2 catalyst/ligand ratio, influenced by ligand ratio and conversion. Distribution plots for PA and PMA in comparison with PMMA homopolymers were illustrated in **Figure 34 C**.

The primary objective of the study was to compare the atom transfer radical polymerization (ATRP) of various biobased monomers derived from cardanol, a sustainable source. Differential scanning calorimetry (DSC) was employed to confirm the crystalline nature of these monomers and investigate the impact of substituents and side chain unsaturation on their melting (T_m) and crystallization (T_c) transitions. Among the polymers, polyPA demonstrated the highest T_m value (16.56°C), while polyPMA exhibited the lowest (1°C). The reduced Tm in polyPMA was attributed to enhanced flexibility due to the methyl substituent, which correspondingly affected the lower crystallization temperature at 18°C. These DSC results indicated that side chain crystallization was preserved in the polymer forms. Notably, the crystallinity of monomers significantly influenced polymerization outcomes; the more crystalline acrylate (PA) led to lower conversion, while methacrylate (PMA) yielded the highest conversion. Comparatively, PMDETA ligand outperformed dNbpy ligand in achieving better conversion during polymerization experiments. Furthermore, the thermal characteristics highlighted the potential of PMA and CA in designing block copolymers and biobased thermoplastic elastomers due to their low polymer glass transition temperatures (T_g). These findings also hold promise for creating value-added products like pour point depressants, lubricant additives, and adhesives with customizable properties, utilizing cardanol as a renewable resource. Ongoing research within the group aims to further explore these potential applications.

2. SUMMARY, CONCLUSIONS & FUTURE PROSPECTS

This work aimed to prepare cardanol-based polymers and copolymers using the ATRP technique successfully. The study used a renewable organic resource created as a byproduct of the cashew industry, cardanol, to describe its production and properties. The vast potential of CNSL to meet a variety of human material needs has been demonstrated by the current study. Numerous copolymers with varying comonomer ratios were produced through ATRP polymerization, indicating a high degree of predictability in copolymer composition and an effect of the side chain length on the polymerization kinetics. This enabled the production of copolymers with adjustable cloud and clearing points. The study developed a unique synergetic modification of plant oil by adding acrylic groups to styrene by ATR polymerization. This modification may significantly improve the synthesis of oil-based copolymers with superior properties. In the meantime, using "green" chemical principles, the polymerization process may make it possible to easily and cleanly synthesize polymeric molecules from renewable resources. The stable co-CA created had a high C-C functionality that was polymerizable, resulting in stiff bioplastics with high crosslink densities and favourable properties.

To achieve narrow molar mass dispersity and learn more about the characteristics related to macromolecular architecture, the work described in this thesis proposes to design and synthesize various living radical polymers using living radical polymerization (LRP) techniques, specifically the ATRP (ATRP) method. Despite being a relatively flexible and practical process to manufacture a variety of homo- and copolymers, free radical polymerization lacks control over the polymer architecture. However, LRP methods are mainly used to prepare well-defined polymer structures. In this research, optimizing the polymerization process is crucial for precisely regulating the molecular weight and design of the polymer. The remaining section of this thesis focuses on investigating different additional characteristics and uses of the polymers that result from macromolecular architecture. The findings from the investigated properties should help improve understanding of the factors that must be considered while building polymeric systems.The aim of this work was the synthesis of ATRP initiator, cardanol-based monomers, and well- defined polymers. The applicability of ATRP on the controlled polymerization of the synthesizedmonomer was thoroughly investigated by optimization of the reaction conditions. In addition, attempts were made to discover the applications of the synthesized polymers.

The entire work carried out here in controlled polymerizations, namely, ATRP, is a valuable technique for synthesizing homo and block copolymers with low ppm of a metal catalyst. However, some problems were met due to the inherent limitations of some reagents or process conditions of ATRP. However, these issues can be resolved by carefully selecting highly active polymerization components under optimum polymerization conditions. Keeping all the results and procedures in mind, one should allow the synthesis of pre-defined polymeric materials with such techniques. This comprehensive study critically compiled research on various monomers, focusing on controlled polymerization processes and cutting-edge organic functionalization methods. The study presents a cohesive and up-to-date overview of the latest advancements in synthesising and functionalizing these monomers for developing advanced polymers with precise

control over their properties and functionalities. By synthesizing and analyzing the current state of research in this field, the study aims to provide valuable insights into the design and development of novel polymers with enhanced performance and applications in various industries.

The aspects of this work are summarized as follows:

- Isolation of cardanol from CNSL
- Synthesis and characterization of cardanol-based acrylate/ methacrylate monomers.
- Optimization of the reaction conditions to achieve controlled polymerization.
- Determination of the thermodynamic parameters of the polymerization reaction.
- Confirmation of the controlled character of the polymerization.
- Confirmation of the "living" characteristics of the synthesized polymers.
- Synthesis and characterization of the copolymer.
- Synthesis and characterization of polymer copolymers and their study.
- Study of polymer properties arising due to macromolecular architecture.
- Finding applications of the synthesized polymers.

CHAPTER-1: Chapter 1 overviews the literature reported on living radical polymerization and its parts. A brief introduction to living radical polymerizations and their types, mechanism, and processes is described. The fundamentals of living radical polymerization can be summarized as follows:

- Since all chains should start to grow practically simultaneously and retain functionality, fast initiation is preferable to propagation.

- The majority of expanding chains are in the dormant state, and only a small fragment is present as propagating free radicals, due to the rapid turnover between active and dormant species.

- There should be a linear relationship between the number average molecular weight (Mn) and the conversion of polymer

***ATRP*:** The monomer, a catalyst, and an initiator with a transferable (pseudo) halogen comprise ATRP as a multicomponent system (Composed of appropriate ligands and a transition metal species). Other elements, such as temperature and solvent, must also be considered for an ATRP to succeed. The following conditions were met for an effective ATRP catalyst:

- Two readily available oxidation states separated by one electron
- Reasonable affinity towards a halogen atom
- Relatively strong complexation with ligands and
- An expandable coordination sphere to accommodate a (pseudo) halogen.

ATRP is a beneficial living radical polymerization technique for it allows:

- Faster reactions at higher temperatures yield acceptable molar mass dispersity.
- Another significant benefit is the potential elimination of catalysts used in controlled polymerization, whereas initiator residues in the final polymer are invariably present in radical polymerization.
- The main benefit of ATRP over other radical polymerization methods is the accessibility of the reagents, which include readily available commercial compounds, including alkyl halides, transition metals, and different ligands.
- The exact management of the polymerization reaction offered by ATRP is another significant benefit. The virtually linear kinetics of the ATRP reaction allows for high reaction yields.

The chapter also discussed cashew nut shell liquid, the method of isolation of cardanol, its characteristics, its various applications as a thermoplastic elastomer in the polymer industry, and the studies on ATRP.

CHAPTER 2: Chapter 2 focused on cleaning chemicals and solvents used in the living radical polymerization technique. Processes for purifying nitrogen gas are studied because reactions must be carried out in an inert atmosphere free of contaminants such as moisture, oxygen, and other reactive gases. This chapter discusses general purification processes, laboratory experimental setups and manipulations, and characterization techniques.

CHAPTER 3: The chapter comprehensively investigated the copolymerization behavior of styrene and pentadecylphenyl methacrylate (PDPMA) using atom transfer radical polymerization (ATRP) at different monomer feed ratios. The reactivity ratios of the resultant copolymers were meticulously determined through a thorough analysis of ^{1}H nuclear magnetic resonance (NMR) composition data, supplemented by information obtained from the Fineman-Ross (FR) and Kelen-Tüdős (KT) methods, a well-established approach in copolymerization studies. The investigation outcomes unveiled a distinct preference for styrene copolymerization, leading to the formation of copolymers with significantly higher styrene content regardless of the initial monomer feed composition. This trend suggests styrene has a higher reactivity than PDPMA in the ATRP process. Notably, while the sequence length of PDPMA demonstrated consistency across various feed ratios, the sequence length of styrene displayed a decline as the initial PDPMA content in the feed increased. This intriguing result can be attributed to the interplay between the reactivity ratios of the monomers and the growing polymer chains during the ATRP process.

The molecular characterization of the copolymers shed light on their molecular weight and polydispersity, which were significantly influenced by the composition of the monomer feed. The dissimilar reactivity and propagation rates between styrene and PDPMA might have altered polymerization kinetics and chain growth dynamics, thus affecting the molecular weight and polydispersity of the copolymers. Intriguingly, the behaviour of the copolymers during the glass transition exhibited variations based on the initial monomer feed composition. Higher styrene content resulted in improved thermal stability of the copolymers. This could be attributed to the

styrene units' inherently rigid and aromatic nature, contributing to enhanced thermal resistance in the copolymer matrix. The examination of the copolymer morphology through transmission electron microscopy (TEM) indicated a phase-separated structure, suggesting that the distinct monomer units did not achieve complete homogeneity at the molecular level. Additionally, rheological and adhesion tests were conducted, providing insights into the potential practical applications of styrene and PDPMA copolymers. The results demonstrated that these copolymers hold promise for use in hot melt adhesives, as they can tailor adhesion properties according to specific requirements, underscoring their versatility and potential utility in applications that demand controlled and tunable adhesion performance.

To conclude, this comprehensive investigation delved into the intricate details of the copolymerization of styrene and PDPMA through ATRP, shedding light on the reactivity, sequence length, molecular properties, and thermal behaviour of the resulting copolymers. These findings contribute to an in-depth understanding of how monomer composition influences the copolymerization process and resultant material properties, which holds implications for various applications across polymer science and technology. The practical applications of these results could span a wide range, including advanced adhesive materials with tailored adhesion properties for specific industrial requirements. This study thus offers valuable insights into the design and utilization of copolymers for enhanced material performance and functionality.

CHAPTER 4: The present study explored the copolymerization dynamics between styrene and cardanyl acrylate (CA) by employing atom transfer radical polymerization (ATRP), focusing on distinct monomer feed ratios. The primary objective was to elucidate these monomers' intricate interaction and reactivity patterns during the polymerization process. To evaluate the reactivity ratios of the formed copolymers, an in-depth analysis was conducted, combining ^{1}H nuclear magnetic resonance (NMR) composition data with insights gained from the Fineman-Ross (FR) and Kelen-Tüdős (KT) methods, which collectively provided a comprehensive understanding of the copolymer composition and behaviour. An intriguing finding emerged from this investigation, revealing a clear preference for the copolymerization of styrene with an alternating pattern, manifesting in copolymers enriched in styrene across the entire spectrum of feed compositions. This preference points to the likelihood of greater reactivity of styrene than CA within the ATRP framework. The distinct reactivity of the monomers influences their incorporation into the polymer chains and ultimately determines the final copolymer composition. The sequence length analysis, a crucial aspect of this study, shed light on the behaviour of CA and styrene sequences within the formed copolymers. Surprisingly, despite varying feed compositions, the sequence length of CA remained relatively stable.

In contrast, the sequence length of styrene showed a noticeable decrease with an elevated CA concentration in the initial feed. This outcome could be attributed to the relative reactivity of CA and styrene during the copolymerization process. The molecular structure of CA seems to exert a consistent influence, while the dynamic nature of the styrene moiety results in sequence length variations.

A further examination of the copolymers' molecular characteristics, particularly their molecular weight and polydispersity, revealed a noteworthy influence on the feed composition. This influence likely originates from the differing reactivity of the monomers and the intricacies of chain propagation. The generated copolymers exhibited a molecular weight range from 2551 to 6934 g/mole and polydispersity values ranging from 1.18 to 3.45, illustrating the diverse nature of the synthesized copolymers and the feed-dependent variations in polymerization kinetics. Intriguingly, the glass transition behaviour of the copolymers exhibited significant variability in response to differing feed compositions. Higher styrene concentration in the feed resulted in improved thermal stability of the copolymers due to the intrinsic rigid and aromatic nature of the styrene units. This aspect enhances the copolymer's overall thermal resistance, underscoring the critical role of monomer composition in dictating the thermal properties of the resultant copolymer.

Moreover, morphological analysis through transmission electron microscopy (TEM) unveiled a phase-separated morphology within the copolymers, indicating the presence of distinct domains of the two monomers. This observation attests to the complexity of the copolymerization process and underscores the need for a nuanced understanding of how monomer interaction influences the resulting structure. The copolymer findings hold significant potential for diverse practical applications, as exemplified by adhesion studies showcasing the adjustable adhesion properties of styrene and CA copolymers. This tunable adhesion behaviour highlights their versatility, rendering them promising contenders for utilization in hot melt adhesive applications. It is especially pertinent for industries requiring customized adhesion performance across various substrates and applications.

In summary, this investigation delved into copolymerization between styrene and cardanyl acrylate (CA) via ATRP, unravelling intricate insights into reactivity patterns, sequence lengths, molecular attributes, and thermal behaviours of the resulting copolymers. The interplay of monomer reactivity, sequence dynamics, and copolymer traits underscores the complexity inherent in copolymerization processes. These findings bear profound implications for crafting copolymeric materials with tailored attributes, particularly in applications like hot melt adhesives where controlled adhesion properties are pivotal. This study contributes substantially to polymer science, charting pathways for advanced materials with precise functionalities. Rigorous structural characterizations are paramount for environmentally friendly methods in a sustainable chemical industry utilizing renewable resources. Incorporating aromatic rings and flexible C15 alkyl chains presents opportunities for cardanol to generate curable coatings with elevated biobased content. The polymerization process provides a streamlined approach to synthesizing polymeric molecules from renewable sources. The copolymerization of styrene with PDPMA or CA via ATRP introduces materials of adaptability, poised for applications across various sectors. The ability to manipulate composition, sequence length, and attributes ushers innovative solutions in domains spanning adhesives and coatings to biomedical devices and microfabrication. As copolymerization research advances, new avenues are poised to emerge, broadening the horizons of these materials in contemporary industries.

3. CURRENT APPROACHES AND CHALLENGES TOWARD RENEWABLE POLYMERS – EVALUATION THROUGH THE STUDY OUTCOME

Renewable polymers are considered a promising alternative to traditional petroleum-based polymers due to their biodegradability, renewability, and potential for carbon neutrality. Current approaches involve using natural resources and biotechnology to produce bioplastics that can replace traditional plastics. However, several challenges must be addressed to make them a viable alternative. Natural resource-based sustainable chemical and polymer production has made significant progress, with a substantial market share difference between petroleum products and renewable alternatives. Cost and performance of various subjects lag behind petroleum products, requiring interdisciplinary collaboration and in-depth investigation.

Using natural resources, such as plants, to produce bioplastics has several advantages, such as reducing greenhouse gas emissions and dependence on fossil fuels. However, there are also limitations to this approach, such as competition with food production and concerns about the environmental impact of large-scale agriculture. Plant-based polymers like cellulose, lignin, and starch can replace traditional petroleum-based plastics. PLA is a biodegradable polymer made from corn starch, while PHAs are produced by certain bacteria. Biotechnology is an approach to renewable polymers that uses microorganisms to produce bioplastics from renewable resources. For example, researchers have used genetic engineering to create bacteria that can make PHAs from various carbon sources. Biotechnology has several advantages over traditional methods, such as being more efficient and reducing waste, but also challenges, such as the high cost of production and the potential for unintended consequences.

Renewable polymers offer a viable alternative to traditional polymers but are currently more expensive. Researchers are exploring new production methods and optimizing existing strategies to reduce costs. They are also using waste streams to produce bioplastics, which can improve sustainability and reduce costs. However, renewable polymers have inferior mechanical and thermal properties, limiting their use in specific applications. To address this, researchers are developing new materials and modifying existing materials to improve performance. Examples include adding nanoparticles to bioplastics to enhance mechanical strength and chemical modification to enhance thermal stability. Renewable polymers are promising due to their biodegradability, renewability, and potential for carbon neutrality. Despite challenges like cost and performance properties, researchers are working to overcome these challenges through new production methods, optimization of existing methods, and the development of new materials. With continued research and development, renewable polymers have the potential to revolutionize the plastics industry and contribute to a more sustainable future.

Renewable polymers derived from CNSL have gained significant attention due to their potential to address environmental concerns and reduce dependence on fossil resources. Current approaches include cardanol as a renewable monomer, Atom Transfer Radical Polymerization (ATRP), copolymerization and functionalization, and multifunctional polymers. Cardanol-based monomers can undergo controlled polymerization through ATRP, allowing for the production of polymers with tailored properties. However, challenges include monomer reactivity, catalyst

compatibility, polymerization conditions, end-group functionalization, scalability and commercial viability, and structural diversity and performance. Optimizing monomer reactivity, selecting catalysts, and ensuring compatibility with solvents, temperature, and reaction parameters are crucial for successful ATRP reactions.

Transitioning from laboratory-scale synthesis to industrial production of cardanol-based polymers presents scalability, cost-effectiveness, and process optimization challenges. Understanding structure-property relationships is crucial for designing polymers with targeted functionalities. Pursuing renewable polymers from cardanol through ATRP is an active research area with promising future directions. Addressing the challenges of monomer reactivity, catalyst compatibility, and polymerization conditions requires innovative catalyst design and reaction engineering. Exploring new copolymerization strategies, such as block and graft copolymers, can lead to materials with enhanced properties and applications in various industries. Endowing cardanol-based polymers with tailored functionalities through functionalization and post-polymerization modifications is a pathway toward advanced materials with specific applications. Developing cardanol-based polymers for emerging fields, such as biomedical materials, electronic devices, and sustainable coatings, holds great potential. Process optimization and cost-effective production methods must be established to overcome scalability challenges, and collaboration between academia, industry, and governmental bodies is crucial for driving the transition from research to commercial production.

4. CONTROLLED POLYMERIZATION OF NEXT-GENERATION RENEWABLE MONOMERS AND BEYOND

Natural molecular biomass is crucial in renewable polymer development due to its petroleum-derived monomers' similarity. It can be used directly or modified for controlled polymerization, providing sustainable and eco-friendly materials advantages.[161] The primary focus of this perspective lies in the monomer approach concerning renewable polymers derived from natural molecular biomass. Biomass-derived monomers are categorized into four distinct groups based on their natural origin. The ultimate goal is to develop renewable polymers that replace and mimic current petroleum-based polymeric materials. While numerous reviews and highlights on this subject have been published in the past decade, this perspective only aims to comprehensively cover some aspects of renewable polymers. Instead, the primary focus is on synthesising renewable polymers using a monomer approach, specifically emphasising naturally occurring molecular biomass. Three main methods for preparing monomers from natural resources are presented in this perspective. The perspective explores challenges and opportunities in renewable polymer synthesis, focusing on monomers derived from natural biomass and controlled polymerizations. It discusses biomass-rich hydrocarbons like vegetable oils, terpenes, terpenoids, and resin acids. In contrast, carboxylic acids and furans are non-hydrocarbon-rich biomass, and carbon dioxide represents biomass without hydrocarbons.[162] This study comprehensively reviews research on various monomers derived from natural molecular biomass. The investigation encompasses controlled polymerization processes and cutting-edge, highly efficient organic functionalization methods.

5. THE 12 PRINCIPLES OF GREEN CHEMISTRY & ITS IMPLEMENTATION IN ATRP

ATRP and reversible-deactivation radical polymerization (RDRP) have limited use due to several potential environmental problems. Environmental concerns, large-scale manufacturing, toxicity (catalysts, additives and monomers), and energy demand hinder ATRP and RDRP development due to transitioning to large-scale manufacturing and energy demands. Improvements in RDRPs in recent years have targeted making the procedures and results more long-lasting.[163] More environmentally friendly polymerizations and polymers need the application of green chemistry concepts and the creation of responsible products and processes. New chemical methods that lessen or do away with producing and consuming harmful substances are known as "green chemistry".[164] To improve present practices, creating innovative and more sustainable materials, chemists should follow the 12 standards for green chemistry developed by Anastas and Warner in 1998.[164] **Table 22** provides a comprehensive outline of the guidelines focused on assessing the environmental impact of chemicals in their intended use (product design) and manufacturing footprint (process design).

Table 22. The summary of 12 principles of green chemistry.

Principle	Summary
P1	Prevent waste.
P2	Design methods to maximize the incorporation of all substrates used in the chemical process into the final product (atom economy).
P3	Design less hazardous chemical synthesis.
P4	Design safer chemicals and other products.
P5	Use safer solvents and auxiliaries.
P6	Design for energy efficiency.
P7	Use renewable feedstocks.
P8	Avoid derivatization because it requires additional reagents and can generate waste.
P9	Use selective catalysts, not stoichiometric reagents.
P10	Design degradable products.
P11	Analyze processes in real-time to prevent pollution.
P12	Minimize the potential for accidents.

The phrase "green methods" in chemistry refers to using catalysts and reagents that are less harmful to the environment (nontoxic), more recyclable, and more effective. Producing goods that are both environmentally friendly and functionally effective is what green chemistry is all about. It is crucial to explore ATRP advancements by focusing on enhancing green attributes and their environmental impact. The current level of green ATRP is summarized in **Table 23**, along

with the guiding concepts that require further study. ATRP remains the technique for producing high-quality polymers from vinyl monomers without endangering human or environmental health. Initiators, catalysts, ligands, additives, and monomers have all had their structure-reactivity relationships well-elucidated thanks to intensive temperature, solvent, and pressure studies. Activator regeneration processes (ATRP) have become more in line with the twelve green chemistry principles thanks to developing technologies that use safe reducing agents and external stimuli. The goals of these guidelines are waste minimization, atom economy, risk mitigation, solvents, safer chemicals, enhanced energy efficiency, auxiliaries, rigorous process control and renewable raw materials. Activator regeneration catalyst regeneration (ATRP) systems may combine highly selective and active catalysts with oxygen tolerance/biocompatibility. They can be degraded on demand, reprocessed, and recycled, making it possible to create unique polymers with the appropriate functions and properties using nonfossil feedstocks. **Table 24** summarizes the key attributes and alignment of the ATRP process with green chemistry principles, showcasing its environmentally friendly characteristics and potential for sustainable, eco-conscious.

The transition to a sustainable chemical industry and circular plastic economy depends on the widespread availability of biobased, biodegradable, or reusable polymeric items. Synthesis of bioconjugates and other novel bioderived polymers or polymer/inorganic hybrids should be performed more regularly in aqueous conditions. The scope of ATRP in green solvents and different heterogeneous and aqueous homogeneous environments needs further work. Fast, efficient, and selective synthesis with oxygen-tolerant techniques must be developed for high-throughput ATRP, which is necessary for optimizing catalytic systems and rapid screening. To better understand structure-property correlations for polymers with intricate architectural designs and to produce more effective catalysts, it is essential to improve ATRP modelling and support it with machine learning methods. Through atom transfer reactions between alkyl halide chain ends and catalysts, ATRP systems may break down halogen-capped polymers into monomers. Improvements might be achieved by aiming for higher monomer yield, lower side reactions, and a wider variety of functional polymers. The Advanced Technology and Research Programme (ATRP) stimulates research on grafting methods for modifying natural polymers and investigating innovative monomers produced from renewable sources. Monomers derived from terpenes and terpenoids, monosaccharides, and lignin are all studied as potential green polymer building blocks. The polymers are considered at some point in manufacturing, although this is optional. However, constant communication and cooperation with industry partners are necessary to ensure that technical improvements are supported in a way that allows ATRP to contribute to a circular economy and sustainable polymer manufacture. Companies interested in green polymers and sustainable practices might benefit from joining the Carnegie Mellon University CRP Consortium, which has advocated using ATRP in industry. E-factor, process mass intensity, atom economy, and material and energy efficiencies are all metrics that may measure how closely ATRP processes comply with green chemistry principles. The promise of RDRPs for green polymer manufacturing and circular plastics can only be realized via collaboration between academia, companies, and government agencies since LCA assesses the influence across the whole product's life cycle.

Table 23. The green features ATRP evaluated by aligning with 12 green chemistry principles, ranging from 0 (not relevant/underdeveloped) to 3 (highly relevant/well-developed). This assessment helps gauge the eco-friendliness and potential of ATRP for sustainable, environmentally conscious polymer synthesis.

Principles	Green features of ATRP													
	Catalytic system				Conditions				Monomers		Materials			
	Ppm loading, high activity	Activator regeneration	Temporal/ spatial control	Catalyst recycling	Aqueous media	Oxygen tolerance	High monomer conversion	Bulk	Scope	Bio based	Segmented copolymers, thermoplastic elastomers	Surface modification, hybrids, dispersants	Bio conjugates	Degradable polymers
P1. Prevent waste	3	3	1	2	3	1	3	3	1	1	2	1	1	2
P2. Atom economy	2	2	1	2	2	0	3	3	2	0	1	1	1	0
P3. Less hazardous synthesis	2	3	3	1	3	2	0	1	1	1	0	0	1	0
P4. Benign chemicals	1	1	0	1	2	1	0	0	1	2	3	3	3	3
P5. Benign solvent &auxiliaries	1	3	0	0	3	1	0	0	2	2	1	1	2	0
P6. Energy efficiency	1	3	2	2	3	2	1	0	0	0	1	1	1	2
P7. Renewable feedstocks	0	0	0	0	0	0	0	0	1	3	2	2	2	2
P8. Reduce derivatives	0	0	0	2	0	0	0	0	3	0	1	2	1	2
P9. Catalysis	3	3	1	3	2	2	1	2	0	0	2	2	2	2
P10. Design for degradation	0	0	1	0	0	0	0	0	3	2	2	1	1	3
P11. Real-time analysis	0	1	2	0	1	1	1	0	1	0	0	0	0	0
P12. Accident prevention	2	3	3	1	2	2	0	0	0	1	0	0	0	0

Figure 24. Application of the principles of green chemistry in ATRP

Principle 1 Prevent waste	Principle 2 Atom Economy	Principle 3 Less Hazardous Synthesis	Principle 4 Design benign chemicals	Principle 5 Benign solvents & auxiliaries	Principle 6 Energy efficiency	Principle 7 Renewable feedstocks	Principle 8 Reduce derivatives	Principle 9 Catalysis	Principle 10 Design for degradation	Principle 11 Real-time analysis	Principle 12 Accident prevention
High monomer conversion	Minimize side reactions	Non-toxic polymerization components and products	(Bio)hybrids	Water	Room temperature with activator regeneration	Carboxylic acid-based monomers & derivatives	Fe-mediated ATRP without ligand and/or initiator	Low catalyst loading	ATRP and radical ring-opening polymerization	Automated Continuous Online Monitoring	Avoid Trommsdorff effect
Bulk Polymerization	Stereocontrol	Catalyst removal	Compatibilizers, Dispersants	Dispersed media	Continuous flow	Lignocellulosic biomass	Dual-role monomers (inimers / inimbramers)	Catalysts removal	Degradable	Exploiting external stimuli	Water-based media
Law catalyst loading	Law catalyst loading	Oxygen tolerance	Commodity upcycling	Ionic Liquids	High-throughput & automation modeling	Monosaccharides and degradation products	No protecting groups	Heterogenous catalysts	Macromolecular architechetcher (Telechelic, stars, brushes)	SI-ATRP (QCM, AFM)	Halting ATRP on demand
	High monomer conversion		Thermoplastic elastomers	Deep Eutectic Solvents		Terpenes and Terpenoids		Fe-based catalysts	Depolymerizations		Ultimate ATRP
			Self-healing polymers	Supercritical CO_2				Organocatalysts			Catalyst scavengers

6. PERSPECTIVES AND FUTURE PROSPECTS

The ATRP community is focused on finding more effective and affordable catalysts with enhanced activity, selectivity, and reduced toxicity. This will enable efficient polymerization with minimal side reactions, accelerating reaction kinetics and improving control over the process. The complex interplay of structural factors, solubility, aggregation behaviour, and ion pairing in ATRP reactions will be crucial for optimizing reaction conditions and tailoring polymer properties. Understanding parameters like monomer type, solvent composition, temperature, and catalyst properties is essential for precise control over the polymerization process. The absence of the Trommsdorf effect in CRP, including ATRP, presents opportunities for solvent-free polymerization processes. This could lead to environmentally friendly processes with reduced energy consumption and simplified purification steps. This greener manufacturing approach contributes to sustainability efforts in the chemical industry.

Understanding the molecular processes of polymerization and deactivation can lead to advanced catalysts and reaction conditions, enabling breakthroughs in control over polymer architecture and functionality. This understanding can facilitate the design of advanced catalysts and reaction conditions, promoting desired outcomes. Expanding monomers and initiators compatible with ATRP holds transformative potential. Incorporating novel monomers with distinct reactivity profiles could synthesize copolymers with tailored properties for specific applications. Exploring cross-propagation processes can engineer complex polymer architectures with well-defined sequences, resulting in materials with precise and predictable behaviours. Enhancing the post-polymerization functionalization capabilities of ATRP products is crucial for creating smart, responsive materials, bioconjugates, and advanced coatings with tailored characteristics. Future efforts should focus on controlled functional group introduction, enabling the creation of smart materials and bioconjugates.

ATRP explores sustainable materials development using cardanol-based monomers like cardanyl acrylate for innovative polymer science and engineering advancements in materials engineering. These versatile monomers offer opportunities for functional polymer synthesis, with researchers focusing on optimizing design and polymerization conditions to achieve targeted properties like enhanced mechanical strength, biocompatibility, or responsiveness. Research on nitroxide-mediated polymerization mediators is expected to expand acrylate polymerization, enabling complex polymer production with desired architectures. New ligands can increase catalytic activity, pushing ATRP reactivity boundaries. Reducing catalyst load and developing hybrid catalyst systems will advance sustainability and greener processes. CRP approaches, including ATRP, have gained significant attention in recent decades. With the discovery of innovative catalysts, mechanistic understanding advancements, and novel monomers, CRP can potentially transform industries like materials science and biomedicine. By harnessing the power of ATRP with styrene-co-PDPMA/cardanyl acrylate monomers and embracing the ongoing evolution of controlled radical polymerization, researchers are poised to revolutionize polymer science and propel it into a new era of tailored functionality, sustainability, and transformative applications.

7. OUTLOOK FOR THE FUTURE

ATRP synthesizes homo and block copolymers, but limitations in reagents and process conditions require optimal component selection. ATRP techniques are being used to synthesize pre-defined polymeric materials, with research focusing on bio-compatible or bio-degradable alternatives. There is no single solution for this problem, as many applications require non-degradable monomers. Water-borne polymerization could help achieve polymers with enhanced properties under mild water-based conditions. With the existing knowledge, there are few limits to be explored using ATRP, and with the development of improved polymerization methods, processes, and techniques that have been considered impossible yet will be achieved in the future. As environmental sustainability becomes an ever-increasing concern, cardanol's origin from renewable cashew nut shell liquid positions it as a sustainable alternative to petroleum-based phenols. This eco-friendly attribute is likely to drive further research and development in cardanol-based ATRP, potentially expanding its applications across sectors such as coatings, adhesives, and high-performance materials. Besides, the tunability of cardanol-based monomers allows for the customization of polymer properties, opening doors to materials with enhanced characteristics like improved adhesion, durability, and corrosion resistance. The biocompatibility of cardanol also hints at its potential role in biomedical applications, including drug delivery systems and medical device coatings. Furthermore, its amphiphilic properties may lead to the creation of innovative smart materials and sensor technologies. In summary, the future of cardanol-based ATRP is marked by sustainability, versatility, and the prospect of novel materials.

8. FUTURE WORK PLAN

- To synthesize more efficient functional ATRP copolymers to enable desired polymerization modifications based on cardanol.
- Synthesis of second-generation polymers for desired application such as coating by block copolymerization.
- Functionalization/post-polymerization modification of polymers by utilizing polymer end groups or pendant groups.
- Synthesis of polymer nanocomposite (eg; incorporation of graphene oxide) to impart the mechanical strength and other useful properties in the polymer.
- Methodology expansion for the range of different monomers.
- Synthesis of well-defined materials with novel and controlled architecture, composition, and functionality by cardanol based monomers.

The current study can be expanded upon in the future to synthesize significant precursors, in which the aliphatic side chain gives prominent hydrophobicity and corrosion-resistant material for coating applications. The material qualities can be achieved through compatibility with various polymers like polyesters, epoxies, and melamine in the future. Its excellent solubility in organic solvents makes it suitable for surface coating applications, offering improved corrosion resistance. Communication between researchers and decision-makers is facilitated by ATRPs, which is crucial for the successful commercialization of goods and technologies.

REFERENCES

(1) Bajpai, P. *Biermann's Handbook of Pulp and Paper: Volume 1: Raw Material and Pulp Making*; Elsevier, 2018.

(2) Namazi, H. Polymers in Our Daily Life. *Bioimpacts* **2017**, *7* (2), 73–74. https://doi.org/10.15171/bi.2017.09.

(3) Wunderlich, B. *Thermal Analysis of Polymeric Materials*; Springer Science & Business Media, 2005.

(4) Council, N. R.; Sciences, D. on E. and P.; Applications, C. on P. S., Mathematics, and; Engineering, C. on P. S. and. *Polymer Science and Engineering: The Shifting Research Frontiers*; National Academies Press, 1994.

(5) Shwartz, Y.; Ben-Zvi, R.; Hofstein, A. The Use of Scientific Literacy Taxonomy for Assessing the Development of Chemical Literacy among High-School Students. *Chemistry Education Research and Practice* **2006**, *7* (4), 203–225. https://doi.org/10.1039/B6RP90011A.

(6) Yao, J.; Yang, M.; Duan, Y. Chemistry, Biology, and Medicine of Fluorescent Nanomaterials and Related Systems: New Insights into Biosensing, Bioimaging, Genomics, Diagnostics, and Therapy. *Chem. Rev.* **2014**, *114* (12), 6130–6178. https://doi.org/10.1021/cr200359p.

(7) Dai, L. *Intelligent Macromolecules for Smart Devices: From Materials Synthesis to Device Applications*; Springer Science & Business Media, 2004.

(8) Pathak, S.; Sneha, C.; Mathew, B. B. Bioplastics: Its Timeline Based Scenario & Challenges. **2014**. https://doi.org/10.12691/jpbpc-2-4-5.

(9) Hayes, G.; Laurel, M.; MacKinnon, D.; Zhao, T.; Houck, H. A.; Becer, C. R. Polymers without Petrochemicals: Sustainable Routes to Conventional Monomers. *Chem. Rev.* **2023**, *123* (5), 2609–2734. https://doi.org/10.1021/acs.chemrev.2c00354.

(10) Gowariker, V. R.; Viswanathan, N. V.; Sreedhar, J. *Polymer Science*; New Age International, 1986.

(11) Martinez, M. R.; Matyjaszewski, K. Degradable and Recyclable Polymers by Reversible Deactivation Radical Polymerization. *CCS Chemistry* **2022**, *4* (7), 2176–2211. https://doi.org/10.31635/ccschem.022.202201987.

(12) Destarac, M. Controlled Radical Polymerization: Industrial Stakes, Obstacles and Achievements. *Macromolecular Reaction Engineering* **2010**, *4* (3–4), 165–179. https://doi.org/10.1002/mren.200900087.

(13) Dey, A.; Haldar, U.; De, P. Block Copolymer Synthesis by the Combination of Living Cationic Polymerization and Other Polymerization Methods. *Frontiers in Chemistry* **2021**,

9.

(14) Nowalk, J. A.; Fang, C.; Short, A. L.; Weiss, R. M.; Swisher, J. H.; Liu, P.; Meyer, T. Y. Sequence-Controlled Polymers Through Entropy-Driven Ring-Opening Metathesis Polymerization: Theory, Molecular Weight Control, and Monomer Design. *J. Am. Chem. Soc*. **2019**, *141* (14), 5741–5752. https://doi.org/10.1021/jacs.8b13120.

(15) Ouchi, M.; Sawamoto, M. *50th Anniversary Perspective* : Metal-Catalyzed Living Radical Polymerization: Discovery and Perspective. *Macromolecules* **2017**, *50* (7), 2603–2614. https://doi.org/10.1021/acs.macromol.6b02711.

(16) Moad, G.; Rizzardo, E.; Thang, S. H. Toward Living Radical Polymerization. *Acc. Chem. Res.* **2008**, *41* (9), 1133–1142. https://doi.org/10.1021/ar800075n.

(17) Pan, X.; Tasdelen, M. A.; Laun, J.; Junkers, T.; Yagci, Y.; Matyjaszewski, K. Photomediated Controlled Radical Polymerization. *Progress in Polymer Science* **2016**, *62*, 73–125. https://doi.org/10.1016/j.progpolymsci.2016.06.005.

(18) Kreutzer, J.; Yagci, Y. Metal Free Reversible-Deactivation Radical Polymerizations: Advances, Challenges, and Opportunities. *Polymers* **2018**, *10* (1), 35. https://doi.org/10.3390/polym10010035.

(19) Chen, M.; Zhong, M.; Johnson, J. A. Light-Controlled Radical Polymerization: Mechanisms, Methods, and Applications. *Chem. Rev.* **2016**, *116* (17), 10167–10211. https://doi.org/10.1021/acs.chemrev.5b00671.

(20) Matyjaszewski, K.; Müller, A. H. E. *Controlled and Living Polymerizations: From Mechanisms to Applications*; John Wiley & Sons, 2009.

(21) Bagheri, A.; Fellows, C.; Boyer, C. Reversible Deactivation Radical Polymerization: From Polymer Network Synthesis to 3D Printing. *Advanced Science* **2021**, *8*, 2003701. https://doi.org/10.1002/advs.202003701.

(22) University, C. M. *Atom Transfer Radical Polymerization - Matyjaszewski Polymer Group - Carnegie Mellon University*. http://www.cmu.edu/maty/chem/fundamentals-atrp/atrp.html (accessed 2023-03-20).

(23) Grishin, I. D.; Zueva, E. I.; Pronina, Y. S.; Grishin, D. F. Novel Copper-Based Catalytic Systems for Atom Transfer Radical Polymerization of Acrylonitrile. *Catalysts* **2023**, *13* (2), 444. https://doi.org/10.3390/catal13020444.

(24) Matyjaszewski, K.; Xia, J. Atom Transfer Radical Polymerization. *Chemical reviews* **2001**, *101*, 2921–2990. https://doi.org/10.1021/cr940534g.

(25) Coessens, V. M. C.; Matyjaszewski, K. Fundamentals of Atom Transfer Radical Polymerization. *J. Chem. Educ.* **2010**, *87* (9), 916–919. https://doi.org/10.1021/ed1002256.

(26) Melville, J. N.; Bernhardt, P. V. Electrochemical Exploration of Active Cu-Based Atom

Transfer Radical Polymerization Catalysis through Ligand Modification. *Inorg. Chem.* **2021**, *60* (13), 9709–9719. https://doi.org/10.1021/acs.inorgchem.1c01001.

(27) Davis, K.; Matyjaszewski, K. Effect of (Pseudo)Halide Initiators and Copper Complexes with Non-halogen Anions on the Atom Transfer Radical Polymerization. *Journal of Macromolecular Science, Part A* **2007**, *41*, 449–465. https://doi.org/10.1081/MA-120030918.

(28) Ribelli, T. G.; Lorandi, F.; Fantin, M.; Matyjaszewski, K. Atom Transfer Radical Polymerization: Billion Times More Active Catalysts and New Initiation Systems. *Macromolecular Rapid Communications* **2019**, *40* (1), 1800616. https://doi.org/10.1002/marc.201800616.

(29) Tang, H.; Arulsamy, N.; Radosz, M.; Shen, Y.; Tsarevsky, N. V.; Braunecker, W. A.; Tang, W.; Matyjaszewski, K. Highly Active Copper-Based Catalyst for Atom Transfer Radical Polymerization. *J. Am. Chem. Soc.* **2006**, *128* (50), 16277–16285. https://doi.org/10.1021/ja0653369.

(30) Xia, J.; Zhang, X.; Matyjaszewski, K. The Effect of Ligands on Copper-Mediated Atom Transfer Radical Polymerization. In *Transition Metal Catalysis in Macromolecular Design*; ACS Symposium Series; American Chemical Society, 2000; Vol. 760, pp 207–223. https://doi.org/10.1021/bk-2000-0760.ch013.

(31) *Copper-Mediated Living Radical Polymerization (Atom Transfer Radical Polymerization and Copper(0) Mediated Polymerization): From Fundamentals to Bioapplications | Chemical Reviews*. https://pubs.acs.org/doi/10.1021/acs.chemrev.5b00396 (accessed 2023-03-20).

(32) Nachtigall, O.; VanderWeide, A. I.; Brennessel, W. W.; Jones, W. D. An Iron-Based Dehydration Catalyst for Selective Formation of Styrene. *ACS Catal.* **2021**, *11* (17), 10885–10891. https://doi.org/10.1021/acscatal.1c03037.

(33) Pasetto, P.; Blas, H.; Audouin, F.; Boissière, C.; Sanchez, C.; Save, M.; Charleux, B. Mechanistic Insight into Surface-Initiated Polymerization of Methyl Methacrylate and Styrene via ATRP from Ordered Mesoporous Silica Particles. *Macromolecules* **2009**, *42* (16), 5983–5995. https://doi.org/10.1021/ma9003506.

(34) Mukumoto, K.; Wang, Y.; Matyjaszewski, K. Iron-Based ICAR ATRP of Styrene with Ppm Amounts of FeIIIBr3 and 1,1′-Azobis(Cyclohexanecarbonitrile). *ACS Macro Lett.* **2012**, *1* (5), 599–602. https://doi.org/10.1021/mz3001463.

(35) Georgi, U.; Erber, M.; Stadermann, J.; Abulikemu, M.; Komber, H.; Lederer, A.; Voit, B. New Approaches to Hyperbranched Poly(4-Chloromethylstyrene) and Introduction of Various Functional End Groups by Polymer-Analogous Reactions. *Journal of Polymer Science Part A: Polymer Chemistry* **2010**, *48* (10), 2224–2235. https://doi.org/10.1002/pola.23995.

(36) Magenau, A. J. D.; Kwak, Y.; Matyjaszewski, K. ATRP of Methacrylates Utilizing

CuIIX2/L and Copper Wire. *Macromolecules* **2010**, *43* (23), 9682–9689. https://doi.org/10.1021/ma102051q.

(37) Zhu, G.; Zhang, L.; Zhang, Z.; Zhu, J.; Tu, Y.; Cheng, Z.; Zhu, X. Iron-Mediated ICAR ATRP of Methyl Methacrylate. *Macromolecules* **2011**, *44* (9), 3233–3239. https://doi.org/10.1021/ma102958y.

(38) Li, X.; Wang, W.-J.; Li, B.-G.; Zhu, S. Kinetics and Modeling of Solution ARGET ATRP of Styrene, Butyl Acrylate, and Methyl Methacrylate. *Macromolecular Reaction Engineering* **2011**, *5* (9–10), 467–478. https://doi.org/10.1002/mren.201100024.

(39) Ohno, S.; Matyjaszewski, K. Controlling Grafting Density and Side Chain Length in Poly(n-Butyl Acrylate) by ATRP Copolymerization of Macromonomers. *Journal of Polymer Science Part A: Polymer Chemistry* **2006**, *44* (19), 5454–5467. https://doi.org/10.1002/pola.21669.

(40) Bergenudd, H.; Coullerez, G.; Jonsson, M.; Malmström, E. Solvent Effects on ATRP of Oligo(Ethylene Glycol) Methacrylate. Exploring the Limits of Control. *Macromolecules* **2009**, *42* (9), 3302–3308. https://doi.org/10.1021/ma8028425.

(41) Truong, N. P.; Jones, G. R.; Bradford, K. G. E.; Konkolewicz, D.; Anastasaki, A. A Comparison of RAFT and ATRP Methods for Controlled Radical Polymerization. *Nat Rev Chem* **2021**, *5* (12), 859–869. https://doi.org/10.1038/s41570-021-00328-8.

(42) Satoh, K.; Kamigaito, M. Stereospecific Living Radical Polymerization: Dual Control of Chain Length and Tacticity for Precision Polymer Synthesis. *Chem. Rev.* **2009**, *109* (11), 5120–5156. https://doi.org/10.1021/cr900115u.

(43) Matyjaszewski, K.; Nanda, A. K.; Tang, W. Effect of [CuII] on the Rate of Activation in ATRP. *Macromolecules* **2005**, *38* (5), 2015–2018. https://doi.org/10.1021/ma047531i.

(44) Fliedel, C.; Dagorne, S.; Roux, E. L. Metal Complexes as Catalysts/Moderators for Polymerization Reactions. **2021**, *9* (Part 19. Applications in Catalysis-Ch. 9.14), 410.

(45) Coessens, V.; Pintauer, T.; Matyjaszewski, K. Functional Polymers by Atom Transfer Radical Polymerization. *Progress in Polymer Science* **2001**, *26*, 337–377. https://doi.org/10.1016/S0079-6700(01)00003-X.

(46) Degirmenci, A.; Yeter Bas, G.; Sanyal, R.; Sanyal, A. “Clickable” Polymer Brush Interfaces: Tailoring Monovalent to Multivalent Ligand Display for Protein Immobilization and Sensing. *Bioconjugate Chem.* **2022**, *33* (9), 1672–1684. https://doi.org/10.1021/acs.bioconjchem.2c00298.

(47) Siegwart, D. J.; Oh, J. K.; Matyjaszewski, K. ATRP in the Design of Functional Materials for Biomedical Applications. *Prog Polym Sci* **2012**, *37* (1), 18–37. https://doi.org/10.1016/j.progpolymsci.2011.08.001.

(48) Seeliger, F.; Matyjaszewski, K. Temperature Effect on Activation Rate Constants in ATRP:

New Mechanistic Insights into the Activation Process. *Macromolecules* **2009**, *42* (16), 6050–6055. https://doi.org/10.1021/ma9010507.

(49) Vargün, E.; Usanmaz, A. Polymerization of 2-Hydroxyethyl Acrylate in Bulk and Solution by Chemical Initiator and by ATRP Method. *Journal of Polymer Science Part A: Polymer Chemistry* **2005**, *43* (17), 3957–3965. https://doi.org/10.1002/pola.20867.

(50) Fantin, M.; Isse, A.; Gennaro, A.; Matyjaszewski, K. Understanding the Fundamentals of Aqueous ATRP and Defining Conditions for Better Control. *Macromolecules* **2015**, *48*, 150918122324008. https://doi.org/10.1021/acs.macromol.5b01454.

(51) Liu, Y.; Klep, V.; Zdyrko, B.; Luzinov, I. Polymer Grafting via ATRP Initiated from Macroinitiator Synthesized on Surface. *Langmuir* **2004**, *20* (16), 6710–6718. https://doi.org/10.1021/la049465j.

(52) Hester, J. F.; Banerjee, P.; Won, Y.-Y.; Akthakul, A.; Acar, M. H.; Mayes, A. M. ATRP of Amphiphilic Graft Copolymers Based on PVDF and Their Use as Membrane Additives. *Macromolecules* **2002**, *35* (20), 7652–7661. https://doi.org/10.1021/ma0122270.

(53) Ran, J.; Wu, L.; Zhang, Z.; Xu, T. Atom Transfer Radical Polymerization (ATRP): A Versatile and Forceful Tool for Functional Membranes. *Progress in Polymer Science* **2014**, *39* (1), 124–144. https://doi.org/10.1016/j.progpolymsci.2013.09.001.

(54) Gualandi, C.; Vo, C. D.; Focarete, M. L.; Scandola, M.; Pollicino, A.; Di Silvestro, G.; Tirelli, N. Advantages of Surface-Initiated ATRP (SI-ATRP) for the Functionalization of Electrospun Materials. *Macromolecular Rapid Communications* **2013**, *34* (1), 51–56. https://doi.org/10.1002/marc.201200648.

(55) Matyjaszewski, K.; Coessens, V.; Nakagawa, Y.; Xia, J.; Qiu, J.; Gaynor, S.; Coca, S.; Jasieczek, C. Synthesis of Functional Polymers by Atom Transfer Radical Polymerization. In *Functional Polymers*; ACS Symposium Series; American Chemical Society, 1998; Vol. 704, pp 16–27. https://doi.org/10.1021/bk-1998-0704.ch002.

(56) Feng, H.; Lu, X.; Wang, W.; Kang, N.-G.; Mays, J. W. Block Copolymers: Synthesis, Self-Assembly, and Applications. *Polymers* **2017**, *9* (10), 494. https://doi.org/10.3390/polym9100494.

(57) *Living/controlled free-radical polymerisation - ProQuest*. https://www.proquest.com/openview/338b3dd1150c811bc27014c811f821fe/1?pq-origsite=gscholar&cbl=2026366&diss=y (accessed 2023-03-21).

(58) Venkataraman, S.; Wooley, K. L. ATRP from an Amino Acid-Based Initiator: A Facile Approach for α-Functionalized Polymers. *Macromolecules* **2006**, *39* (26), 9661–9664. https://doi.org/10.1021/ma0619583.

(59) Zoppe, J. O.; Ataman, N. C.; Mocny, P.; Wang, J.; Moraes, J.; Klok, H.-A. Surface-Initiated Controlled Radical Polymerization: State-of-the-Art, Opportunities, and Challenges in Surface and Interface Engineering with Polymer Brushes. *Chem. Rev.* **2017**, *117* (3), 1105–

1318. https://doi.org/10.1021/acs.chemrev.6b00314.

(60) Lee, S.; Russell, A.; Matyjaszewski, K. ATRP Synthesis of Amphiphilic Random, Gradient, and Block Copolymers of 2-(Dimethylamino)Ethyl Methacrylate and n -Butyl Methacrylate in Aqueous Media. *Biomacromolecules* **2003**, *4*, 1386–1393. https://doi.org/10.1021/bm034126a.

(61) Arriola, D. J.; Carnahan, E. M.; Hustad, P. D.; Kuhlman, R. L.; Wenzel, T. T. Catalytic Production of Olefin Block Copolymers via Chain Shuttling Polymerization. *Science* **2006**, *312* (5774), 714–719. https://doi.org/10.1126/science.1125268.

(62) Aoshima, S.; Kanaoka, S. A Renaissance in Living Cationic Polymerization. *Chem. Rev.* **2009**, *109* (11), 5245–5287. https://doi.org/10.1021/cr900225g.

(63) Nedeljkovic, D. Polystyrene-b-Poly(2-(Methoxyethoxy)Ethyl Methacrylate) Polymerization by Different Controlled Polymerization Mechanisms. *Polymers* **2021**, *13* (20), 3505. https://doi.org/10.3390/polym13203505.

(64) Kajiwara, A.; Matyjaszewski, K. Formation of Block Copolymers by Transformation of Cationic Ring-Opening Polymerization to Atom Transfer Radical Polymerization (ATRP). *Macromolecules* **1998**, *31* (11), 3489–3493. https://doi.org/10.1021/ma971445j.

(65) Huang, C.-F.; Kuo, S.-W.; Lee, H.-F.; Chang, F.-C. A New Strategy for the One-Step Synthesis of Block Copolymers through Simultaneous Free Radical and Ring Opening Polymerizations Using a Dual-Functional Initiator. *Polymer* **2005**, *46* (5), 1561.

(66) Roka, N.; Kokkorogianni, O.; Kontoes-Georgoudakis, P.; Choinopoulos, I.; Pitsikalis, M. Recent Advances in the Synthesis of Complex Macromolecular Architectures Based on Poly(N-Vinyl Pyrrolidone) and the RAFT Polymerization Technique. *Polymers* **2022**, *14* (4), 701. https://doi.org/10.3390/polym14040701.

(67) *ATRP | PDF | Polymerization | Catalysis*. Scribd. https://www.scribd.com/document/345220053/ATRP (accessed 2023-03-21).

(68) Shunmugam, R. *Functional Polymers: Design, Synthesis, and Applications*; CRC Press, 2017.

(69) Ouchi, M.; Terashima, T.; Sawamoto, M. Transition Metal-Catalyzed Living Radical Polymerization: Toward Perfection in Catalysis and Precision Polymer Synthesis. *Chem. Rev.* **2009**, *109* (11), 4963–5050. https://doi.org/10.1021/cr900234b.

(70) Deepa, T.; Satheeshkumar, K. S.; Arun, A. Study of Thermoplastic Elastomer Synthesis, Characterization, Crystallization Based on Crystallizable Amide Segment Contains Conducting Moiety. *Materials Today: Proceedings* **2022**, *60*, 1297–1302. https://doi.org/10.1016/j.matpr.2021.09.265.

(71) Gao, C.; Yan, D. Hyperbranched Polymers: From Synthesis to Applications. *Progress in Polymer Science* **2004**, *29* (3), 183–275.

https://doi.org/10.1016/j.progpolymsci.2003.12.002.

(72) Zhong, W.; Zhang, M.; Zhu, L.; Zhang, Y.; Liu, F. Complex Multilength-Scale Morphology in Organic Photovoltaics. *Trends in Chemistry* **2022**, *4* (8), 699–713. https://doi.org/10.1016/j.trechm.2022.05.004.

(73) Niesten, M. C. E. J.; Feijen, J.; Gaymans, R. J. Synthesis and Properties of Segmented Copolymers Having Aramid Units of Uniform Length. *Polymer* **2000**, *41* (24), 8487–8500. https://doi.org/10.1016/S0032-3861(00)00252-4.

(74) Martin, D. J.; Meijs, G. F.; Renwick, G. M.; Gunatillake, P. A.; Mccarthy, S. J. Effect of Soft-Segment CH2/O Ratio on Morphology and Properties of a Series of Polyurethane Elastomers. *Journal of Applied Polymer Science* **1996**, *60* (4), 557–571. https://doi.org/10.1002/(SICI)1097-4628(19960425)60:4<557::AID-APP9>3.0.CO;2-N.

(75) Luckachan, G. E.; Pillai, C. K. S. Random Multiblock Poly(Ester Amide)s Containing Poly(L-Lactide) and Cycloaliphatic Amide Segments: Synthesis and Biodegradation Studies. *Journal of Polymer Science Part A: Polymer Chemistry* **2006**, *44* (10), 3250–3260. https://doi.org/10.1002/pola.21417.

(76) Prisacariu, C. *Polyurethane Elastomers: From Morphology to Mechanical Aspects*; Springer Science & Business Media, 2011.

(77) Shah, V.; Bhaliya, J.; Patel, G. M.; Deshmukh, K. Advances in Polymeric Nanocomposites for Automotive Applications: A Review. *Polymers for Advanced Technologies* **2022**, *33* (10), 3023–3048. https://doi.org/10.1002/pat.5771.

(78) Kalogeras, I. M. Glass-Transition Phenomena in Polymer Blends. In *Encyclopedia of Polymer Blends*; John Wiley & Sons, Ltd, 2016; pp 1–134. https://doi.org/10.1002/9783527653966.ch1.

(79) Melo, L.; Benavides, R.; Martínez, G.; Da Silva, L.; Paula, M. M. S. Degradation Reactions during Sulphonation of Poly(Styrene-Co-Acrylic Acid) Used as Membranes. *Polymer Degradation and Stability* **2014**, *109*, 343–352. https://doi.org/10.1016/j.polymdegradstab.2014.06.002.

(80) Richardson, M. J.; Savill, N. G. Volumetric Properties of Polystyrene: Influence of Temperature, Molecular Weight and Thermal Treatment. *Polymer* **1977**, *18* (1), 3–9. https://doi.org/10.1016/0032-3861(77)90253-1.

(81) Singh, L.; Ludovice, P. J.; Henderson, C. L. Influence of Molecular Weight and Film Thickness on the Glass Transition Temperature and Coefficient of Thermal Expansion of Supported Ultrathin Polymer Films. *Thin Solid Films* **2004**, *449* (1), 231–241. https://doi.org/10.1016/S0040-6090(03)01353-1.

(82) Fox, T. G.; Flory, P. J. Second-Order Transition Temperatures and Related Properties of Polystyrene. I. Influence of Molecular Weight. *Journal of Applied Physics* **1950**, *21* (6), 581–591. https://doi.org/10.1063/1.1699711.

(83) Spontak, R. J.; Patel, N. P. Thermoplastic Elastomers: Fundamentals and Applications. *Current Opinion in Colloid & Interface Science* **2000**, *5* (5), 333–340. https://doi.org/10.1016/S1359-0294(00)00070-4.

(84) Drobny, J. G. *Handbook of Thermoplastic Elastomers*; Elsevier, 2014.

(85) Feldman, D. Polymer History. *Designed Monomers and Polymers* **2008**, *11* (1), 1–15. https://doi.org/10.1163/156855508X292383.

(86) Mamun, A. A.; Chen, J. Y. *Industrial Applications of Biopolymers and Their Environmental Impact*; CRC Press, 2020.

(87) Bonart, R. Thermoplastic Elastomers. *Polymer* **1979**, *20* (11), 1389–1403. https://doi.org/10.1016/0032-3861(79)90280-5.

(88) Wang, W.; Lu, W.; Goodwin, A.; Wang, H.; Yin, P.; Kang, N.-G.; Hong, K.; Mays, J. W. Recent Advances in Thermoplastic Elastomers from Living Polymerizations: Macromolecular Architectures and Supramolecular Chemistry. *Progress in Polymer Science* **2019**, *95*, 1–31. https://doi.org/10.1016/j.progpolymsci.2019.04.002.

(89) Matyjaszewski, K. Atom Transfer Radical Polymerization: From Mechanisms to Applications. *Israel Journal of Chemistry* **2012**, *52* (3–4), 206–220. https://doi.org/10.1002/ijch.201100101.

(90) Yan, J.; Bockstaller, M. R.; Matyjaszewski, K. Brush-Modified Materials: Control of Molecular Architecture, Assembly Behavior, Properties and Applications. *Progress in Polymer Science* **2020**, *100*, 101180. https://doi.org/10.1016/j.progpolymsci.2019.101180.

(91) Delidovich, I.; Hausoul, P. J. C.; Deng, L.; Pfützenreuter, R.; Rose, M.; Palkovits, R. Alternative Monomers Based on Lignocellulose and Their Use for Polymer Production. *Chem. Rev.* **2016**, *116* (3), 1540–1599. https://doi.org/10.1021/acs.chemrev.5b00354.

(92) Pillai, C. K. S. Challenges for Natural Monomers and Polymers: Novel Design Strategies and Engineering to Develop Advanced Polymers. *Designed Monomers and Polymers* **2010**, *13* (2), 87–121. https://doi.org/10.1163/138577210X12634696333190.

(93) Lubi, M. C.; Thachil, E. T. Cashew Nut Shell Liquid (CNSL) - a Versatile Monomer for Polymer Synthesis. *Designed Monomers and Polymers* **2000**, *3* (2), 123–153. https://doi.org/10.1163/156855500300142834.

(94) Padinjakkara, A.; Thankappan, A.; Jr, F. G. S.; Thomas, S. *Biopolymers and Biomaterials*; CRC Press, 2018.

(95) Tyman, J. H. P.; Johnson, R. A.; Muir, M.; Rokhgar, R. The Extraction of Natural Cashew Nut-Shell Liquid from the Cashew Nut (Anacardium Occidentale). *JAOCS* **1989**, *66* (4), 553–557. https://doi.org/10.1007/BF02885447.

(96) Patel, V. *Advances in Petrochemicals*; BoD – Books on Demand, 2015.

(97) O, A. O.; O, O. F.; D, A. B.; A, M. A. A Review on Cashew Research and Production in Nigeria in the Last Four Decades. *SRE* **2015**, *10* (5), 196–209. https://doi.org/10.5897/SRE2014.5953.

(98) Rickson, F. R.; Rickson, M. M. The Cashew Nut, Anacardium Occidentale (Anacardiaceae), and Its Perennial Association with Ants: Extrafloral Nectary Location and the Potential for Ant Defense. *American Journal of Botany* **1998**, *85* (6), 835–849. https://doi.org/10.2307/2446419.

(99) Idah, P. A.; Simeon, M. I.; Mohammed, M. A. Extraction and Characterization of Cashew Nut (Anacardium Occidentale) Oil and Cashew Shell Liquid Oil. **2014**.

(100) Liaotrakoon, W.; Namhong, T.; Yu, C.-H.; Chen, H.-H. Impact of Roasting on the Changes in Composition and Quality of Cashew Nut (Anacardium Occidentale) Oil. *International Food Research Journal* **2016**, *23* (3), 986–991.

(101) *CNSL processing technology*. MEKONG TECHNOLOGY VIETNAM. https://www.mktech.vn/cnsl-processing-technology/ (accessed 2023-03-22).

(102) Lubi, M. C.; Thachil, E. T. Cashew Nut Shell Liquid (CNSL) - a Versatile Monomer for Polymer Synthesis. *Designed Monomers and Polymers* **2000**, *3* (2), 123–153. https://doi.org/10.1163/156855500300142834.

(103) Gandhi, Dr. T.; Patel, M.; Dholakiya, B. Studies on Effect of Various Solvents on Extraction of Cashew Nut Shell Liquid (CNSL) and Isolation of Major Phenolic Constituents from Extracted CNSL. *Scholars Research Library* **2012**, *2 (1):135-142*, 8.

(104) Balgude, D.; Sabnis, A. S. CNSL: An Environment Friendly Alternative for the Modern Coating Industry. *J Coat Technol Res* **2014**, *11* (2), 169–183. https://doi.org/10.1007/s11998-013-9521-3.

(105) Attanasi, O. A.; Berretta, S.; Fiani, C.; Filippone, P.; Mele, G.; Saladino, R. Synthesis and Reactions of Nitro Derivatives of Hydrogenated Cardanol. *Tetrahedron* **2006**, *62* (25), 6113–6120. https://doi.org/10.1016/j.tet.2006.03.105.

(106) Kathalewar, M.; Sabnis, A.; D'Mello, D. Isocyanate Free Polyurethanes from New CNSL Based Bis-Cyclic Carbonate and Its Application in Coatings. *European Polymer Journal* **2014**, *57*, 99–108. https://doi.org/10.1016/j.eurpolymj.2014.05.008.

(107) L. Quirino, R.; F. Garrison, T.; R. Kessler, M. Matrices from Vegetable Oils, Cashew Nut Shell Liquid, and Other Relevant Systems for Biocomposite Applications. *Green Chemistry* **2014**, *16* (4), 1700–1715. https://doi.org/10.1039/C3GC41811A.

(108) Rudnick, L. R. *Lubricant Additives: Chemistry and Applications, Third Edition*; CRC Press, 2017.

(109) Voirin, C.; Caillol, S.; V. Sadavarte, N.; V. Tawade, B.; Boutevin, B.; P. Wadgaonkar, P. Functionalization of Cardanol: Towards Biobased Polymers and Additives. *Polymer*

Chemistry **2014**, *5* (9), 3142–3162. https://doi.org/10.1039/C3PY01194A.

(110) *Cardanol Production from Cashew Nut Shell Liquid (CNSL)*. Niir Project Consultancy Services. https://npcsblog.wordpress.com/2018/12/24/cardanol-production-from-cashew-nut-shell-liquid-cnsl/ (accessed 2023-03-22).

(111) Deutsch, J.; Köckritz, A. Synthesis of Novel Chemicals from Cardanol as a Product of Cashew Nutshell Processing. *Food Science & Nutrition* **2020**, *8* (7), 3081–3088. https://doi.org/10.1002/fsn3.1480.

(112) Mohammed, A. N. Development of High Performance Cashew Nut Shell Liquid (CNSL) Based Surface Coatings Cross Linked with Styrene and MethylMethacrylate. Thesis, 2015. http://localhost/xmlui/handle/123456789/1884 (accessed 2023-03-22).

(113) Jia, P.; Song, F.; Li, Q.; Xia, H.; Li, M.; Shu, X.; Zhou, Y. Recent Development of Cardanol Based Polymer Materials-A Review. *Journal of Renewable Materials* **2019**, *7*, 601–619. https://doi.org/10.32604/jrm.2019.07011.

(114) Voirin, C.; Caillol, S.; V. Sadavarte, N.; V. Tawade, B.; Boutevin, B.; P. Wadgaonkar, P. Functionalization of Cardanol: Towards Biobased Polymers and Additives. *Polymer Chemistry* **2014**, *5* (9), 3142–3162. https://doi.org/10.1039/C3PY01194A.

(115) Perdriau, S.; Harder, S.; Heeres, H. J.; de Vries, J. G. Selective Conversion of Polyenes to Monoenes by RuCl3-Catalyzed Transfer Hydrogenation: The Case of Cashew Nutshell Liquid. *ChemSusChem* **2012**, *5* (12), 2427–2434. https://doi.org/10.1002/cssc.201200503.

(116) Caillol, S. Cardanol: A Promising Building Block for Biobased Polymers and Additives. *Current Opinion in Green and Sustainable Chemistry* **2018**, *14*, 26–32. https://doi.org/10.1016/j.cogsc.2018.05.002.

(117) Shankar Balachandran, V.; Rohidas Jadhav, S.; Kumar Vemula, P.; John, G. Recent Advances in Cardanol Chemistry in a Nutshell: From a Nut to Nanomaterials. *Chemical Society Reviews* **2013**, *42* (2), 427–438. https://doi.org/10.1039/C2CS35344J.

(118) Kathalewar, M.; Sabnis, A.; D'Melo, D. Polyurethane Coatings Prepared from CNSL Based Polyols: Synthesis, Characterization and Properties. *Progress in Organic Coatings* **2014**, *77* (3), 616–626. https://doi.org/10.1016/j.porgcoat.2013.11.028.

(119) Balgude, D.; Sabnis, A. S. CNSL: An Environment Friendly Alternative for the Modern Coating Industry. *J Coat Technol Res* **2014**, *11* (2), 169–183. https://doi.org/10.1007/s11998-013-9521-3.

(120) Muringayil Joseph, T.; Murali Nair, S.; Kattimuttathu Ittara, S.; Haponiuk, J. T.; Thomas, S. Copolymerization of Styrene and Pentadecylphenylmethacrylate (PDPMA): Synthesis, Characterization, Thermomechanical and Adhesion Properties. *Polymers* **2020**, *12* (1), 97. https://doi.org/10.3390/polym12010097.

(121) Rajender, N.; Suresh, K. I.; Sreedhar, B. Comb-like Polymer-Graphene Nanocomposites

with Improved Adhesion Properties via Surface-Initiated Atom Transfer Radical Polymerization (SI-ATRP). *Journal of Applied Polymer Science* **2018**, *135* (8), 45885. https://doi.org/10.1002/app.45885.

(122) Kim, D.-G.; Kang, H.; Choi, Y.-S.; Han, S.; Lee, J.-C. Photo-Cross-Linkable Star-Shaped Polymers with Poly(Ethylene Glycol) and Renewable Cardanol Side Groups: Synthesis, Characterization, and Application to Antifouling Coatings for Filtration Membranes. *Polym. Chem.* **2013**, *4* (19), 5065–5073. https://doi.org/10.1039/C3PY00756A.

(123) Choi, Y.-S.; Kim, N. K.; Kang, H.; Jang, H.-K.; Noh, M.; Kim, J.; Shon, D.-J.; Kim, B.-S.; Lee, J.-C. Antibacterial and Biocompatible ABA-Triblock Copolymers Containing Perfluoropolyether and Plant-Based Cardanol for Versatile Coating Applications. *RSC Adv.* **2017**, *7* (60), 38091–38099. https://doi.org/10.1039/C7RA07689D.

(124) Wang, R.; Luo, Y.; Cheng, C.-J.; Huang, Q.-H.; Huang, H.-S.; Qin, S.-L.; Tu, Y.-M. Syntheses of Cardanol-Based Cationic Surfactants and Their Use in Emulsion Polymerisation. *Chemical Papers* **2016**, *70* (9), 1218–1227. https://doi.org/10.1515/chempap-2016-0052.

(125) 손다정; 최용석; 강효; 노명경; 장현기; 김병수; 이종찬. Synthesis and Characterization of Antifouling and Bactericidal ABA Tri-block Copolymers Having Perfluoropolyether and Cardanol-Containing Methacrylate Polymer Segments for Surface Coating Applications. 한국고분자학회 학술대회 연구논문 초록집 **2015**, 91–91.

(126) K. I., S.; Nutenki, R.; Joseph, T. M.; Murali, S. Structural, Molecular and Thermal Properties of Cardanol Based Monomers and Polymers Synthesized via Atom Transfer Radical Polymerization (ATRP). *Journal of Macromolecular Science, Part A* **2022**, *59* (6), 403–410. https://doi.org/10.1080/10601325.2022.2053288.

(127) Vitale, A.; Molina-Gutiérrez, S.; Li, W. S. J.; Caillol, S.; Ladmiral, V.; Lacroix-Desmazes, P.; Dalle Vacche, S. Biobased Composites by Photoinduced Polymerization of Cardanol Methacrylate with Microfibrillated Cellulose. *Materials* **2022**, *15* (1), 339. https://doi.org/10.3390/ma15010339.

(128) Cheng, C.; Bai, X.; Liu, S.; Huang, Q.; Tu, Y.; Wu, H.; Wang, X. UV Cured Polymer Based on a Renewable Cardanol Derived RAFT Agent. *J Polym Res* **2013**, *20* (7), 197. https://doi.org/10.1007/s10965-013-0197-2.

(129) Clementine. *Controlled radical polymerization - Design the architecture of polymers*. specific polymers. https://specificpolymers.com/controlled-radical-polymerization-how-to-design-the-architecture-of-polymers/ (accessed 2023-03-20).

(130) Sollka, L.; Lienkamp, K. Progress in the Free and Controlled Radical Homo- and Co-Polymerization of Itaconic Acid Derivatives: Toward Functional Polymers with Controlled Molar Mass Distribution and Architecture. *Macromolecular Rapid Communications* **2021**, *42* (4), 2000546. https://doi.org/10.1002/marc.202000546.

(131) Lorandi, F.; Fantin, M.; Matyjaszewski, K. Atom Transfer Radical Polymerization: A

Mechanistic Perspective. *J. Am. Chem. Soc.* **2022**, *144* (34), 15413–15430. https://doi.org/10.1021/jacs.2c05364.

(132) Abraham, S.; Ha, C.-S.; Kim, I. Synthesis of Poly(Styrene-Block-Tert-Butyl Acrylate) Star Polymers by Atom Transfer Radical Polymerization and Micellization of Their Hydrolyzed Polymers. *Journal of Polymer Science Part A: Polymer Chemistry* **2005**, *43* (24), 6367.

(133) Aydogan, C.; Aykac, F. S.; Yilmaz, G.; Chew, Y. Q.; Goto, A.; Yagci, Y. Synthesis of Block Copolymers by Mechanistic Transformation from Reversible Complexation Mediated Living Radical Polymerization to the Photoinduced Radical Oxidation/Addition/Deactivation Process. *ACS Macro Lett.* **2022**, *11* (3), 342–346. https://doi.org/10.1021/acsmacrolett.2c00004.

(134) Cölfen, H. Double-Hydrophilic Block Copolymers: Synthesis and Application as Novel Surfactants and Crystal Growth Modifiers. *Macromolecular Rapid Communications* **2001**, *22* (4), 219–252. https://doi.org/10.1002/1521-3927(20010201)22:4<219::AID-MARC219>3.0.CO;2-G.

(135) Mori, H.; Müller, A. H. E. New Polymeric Architectures with (Meth)Acrylic Acid Segments. *Progress in Polymer Science* **2003**, *28* (10), 1403–1439. https://doi.org/10.1016/S0079-6700(03)00076-5.

(136) Gupta, J.; Keddie, D. J.; Wan, C.; Haddleton, D. M.; McNally, T. Functionalisation of MWCNTs with Poly(Lauryl Acrylate) Polymerised by Cu(0)-Mediated and RAFT Methods. *Polym. Chem.* **2016**, *7* (23), 3884–3896. https://doi.org/10.1039/C6PY00522E.

(137) John, G.; Pillai, C. K. S. Self-Crosslinkable Monomer from Cardanol: Crosslinked Beads of Poly(Cardanyl Acrylate) by Suspension Polymerization. *Die Makromolekulare Chemie, Rapid Communications* **1992**, *13* (5), 255–259. https://doi.org/10.1002/marc.1992.030130502.

(138) Pandit, P.; Nadathur, G. T.; Maiti, S.; Regubalan, B. Functionality and Properties of Bio-Based Materials. In *Bio-based Materials for Food Packaging: Green and Sustainable Advanced Packaging Materials*; Ahmed, S., Ed.; Springer: Singapore, 2018; pp 81–103. https://doi.org/10.1007/978-981-13-1909-9_4.

(139) Vukovic, I.; Brinke, G. ten; Loos, K. Block Copolymer Template-Directed Synthesis of Well-Ordered Metallic Nanostructures. *Polymer* **2013**, *54* (11), 2591–2605. https://doi.org/10.1016/j.polymer.2013.03.013.

(140) Nutenki, R.; Darapureddi, P. R.; Nayak, R. R.; Kattimuttathu, S. I. Amphiphilic Comb-like Polymer-Modified Graphene Oxide and Its Nanocomposite with Polystyrene via Emulsion Polymerization. *Colloid Polym Sci* **2018**, *296* (1), 133–144. https://doi.org/10.1007/s00396-017-4228-0.

(141) Ziegenbalg, N.; V. Gruschwitz, F.; Adermann, T.; Mayr, L.; Guriyanova, S.; C. Brendel, J. Vinyl Mercaptoethanol as a Reactive Monomer for the Preparation of Functional Homo- and Copolymers with (Meth)Acrylates. *Polymer Chemistry* **2022**, *13* (34), 4934–4943.

https://doi.org/10.1039/D2PY00598K.

(142) Koiry, B. P.; Singha, N. K. Copper Mediated Controlled Radical Copolymerization of Styrene and 2-Ethylhexyl Acrylate and Determination of Their Reactivity Ratios. *Frontiers in Chemistry* **2014**, *2*.

(143) Mieras, H. J. M. A. Solution and Bulk Flow Properties of Linear and Branched Styrene–Butadiene Rubbers. *Journal of Polymer Science: Polymer Symposia* **1973**, *42* (2), 987–1000. https://doi.org/10.1002/polc.5070420250.

(144) Suresh, K. I.; Jaikrishna, M. Synthesis of Novel Crosslinkable Polymers by Atom Transfer Radical Polymerization of Cardanyl Acrylate. *Journal of Polymer Science Part A: Polymer Chemistry* **2005**, *43* (23), 5953–5961. https://doi.org/10.1002/pola.21088.

(145) Matyjaszewski, K.; Xia, J. Atom Transfer Radical Polymerization. *Chem. Rev.* **2001**, *101* (9), 2921–2990. https://doi.org/10.1021/cr940534g.

(146) Pirman, T.; Ocepek, M.; Likozar, B. Radical Polymerization of Acrylates, Methacrylates, and Styrene: Biobased Approaches, Mechanism, Kinetics, Secondary Reactions, and Modeling. *Ind. Eng. Chem. Res.* **2021**, *60* (26), 9347–9367. https://doi.org/10.1021/acs.iecr.1c01649.

(147) John, G.; Pillai, C. K. S. Synthesis and Characterization of a Self-Crosslinkable Polymer from Cardanol: Autooxidation of Poly(Cardanyl Acrylate) to Crosslinked Film. *Journal of Polymer Science Part A: Polymer Chemistry* **1993**, *31* (4), 1069–1073. https://doi.org/10.1002/pola.1993.080310429.

(148) Kattimuttathu I, S.; Foerst, G.; Schubert, R.; Bartsch, E. Synthesis and Micellization Properties of New Anionic Reactive Surfactants Based on Hydrogenated Cardanol. *Journal of Surfactants and Detergents* **2012**, *15* (2), 207–215. https://doi.org/10.1007/s11743-011-1294-z.

(149) Luyten, M. C.; Alberda van Ekenstein, G. O. R.; ten Brinke, G.; Ruokolainen, J.; Ikkala, O.; Torkkeli, M.; Serimaa, R. Crystallization and Cocrystallization in Supramolecular Comb Copolymer-like Systems: Blends of Poly(4-Vinylpyridine) and Pentadecylphenol. *Macromolecules* **1999**, *32* (13), 4404–4410. https://doi.org/10.1021/ma9900481.

(150) Ruokolainen, J.; Saariaho, M.; Ikkala, O.; ten Brinke, G.; Thomas, E. L.; Torkkeli, M.; Serimaa, R. Supramolecular Routes to Hierarchical Structures: Comb-Coil Diblock Copolymers Organized with Two Length Scales. *Macromolecules* **1999**, *32* (4), 1152–1158. https://doi.org/10.1021/ma980189n.

(151) Hofman, A. H.; Chen, Y.; ten Brinke, G.; Loos, K. Interaction Strength in Poly(4-Vinylpyridine)–n-Alkylphenol Supramolecular Comb-Shaped Copolymers. *Macromolecules* **2015**, *48* (5), 1554–1562. https://doi.org/10.1021/acs.macromol.5b00141.

(152) Nguyen, L. H.; Koerner, H.; Lederer, K. Free radical Co- and terpolymerization of styrene, hydrogenated cardanyl acrylate, and cardanyl acetate. *Journal of Applied Polymer Science*

2003, *88* (6), 1399–1409. https://doi.org/10.1002/app.11635.

(153) O'Leary, K. A.; Paul, D. R. Physical Properties of Poly(n-Alkyl Acrylate) Copolymers. Part 1. Crystalline/Crystalline Combinations. *Polymer* **2006**, *47* (4), 1226–1244. https://doi.org/10.1016/j.polymer.2005.12.005.

(154) Inomata, K.; Sakamaki, Y.; Nose, T.; Sasaki, S. Solid-State Structure of Comb-Like Polymers Having n-Octadecyl Side Chains I. Cocrystallization of Side Chain with n-Octadecanoic Acid. *Polym J* **1996**, *28* (11), 986–991. https://doi.org/10.1295/polymj.28.986.

(155) Inomata, K.; Sakamaki, Y.; Nose, T.; Sasaki, S. Solid-State Structure of Comb-Like Polymers Having n-Octadecyl Side Chains II. Crystalline-Amorphous Layered Structure. *Polym J* **1996**, *28* (11), 992–999. https://doi.org/10.1295/polymj.28.992.

(156) Faber, M.; Hofman, A. H.; Polushkin, E.; van Ekenstein, G. A.; Seitsonen, J.; Ruokolainen, J.; Loos, K.; ten Brinke, G. Hierarchical Self-Assembly in Supramolecular Double-Comb Diblock Copolymer Complexes. *Macromolecules* **2013**, *46* (2), 500–517. https://doi.org/10.1021/ma302295v.

(157) Li, S.; Wang, H.; Liu, L.; Xu, H.; Shi, H. On the Crystallization Behavior of a Poly(Stearyl Methacrylate) Comb-like Polymer inside a Nanoscale Environment. *CrystEngComm* **2018**, *20* (45), 7348–7356. https://doi.org/10.1039/C8CE01378K.

(158) Shi, H.; Zhao, Y.; Zhang, X.; Jiang, S.; Wang, D.; Han, C. C.; Xu, D. Phase Transition and Conformational Variation of N-Alkylated Branched Poly(Ethyleneimine) Comblike Polymer. *Macromolecules* **2004**, *37* (26), 9933–9940. https://doi.org/10.1021/ma0480704.

(159) Shi, H.; Zhao, Y.; Jiang, S.; Xin, J. H.; Rottstegge, J.; Xu, D.; Wang, D. Order–Disorder Transition in Eicosylated Polyethyleneimine Comblike Polymers. *Polymer* **2007**, *48* (9), 2762–2767. https://doi.org/10.1016/j.polymer.2007.03.012.

(160) Chapman, D. 904. The 720 Cm.–1 Band in the Infrared Spectra of Crystalline Long-Chain Compounds. *J. Chem. Soc.* **1957**, No. 0, 4489–4491. https://doi.org/10.1039/JR9570004489.

(161) Yao, K.; Tang, C. Controlled Polymerization of Next-Generation Renewable Monomers and Beyond. *Macromolecules* **2013**, *46*, 1689–1712. https://doi.org/10.1021/ma3019574.

(162) Gandini, A.; M. Lacerda, T. Monomers and Macromolecular Materials from Renewable Resources: State of the Art and Perspectives. *Molecules* **2022**, *27* (1), 159. https://doi.org/10.3390/molecules27010159.

(163) Yuan, M.; Cui, X.; Zhu, W.; Tang, H. Development of Environmentally Friendly Atom Transfer Radical Polymerization. *Polymers* **2020**, *12* (9), 1987. https://doi.org/10.3390/polym12091987.

(164) Applications of the 12 Principles of Green Chemistry in the Crop Protection Industry. *Organic Process Research & Development* **2019**, *23* (10), 2109–2121. https://doi.org/10.1021/acs.oprd.9b00305.

RESEARCH ACHIEVEMENTS

Publications

1. Muringayil Joseph, Tomy; Murali Nair, Sumi; Kattimuttathu Ittara, Suresh; Haponiuk, Jozef T; Thomas, Sabu. Copolymerization of styrene and pentadecylphenylmethacrylate (PDPMA): Synthesis, characterization, thermomechanical and adhesion properties. Polymers. 12,1,97,2020. MDPI.

2. Joseph, Tomy Muringayil; Luke, P Mereena. Transferosomes: Novel Delivery System for Increasing The skin Permeation of Drugs, Int J Med Phar Sci. Vol,10,02,1. 2020.

3. Mahapatra, Debarshi Kar; Gupta, Sayan Dutta; Bharti, Sanjay Kumar; Joseph, Tomy Muringayil; Haponiuk, Jozef T; Thomas, Sabu. Heat Shock Protein 90 (Hsp90) Inhibitory Potentials of Some Chalcone Compounds as Novel Anti-Proliferative Candidates, Advanced Studies in Experimental and Clinical Medicine.107-122, 2021, Apple Academic Press.

4. Luke, P Mereena; Dhanya, KR; Joseph, Tomy Muringayil; Haponiuk, Jozef T; Rouxel, Didier; Thomas, Sabu. Developments of Health Care: A Brief History of Medicine, Advanced Studies in Experimental and Clinical Medicine. 3-30,2021, Apple Academic Press.

5. Joseph, Tomy Muringayil; Mahapatra, Debarshi Kar; Luke, P Mereena; Haponiuk, Jozef T; Thomas, Sabu. Perspectives of Cashew Nut Shell Liquid (CNSL) in a Pharmacotherapeutic Context, Advanced Studies in Experimental and Clinical Medicine. 123-133,2021. Apple Academic Press.

6. Joseph, Tomy Muringayil; Pallikkunnel, Mereena Luke; Mahapatra, Debarshi Kar; Kallingal, Anoop; Thomas, Sabu; Haponiuk, Jozef T. Polyurethane Epoxy Composites: Recent Developments and Future Perspectives, Polyurethane Chemistry: Renewable Polyols and Isocyanates. 257-280,2021. American Chemical Society.

7. Kallingal, Anoop; Thachan Kundil, Varun; Ayyolath, Aravind; Muringayil Joseph, Tomy; Kar Mahapatra, Debarshi; Haponiuk, Jozef T; Variyar, E Jayadevi; Identification of sustainable trypsin active site inhibitors from Nigrospora sphaerica strain AVA1. Journal of Basic Microbiology. 61,8,709-720,2021.

8. Kallingal, Anoop; Ayyolath, Aravind; Thachan Kundil, Varun; Joseph, Tomy M; Chandra D, Naveen; Haponiuk, Jozef T; Thomas, Sabu; Variyar E, Jayadevi. Extraction and optimization of Penicillium sclerotiorum strain AKT1 pigment for fabric dyeing. Journal of Basic Microbiology,61,10,900-909,2021.

9. Joseph, Tomy M. Knowing What the COVID-19 Vaccine Does to Your Body?, International Journal of Current Research and Review. 13. 1-1,202. 2021.

10. Jose Varghese, R; Vidya, L; Joseph, Tomy Muringayil; Gudimalla, Apparao; Harini Bhuvaneswari, G; Thomas, Sabu. Potential Applications of XLPE Nanocomposites in the Field of Cable Insulation, Crosslinkable Polyethylene Based Blends, and Nanocomposites. 197-213,2021, Springer Singapore.

11. Luke, P Mereena; Joseph, Tomy Muringayil. Ufasomes: Rising technology for delivery of drugs. Int J Med Phar Sci. Vol,11,11,1,2021.

12. Kallingal, Anoop; Thachan Kundil, Varun; Ayyolath, Aravind; Karlapudi, Abraham Peele; Muringayil Joseph, Tomy; E, Jayadevi Variyar. Molecular modeling study of tectoquinone and acteoside from Tectona grandis linn: a new SARS-CoV-2 main protease inhibitor against COVID-19. Journal of Biomolecular Structure and Dynamics. 40,4,1764-1775,2022, Taylor & Francis.

13. KI, Suresh; Nutenki, Rajender; Joseph, Tomy Murugayil; Murali, Sumi. Structural, molecular, and thermal properties of cardanol-based monomers and polymers synthesized via ATRP (ATRP). Journal of Macromolecular Science, Part A. 59,6,403-410,2022. Taylor & Francis.

14. Muringayil Joseph, Tomy; Mariya, Hanna J; Haponiuk, Jozef T; Thomas, Sabu; Esmaeili, Amin; Sajadi, S Mohammad. Electromagnetic Interference Shielding Effectiveness of Natural and Chlorobutyl Rubber Blend Nanocomposite. Journal of Composites Science. 6,8,240,2022, MDPI.

15. Joseph, Tomy Muringayil; Kallingal, Anoop; Suresh, Akshay Maniyeri; Mahapatra, Debarshi Kar; Haponiuk, Jozef; Thomas, Sabu; Sajadi, S Mohammad. Orthomolecular Medicine Against COVID-19: Getting Prepared for Future Pandemic Recurrence. Acta Scientific Applied Physics. Volume,2,10, 2022.

16. Kallingal, Anoop; Ayyolath, Aravind; Thachan Kundil, Varun; Maniyeri Suresh, Akshay; Muringayil Joseph, Tomy; Haponiuk, Jozef; Thomas, Sabu; Augustine, Anu. Divulging the anti-acetylcholinesterase activity of Colletotrichum lentis strain KU1 extract as sustainable AChE active site inhibitors. Archives of Microbiology. 204,12,713, 2022. Springer.

17. Joseph, Tomy Muringayil; Suresh, Akshay Maniyeri; Kar Mahapatra, Debarshi; Haponiuk, Jozef; Thomas, Sabu. The Efficacious Benefit of 25-Hydroxy Vitamin D to Prevent COVID-19: An In-Silico Study Targeting SARS-CoV-2 Spike Protein. Nutrients. 14,23,4964,2022. MDPI.

18. Joseph, Tomy Muringayil; Sathian, Aiswarya; Unni, Aparna Beena; Mahapatra, Debarshi Kar; Kallingal, Anoop; K. S, Joshy; Hapniuk, Josef; Thomas, Sabu. Modulation of Aroma and Flavor Using Plasma Technology. Flavors and Fragrances in Food Processing: Preparation and Characterization Methods. 327-339,2022. ACS

19. Joseph, Tomy Muringayil; Sathian, Aiswarya; Unni, Aparna Beena; Mahapatra, Debarshi Kar; Kallingal, Anoop; K. S, Joshy; Haponiuk, Jozef; Thomas, Sabu. Applications of Flavors and Fragrances in Meat Products. Flavors and Fragrances in Food Processing: Preparation and Characterization Methods. 405-435,2022. ACS

20. Kumar, Pranesh; Mahapatra, Debarshi Kar; Kumar, Dileep; Taleuzzaman, Mohamad; Borikar, Sachin; Gulecha, Vishal S; Zalte, Amar G; Dadure, Kanhaiya M; Puranik, Manisha; Das, Manik; Joseph, Tomy Muringayil. Liposomal Delivery System for the Effective Delivery of Nutraceuticals and Functional Foods. Nutraceutical Delivery Systems. 173-184,2023. Apple Academic Press.

21. Joseph, Tomy Muringayil; Kallingal, Anoop; Suresh, Akshay Maniyeri; Mahapatra, Debarshi Kar; Hasanin, Mohamed S; Haponiuk, Jozef; Thomas, Sabu. 3D printing of polylactic acid: recent advances and opportunities, The International Journal of Advanced Manufacturing Technology.1-21,2023. Springer.

22. Joseph, Tomy Muringayil; Kar Mahapatra, Debarshi; Esmaeili, Amin; Piszczyk, Lukasz; Hasanin, Mohamed S; Kattali, Mashhoor; Haponiuk, Jozef; Thomas, Sabu. Nanoparticles: Taking a unique position in medicine. Nanomaterials. 13,3,574,2023, MDPI.

23. Joseph, Tomy Muringayil; Unni, Aparna Beena; Joshy, KS; Kar Mahapatra, Debarshi; Haponiuk, J┣┃zef; Thomas, Sabu. Emerging Bio-Based Polymers from Lab to Market: Current Strategies, Market Dynamics and Research Trends. Carbon,9,1,30,2023, MDPI.

24. Joseph, Tomy Muringayil, Mohamed S. Hasanin, Aparna Beena Unni, Debarshi Kar Mahapatra, Jozef Haponiuk, and Sabu Thomas. Macromolecules: Contemporary Futurist Thoughts on Progressive Journey. Eng 4, no. 1: 678-702, 2023. MDPI.

NCBI Genbank Entries

1. MW057418.1Curvulariapseudorobusta strain TMJ 1, Tomy,M.J. and Anoop,K.
2. MW057715.1Bacillus licheniformis strain AK 1, Tomy,M.J. and Anoop,K.
3. MW057760.1Uncultured Escherichia sp. clone TMJ 3, Tomy, M.J. and Anoop, K.
4. MW057764.1Bacillus thuringiensis strain AK 2, Tomy,M.J. and Anoop,K.

5. MW057763.1Klebsiella pneumoniae strain GDU 2, Tomy, M.J. and Anoop, K.
6. MW057781.1Bacillus anthracis strain VTK 1, Tomy, M.J. and Anoop, K.
7. MW057852.1Bacillus flexus strain ARA 1, Tomy, M.J. and Anoop, K.
8. MW058059.1Bacillus cereus strain GDU 1, Tomy, M.J. and Anoop, K.
9. MW058055.1Stenotrophomonas maltophilia strain UK 1, Mahapatra, D.K., Tomy, M.J. and Anoop, K.
10. MW058061.1Streptomyces sp. strain AK 1, Mahapatra, D.K., Tomy, M.J. and Anoop, K.
11. MW058064.1Aspergillus oryzae strain AOS-KU, Mahapatra, D.K., Tomy, M.J. and Anoop, K.
12. MW058063.1Aspergillus flavus strain AF-1, Mahapatra, D.K., Tomy, M.J. and Anoop, K.
13. MW063264.1Rhizopus sp. strain RHS-ANU-1, Mahapatra, D.K., Tomy, M.J. and Anoop, K.
14. MW063265.1Aspergillus terreus strain KUN F 1, Mahapatra,D.K., Tomy, M.J. and Anoop, K.
15. MW067299.1Bacillus licheniformis strain DKM 2, Mahapatra,D.K., Tomy, M.J. and Anoop, K.

Participation in conferences & workshops

1. Seminar and workshop on 'Accustomic Pharmaceutical Professionals with Upcoming Future Challenges' organized by Gurunanak College of Pharmacy, Nagpur, 44002. [May29-31, 2020]

2. Workshop on Polymer Nanocomposites and Applications (IWPNA), Mahatma Gandhi University Kottayam Gandhi University Kottayam, 30 December 2019.

3. International Workshop on Engineered Polymer Nanocomposites Mahatma Gandhi University Kottayam Gandhi University Kottayam, December 5-7, 2019.

4. International Workshop on Medical Imaging and Nanotechnology- Latest Trends (IWMN-2020), 9-11 January 2020.

5. Conference organized by the Centre for Interdisciplinary science JISIASAR, Kolkota, JIS University. India.

6. Fourth International Conference on Reuse and Recycling of Materials and their Products (ICRM-2018) 10-12 March 2018.

7. Seminar and workshop on 'Accustomic Pharmaceutical Professionals with Upcoming Future Challenges' organized by Gurunanak College of Pharmacy, Nagpur, 44002. [May29-31, 2020].

8. International Workshop on Medical Imaging and Nanotechnology- Latest Trends (IWMN-2020), 9-11 January 2020.

9. Mereena Luke, Tomy Muringayil Joseph, Józef T. Haponiuk, Sabu Thomas, "Rifampicin Incorporated Sodium Alginate Microspheres: Effect Of Crosslinking Metal Ions" Advance in Petroleum and Gas Industry and Petrochemistry" (APGIP-11) May 2022 Lviv Polytechnic National University, Lviv, Ukraine.

10. Tomy Muringayil Joseph, Mereena Luke P, T. Józef Haponiuk and Sabu Thomas "Challenges in polymer nanocomposite processing techniques; An overview in brief" (APGIP-10) May 18-23, 2020 Lviv Polytechnic National University, Lviv, Ukraine.

11. Mereena Luke P Tomy Muringayil Joseph, Józef T. Haponiuk, S. Thomas "Preparation and Evaluation of Curcumin Incorporated Sodium Alginate Microspheres" (APGIP-10) May 18- 23, 2020 Lviv Polytechnic National University, Lviv, Ukraine

12. Tomy Muringayil Joseph, K I Suresh, Józef T. Haponiuk, Sabu Thomas, "Copolymerization of styrene and cardanyl acrylate (CA): Synthesis, characterization, thermomechanical and adhesion properties" (APGIP-11) May 2022 Lviv Polytechnic National University, Lviv, Ukraine.